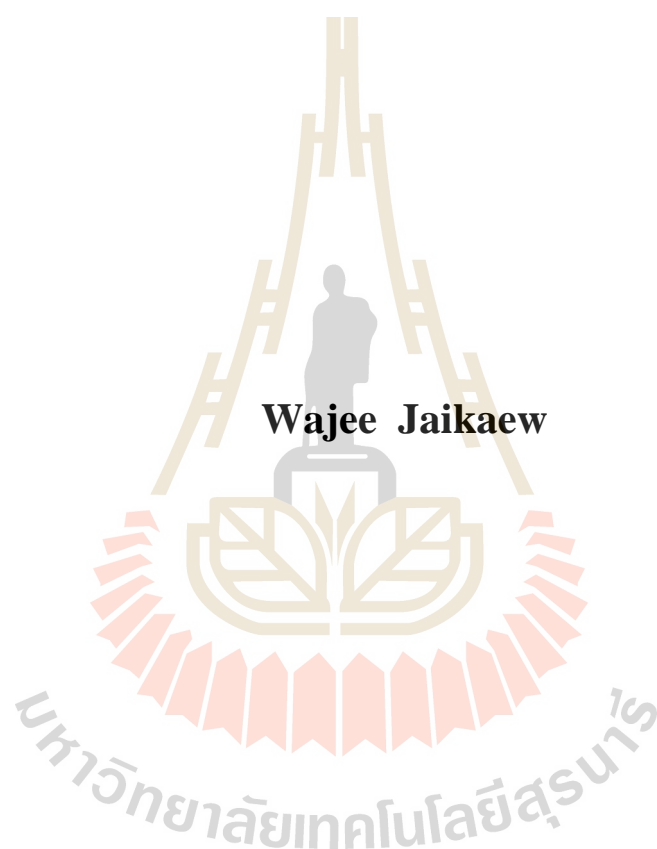


โรบติกโวลแทมเมตรีสำหรับการทดสอบการละลายยา และการใช้
ไบโอเซนเซอร์ชนิดลวดทองแดงซึ่งปราศจากสิ่งรบกวน



วิทยานิพนธ์นี้เป็นส่วนหนึ่งของการศึกษาตามหลักสูตรปริญญาวิทยาศาสตรดุษฎีบัณฑิต
สาขาวิชาเคมี
มหาวิทยาลัยเทคโนโลยีสุรนารี
ปีการศึกษา 2560

**ROBOTIC VOLTAMMETRY FOR DRUG DISSOLUTION
TESTING AND INTERFERENCE-FREE COPPER-BASED
BIOSENSOR PLATFORM**



**A Thesis Submitted in Partial Fulfillment of the Requirements for the
Degree of Doctor of Philosophy in Chemistry
Suranaree University of Technology
Academic Year 2017**

**ROBOTIC VOLTAMMETRY FOR DRUG DISSOLUTION
TESTING AND INTERFERENCE-FREE COPPER-BASED
BIOSENSOR PLATFORM**

Suranaree University of Technology has approved this thesis submitted in partial fulfillment of the requirements for the Degree of Doctor of Philosophy.

Thesis Examining Committee



(Prof. Dr. James R. Ketudat-Cairns)

Chairperson



(Asst. Prof. Dr. Panida Khunkaewla)

Member (Thesis Advisor)



(Prof. Dr. Albert Schulte)

Member



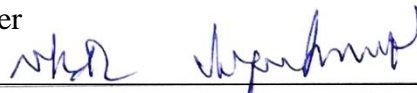
(Prof. Dr. Wolfgang Schuhmann)

Member



(Prof. Dr. Kritsana Sagarik)

Member



(Asst. Prof. Dr. Sanchai Prayoonpokarach)

Member



(Asst. Prof. Dr. Worawat Meevasana)



(Prof. Dr. Santi Maensiri)

Vice Rector for Academic Affairs
and Internationalization

Dean of Institute of Science

วชิ ใจแก้ว : โรโบติกโวลแทมเมตรีสำหรับการทดสอบการละลายยา และการใช้
ไบโอเซนเซอร์ชนิดลวดทองแดงซึ่งปราศจากสิ่งรบกวน (ROBOTIC VOLTAMMETRY
FOR DRUG DISSOLUTION TESTING AND INTERFERENCE-FREE COPPER-
BASED BIOSENSOR PLATFORM). อาจารย์ที่ปรึกษา : ผู้ช่วยศาสตราจารย์
ดร.พนิดา ชันแก้วหาล้า, 178 หน้า.

อัตรโนมัตติ การทดสอบการละลายยา เอนไซม์ไบโอเซนเซอร์ สายไฟฟ้าทองแดง การวัด H_2O_2 ที่กระแส
แคโทดิก

ภารกิจในแต่ละวันของการพัฒนาและควบคุมคุณภาพของยาคือการวิเคราะห์ตัวอย่างจำนวนมาก
ที่ได้จากการทดสอบการสลายตัวของยา ระบบอัตรโนมัตติจึงเป็นสิ่งสำคัญเพื่อลดค่าใช้จ่ายและเพิ่ม
ประสิทธิภาพของผู้ปฏิบัติงาน วิทยานิพนธ์นี้ใช้โรโบติกโวลแทมเมตรีขั้นสูงชนิดไมโครเพลทที่สะดวก
สำหรับตรวจสอบการปลดปล่อยยา ยาต้นแบบที่นำมาใช้คือพาราเซตามอล (PCT) ในรูปแบบยาเม็ดซึ่ง
ปลดปล่อยยาทันทีและปลดปล่อยยาอย่างช้า หรือยาที่อยู่ในรูปแบบของเจลหรือพอลิเมอร์ฟิล์ม การเพิ่ม
ประสิทธิภาพของเซนเซอร์เพื่อโวลแทมเมตรีของพาราเซตามอลที่ดี ทำโดยการตั้งค่าและติดตั้งซอฟต์แวร์
ระบบสำหรับการสร้างโปรไฟล์การปลดปล่อยยาพาราเซตามอล ด้วยระบบอัตรโนมัตติ โรโบติกโวลแทมเมตรี
สามารถวัดการละลายของเม็ดยาพาราเซตามอลตามคุณสมบัติการปลดปล่อยยาได้ดี นอกจากนี้ ได้มีการ
เพิ่มระบบปั๊มและเวลาที่ใช้ในการดูดสารละลายอิเล็กโทรไลต์สู่หลุมตัวอย่างยาในไมโครเพลท เมทริกซ์
ทั้งหมด 11 ชนิด กราฟการปลดปล่อยยาของแต่ละชนิดถูกสร้างขึ้น โดยเทคนิคโรโบติกโวลแทมเมตรี
เช่นกัน เมื่อเปรียบเทียบกับการวิเคราะห์แบบดั้งเดิมของการศึกษาการละลายของตัวอย่างยา เทคนิคนี้
สามารถลดความสับสนจากการทำงานซ้ำ ๆ ในตัวอย่างจำนวนมากของผู้วิเคราะห์ และยังสะดวก ลดความ
ผิดพลาดที่อาจเกิดจากผู้วิเคราะห์เอง และสามารถมีเวลาทำงานอื่น ๆ ควบคู่กันได้ ดังนั้นเทคนิคโรโบติก
โวลแทมเมตรีจึงมีศักยภาพในการใช้ศึกษาการปลดปล่อยยามีความคุ้มค่าทางเศรษฐกิจ สามารถนำมาใช้
ศึกษาการปลดปล่อยสารตัวอย่างที่มีตัวเกิดปฏิกิริยารีดอกซ์ การวิเคราะห์นี้ได้ถูกนำเสนอให้เป็น
เครื่องมือวิเคราะห์ที่มีความเป็นไปได้สูงในการนำมาใช้งานอีกวิธีหนึ่งสำหรับการศึกษาการปลดปล่อย
ตัวอย่างยา

แอมเพอโรเมตริกออกซิเดสไบโอเซนเซอร์ทำงานร่วมกับกระแสแอโนดิกของไฮโดรเจนเปอร์
ออกไซด์ (H_2O_2) ซึ่งเป็นผลจากปฏิกิริยารีดอกซ์ของเอนไซม์/สารตั้งต้น แต่ในตัวอย่างที่มีสารอื่นที่สามารถถูก
ออกซิไดซ์ได้นั้น สัญญาณจากกระแสแคโทดิกของไฮโดรเจนเปอร์ออกไซด์ เป็นทางเลือกที่ดีกว่า
เนื่องจากมีเพียงไฮโดรเจนเปอร์ออกไซด์เท่านั้นที่จะสามารถตรวจวัดได้โดยปฏิกิริยารีดอกซ์ด้วยไฟฟ้า

และไม่มีสิ่งรบกวนจากตัวอย่างในการวัด ส่วนที่สองของวิทยานิพนธ์ เป็นการนำเอาหลอดทองแดงมาใช้เตรียมขั้วไฟฟ้าใช้งานสำหรับการทำออกซิเดสไปโอเซนเซอร์ที่กระแสแคโทดิก พบว่าที่ -0.15 โวลต์ เทียบกับขั้วอ้างอิง การตอบสนองต่อสัญญาณแบบเส้นตรงอยู่ระหว่าง $20 - 1500 \mu\text{M}$ ความไวในการวิเคราะห์มีค่าเป็น $7 \text{ nA } \mu\text{M}^{-1} \text{ cm}^2$ และในการวิเคราะห์หาปริมาณกลูโคสที่เติมลงในสารละลายพบว่าร้อยละการได้กลับคืนคือ $106 \pm 4\%$ ($n=3$) ประโยชน์หลักของกลูโคสไปโอเซนเซอร์ที่ใช้ขั้วไฟฟ้าทองแดงเปรียบเทียบกับตัวเลือกอื่น ๆ คือ เรียบง่ายและประหยัดในการวิเคราะห์ไฮโดรเจนเปอร์ออกไซด์ เนื่องจากการใช้งานไม่ต้องใช้วัสดุพิเศษเป็นตัวเร่งปฏิกิริยาเชิงไฟฟ้าเคมีในการวัดไฮโดรเจนเปอร์ออกไซด์



สาขาวิชาเคมี

ปีการศึกษา 2560

ลายมือชื่อนักศึกษา ศ. ใจแก้ว
 ลายมือชื่ออาจารย์ที่ปรึกษา P. S.
 ลายมือชื่ออาจารย์ที่ปรึกษาร่วม Allert Schultz

WAJEE JAIKAEW : ROBOTIC VOLTAMMETRY FOR DRUG
DISSOLUTION TESTING AND INTERFERENCE-FREE COPPER-
BASED BIOSENSOR PLATFORM. THESIS ADVISOR :
ASST. PROF. PANIDA KHUNKAEWLA, Ph.D. 178 PP.

AUTOMATION, DRUG DISSOLUTION TESTING, ENZYME BIOSENSOR,
CABLE-COPPER, CATHODIC H₂O₂ DETECTION


A daily task of drug development and drug formulation quality control is analysis of many samples from dissolution testing. Automation of that duty is crucial for cost reduction and labor efficiency perfection. This thesis advanced robotic microplate-based voltammetry into a convenient solution for automated analysis of samples from drug release studies. Model drug was Paracetamol[®] (PCT), as immediate (IR) and extended (ER) release tablets or stored in hydrogels or polymer thin films. Sensor optimization for good PCT voltammetry and setup and software adaptation was completed to gain the system for non-manual PCT release profile creation. Robotic electroanalysis of samples from PCT tablet dissolution tests reproduced well their known release features. Addition of a syringe pump to the used system and timed electrolyte filling enabled direct robotic drug release trials from drug formulations in microplate wells. For 11 polymer matrices the release profiles were created with data from robotic voltammetry. Compared to normal manual inspection of dissolution study samples, the tactic from this work frees laboratory staff from repetitions of many identical actions, leading to convenience, and human error exclusion. Robotic microplate well voltammetry has potential to make drug release profiling economic and

pleasant, if drugs are redox active. The assay is hence suggested as a promising complementary analytical tool for drug release trials.

Common amperometric oxidase biosensors work with anodic detection of hydrogen peroxide (H_2O_2), which is product of enzyme/substrate interaction. In samples with other oxidizable species cathodic H_2O_2 signaling is better as only H_2O_2 is detected via electro-reduction but not interferences. In a second thesis part copper disk electrodes made from electrical cable were explored as cathodic platform for oxidase biosensors. At -0.15 V vs. reference, the linear glucose response of Cu glucose biosensors stretched from 20 to 1500 μM , with a sensitivity of about $7 \text{ nA } \mu\text{M}^{-1} \text{ cm}^{-2}$. Analysis of glucose supplemented buffer solutions revealed recovery rates of $106 \pm 4\%$ ($n=3$). Main benefit of cable Cu-based glucose biosensors, compared to other options, is the simplicity and cheapness of the H_2O_2 readout, which works without involvement of electrocatalytic micro- or nanomaterials in competitive manner for reductive H_2O_2 detection.

School of Chemistry

Academic Year 2017

Student's signature 

Advisor's signature 

Co-advisor's signature 

ACKNOWLEDGEMENTS

First, I would like to express sincere appreciation to my Ph.D. advisors, Prof. Dr. Albert Schulte, School of Biomolecular Science and Engineering, Vidyasirimedhi Institute of Science and Technology (VISTEC), Rayong, Thailand, and Assistant Professor Dr. Panida Khunkaewla, School of Chemistry, Suranaree University of Technology, Thailand, for their guidance, support and ideas that made this work interesting for me and gave me a lot of inspiration. Their valuable inputs helped to make this thesis successful.

I recognize that this research would not have been possible without the kind financial support through the Royal Golden Jubilee Ph.D. Program of the Thailand Research Fund and without the provision of good research facilities by the Suranaree University of Technology and Ruhr-University of Bochum and I express my sincere gratitude to these three organizations.

I am also deeply grateful to Prof. Dr. Wolfgang Schuhmann, Analytische Chemie Elektroanalytik und Sensorik (ELAN), Department of Chemistry and Biochemistry, Ruhr-Universität Bochum, Bochum, Germany, for providing precious advice and quality laboratory facilities during my one-year research work in his group in Germany. My stay in his laboratory was enjoying, very fruitful and I have gained there a lot of knowledge related to my project.

I also would like to thank Dr. Thomas Erichsen and Dr. Adrian Ruff for their support valuable support and supervision of my Bochum laboratory time and Bettina Stetzka for her kind help in administrative issues and the organization of my research

visit to Bochum. Dr. Piyanut Pinyou and all other “ELAN” group members are acknowledged for offering a nice and friendly working environment, as well as spending for the time together throughout my stay. Dr. Alberto Ganassin’s help in improving the writing of this thesis is also very much appreciated.

I am furthermore thankful to Professor Wipa Suginta and Assistant Professor Panida Khunkaewla for their continuous efforts in maintaining the Biochemistry-Electrochemistry Research Unit (BECRU) as well-organized laboratory environment and also acknowledge all BECRU members for their discussions, help in laboratory issues and the many celebrations in a warm atmosphere.

All lecturers of my courses at the School of Chemistry, Suranaree University of Technology, Thailand are acknowledged.

And finally my deep sense of gratitude goes to my beloved family members and all those who have helped me during this project for their endless encouragement and heartiest assistance.

Wajee Jaikaew

มหาวิทยาลัยเทคโนโลยีสุรนารี

CONTENTS

	Page
ABSTRACT IN THAI.....	I
ABSTRACT IN ENGLISH.....	III
ACKNOWLEDGEMENTS.....	V
CONTENTS.....	VII
LIST OF TABLES.....	XIV
LIST OF FIGURES.....	XV
LIST OF ABBREVIATIONS.....	XXIII
CHAPTER	
I INTRODUCTION.....	1
1.1 Research objectives.....	4
II LITERATURE REVIEWS.....	7
2.1 State of the art of drug dissolution testing.....	7
2.1.1 Automated electrochemistry.....	15
2.1.2 Robotic electrochemical for assessment of drug analysis.....	19
2.1.3 Drug dissolution testing of paracetamol tablet analysis.....	21
2.1.4 Drug release from polymer as a controlled drug delivery system.....	24
2.2 State of the art of electrochemical glucose biosensors based copper disk electrode.....	27

CONTENTS (Continued)

	Page
2.2.1 Electrochemical sensors.....	27
2.2.2 Evolution from 1 st to 3 rd generation biosensors	29
2.2.3 Electroactive interferences.....	31
III RESEARCH METHODOLOGY.....	34
3.1 Experimental and methods	34
3.1.1 Materials and chemicals.....	34
3.1.2 Instruments.....	36
3.2 Research methodology	37
3.2.1 Counter electrode (CE).....	37
3.2.2 Reference electrode (RE).....	37
3.2.3 Working electrode (WE).....	38
3.2.3.1 Bare glassy carbon electrodes.....	38
3.2.3.2 Preparation of CNT-modified glassy carbon electrodes	38
3.2.3.3 Cu electrode and GOx immobilization.....	39
3.3 Robotic electrochemical workstation	41
3.4 Robotic voltammetry for drug tablet dissolution testing with CNT modified glassy carbon electrode	42
3.4.1 Differential pulse voltammetry of PCT	43
3.4.2 Calibration curve for drug via robotic DPV in 24-well plate	44

CONTENTS (Continued)

	Page
3.4.3 Reproducibility for drug quantification via robotic electrochemical measurements	44
3.4.4 Robotic DPV for drug profiling measurements in drug tablets.....	44
3.4.4.1 In vitro drug dissolution testing with the basket method	44
3.4.4.2 Dissolution testing of PCT drugs used DPV via robotic measurements in calibration curve mode	46
3.5 Robotic microtiter plate based drug voltammetry and controlled released from hydrogel drug formulations	46
3.5.1 Square wave voltammetry of PCT.....	47
3.5.2 Stability of the working electrode.....	47
3.5.3 Robotic SWV for drug release from agarose natural hydrogels.....	48
3.5.3.1 PCT drug loading with agarose hydrogel in microtiter plate.....	48
3.5.3.2 Robotic voltammetry determination of PCT release from agarose hydrogels in 24-well microtiter plate.....	49
3.6 Drug release from natural and artificial hydrogels by means of the electrochemical robotic system	50

CONTENTS (Continued)

	Page
3.6.1 The application of robotic SWV for drug release from artificial and natural hydrogels	51
3.6.1.1 PCT drug loading in one-component hydrogel in microtiter plate.....	51
3.6.1.2 PCT drug loading in two-component hydrogel in microtiter plate modelling	52
3.6.1.3 Drug loading in three-component hydrogel in microtiter plate.....	54
3.7 Cathodic H ₂ O ₂ analysis with electricity cable Cu disk electrodes as Oxidase biosensor platforms	54
3.7.1 Calibration curve of H ₂ O ₂ with Cu disk electrode.....	54
3.7.2 Cu disk electrode testing interference in amperometric method	55
3.7.3 Determining ability of Cu disk electrode to determine H ₂ O ₂	55
3.7.4 Calibration curve of glucose biosensor via Cu disk electrode at cathodic potential	55
3.7.5 Determination of the glucose with GOx/Nafion-modified Cu disk electrode	56
IV RESULTS AND DISCUSSION.....	57

CONTENTS (Continued)

	Page
4.1	Robotic voltammetry as convenient tool for analysis in course of tablet dissolution testing58
4.1.1	Required methodological adaptations and consistency verification58
4.1.2	Tablet drug dissolution testing with microplate-based robotic voltammetry sample analysis70
4.2	Application of robotic voltammetry in 24-well microtiter plates as screening tool for drug release from agarose-based hydrogels matrices and polymer thin films82
4.2.1	24-well microtiter plate voltammetry as convenient screening tool for drug release from hydrogel drug formulations88
4.2.2	Robotic microplate-based voltammetry as screening tool for drug release from synthetic and natural polymer thin films and their blends with agarose hydrogels: A comparative case study100
4.2.2.1	Release characteristics for the film-like one-component chitosan, S1-1 or S2-2 PCT formulations104

CONTENTS (Continued)

	Page
4.2.2.2 Release characteristics of the agarose+chitosan, agarose+S1-1 or S2-2, chitosan+S1-1 or S2-2 and agarose+chitosan+S1-1 or S2-2 PCT formulations.	108
4.3 Electrical copper disk electrodes as oxidase biosensor platforms with cathodic of H ₂ O ₂ assessment	117
V CONCLUSIONS AND OUTLOOK	128
5.1 Robotic voltammetry for drug product dissolution testing.....	128
5.2 Cable copper disk electrodes as oxidase biosensor platforms	130
REFERENCES	132
APPENDICES	
APPENDIX A SOLUTION PREPARATION	152
APPENDIX B DESIGN OF SOFTWARE FOR THE EXECUTION OF ROBOTIC ELECTROCHEMICAL ANALYSIS IN 24-WELL MICROTITER PLATES	155
APPENDIX C ROBOTIC ELECTROCHEMICAL ANALYSIS OF DRUG DISSOLUTION SAMPLES	157
APPENDIX D ROBOTIC ELECTROCHEMICAL ANALYSIS OF CONTROLLED DRUG RELEASE FROM THE NATURAL AND ARTIFICIAL POLYMERS	164

CONTENTS (Continued)

	Page
APPENDIX E PUBLICATIONS.....	170
CURRICULUM VITAE	179



LIST OF TABLES

Table		Page
4.1	Recovery rate performance of robotic PCT voltammetry in the standard addition method.	69
4.2	Comparison of the recovery rate performance of robotic PCT voltammetry in the standard addition and the calibration method.	70
4.3	Materials trialed via microplate robotic voltammetry as to the time course of their PCT storage properties.	103

LIST OF FIGURES

Figure		Page
2.1	Steps in course of drug discovery and development.....	8
2.2	Time course of blood drug levels after uptake of immediate, controlled and sustained release tablets.	8
2.3	Controlled drug release out of macro-, and micrometric polymer capsules.....	10
2.4	Schematic illustration of the apparatus for standardized in vitro drug dissolution testing.....	12
2.5	Identification of a drug molecule electro-activity for voltammetry.....	14
2.6	Simple schematic of flow-based electroanalysis of samples from drug release testing.....	16
2.7	The device for automatic sequential electrochemistry in the wells of microtiter plate.	16
2.8	Chemical structure of paracetamol, PCT, and the reaction scheme for the redox reaction	20
2.9	Drug release profiles of immediate release paracetamol formulation compared to the release profile from two sustaineds release formula in 0.1 N HCl pH 1.2 dissolution media.....	23
2.10	Schematic of the concept or design of biosensors.	28
2.11	Three generations of amperometric enzyme electrodes for glucose.....	31

LIST OF FIGURES (Continued)

Figure	Page
3.1	The photograph of a miniaturized A) Pt wire counter electrode, B) Ag/AgCl reference electrode.37
3.2	Schematic diagram of the procedure used for the preparation of CNT-modified GCE used in this study for drug measurements in the robotic electrochemical workstation.39
3.3	Digital photographs of A) the electrical cable used as the precursor for Cu electrode fabrication B) a completed Cu disk electrode.40
3.4	Digital photographs of modification of cable Cu disk electrodes via coating with a GOx-immobilizing Nafion thin film and the electrochemical cells set up.....41
3.5	Photo of the robotic electrochemical system.42
3.6	Drug dissolution testing via standardized “basket” method as suggested and standardized by the United States Pharmacopeia (USP).....45
3.7	Display of the schedule for sample collection within a PCT tablet dissolution test.....46
3.8	The microplate layout for response stability tests with a 200 μ M PCT sample.48
3.9	Scheme of the preparation of PCT-loaded agarose hydrogels in individual wells of microplates.49

LIST OF FIGURES (Continued)

Figure	Page
3.10	Molecular structure of the artificial immobilization matrix P(SS-GMA-BA) and nominal composition.51
3.11	Scheme of the preparation of PCT-loaded chitosan or P(SS-GMA-BA) films in individual wells of microplates.....52
3.12	Scheme of the preparation of PCT-loaded two- and three-components hydrogel/polymer formulations in individual wells of microplates.....53
4.1	Schematic illustration of paracetamol drug tablets in the immediate-release (IR) and extended-release (ER) release form.59
4.2	Differential pulse voltammograms of 100 μ M PCT in 0.1 M H_2SO_4 - K_2SO_4 mixed with 0.1 M KCl (pH 1.02) at a bare and a CNT-modified GCE.....60
4.3	Robotic PCT calibration measurements with a CNT/GCE working electrode in sequential action in the containers of a pre-loaded 24-well microtiter plate62
4.4	Calibration plot for robotic PCT DPV with a CNT/GCE working electrode.63
4.5	Robotic PCT differential pulse voltammetry in 24-well microtiter plates: Stability test I.....65
4.6	Robotic PCT differential pulse voltammetry in 24-well microtiter plates: Stability test II67

LIST OF FIGURES (Continued)

Figure	Page
4.7	Quantification of PCT in a model sample with an adjusted 20 μ M level by the standard addition method.69
4.8	Illustration of the in vitro Paracetamol [®] tablet dissolution testing with the basket method and subsequent sample analysis via robotic voltammetry72
4.9	Illustration of the protocol for the analysis of samples from Paracetamol [®] tablet dissolution testing74
4.10	Robotic voltammetric quantification of PCT in samples from PCT tablet dissolution testing76
4.11	Time course of PCT release from a) an immediate-release and, b) an extended-release at room temperature.77
4.12	A comparison of the averaged drug release profiles of an immediate and an extended release PCT tablet79
4.13	Shows comparison of averaged drug release profiles different temperature as body and as room of the dissolution medium at pH 1.02 with the immediate release formulation.80
4.14	Schematic of the robotic electrochemical workstation as used for voltammetric drug release measurement from drug-loaded materials in individual containers of 24-well microplates84

LIST OF FIGURES (Continued)

Figure	Page
4.15	Calibration of a bare GCE working electrode in the robotic SWV mode.....85
4.16	Display of the plot of the peak height of PCT SWVs displayed in Figure 4.15b) as a function of the PCT concentration86
4.17	Response stability of robotic SWV at bare GCEs toward PCT87
4.18	Illustration of the charging of microplate wells with transparent PCT-loaded agarose hydrogels90
4.19	The microplate load a) and the protocol (event sequence) of well approach/activity b) of a typical triplicate robotic voltammetry quantification trial of the release of PCT from gelled agarose.91
4.20	Typical data of a robotic voltammetry quantification trial regarding the release of PCT from 1% agarose hydrogels in a microplate well92
4.21	Time dependence of PCT release from a 1% agarose hydrogel as assessed with a robotic trial as outlined94
4.22	Distribution of PCT within a 0.3 mm thick hydrogel pellet in a microplate well.....95
4.23	PCT release profiles as constructed with data from a triplicate comparative robotic voltammetry release trial at room temperature for 1% agarose hydrogels with 4, 2, 1 and 0.5 mM PCT load.....96

LIST OF FIGURES (Continued)

Figure		Page
4.24	TriPLICATE comparative robotic voltammetry release trials at room temperature for 1% agarose hydrogels with 4, 2, 1 and 0.5 mM PCT load	97
4.25	PCT release profiles as constructed with data from triplicate comparative robotic voltammetry release trials at room temperature for 1% agarose hydrogels with a 2 mM PCT load at pH 1.2 and 8.0	99
4.26	Origin and molecular structures of the biopolymer chitosan	101
4.27	Molecular structures of polymers S1-1 and S2-2.....	102
4.28	Schematic and photographs of the preparation of PCT-loaded chitosan+S1-1 or S2-2 blends with agarose hydrogels and pure chitosan, S1-1, or S2-2 films with PCT charge in 24-well microtiter plate containers.....	102
4.29	Cumulative PCT release (in %) from chitosan, S1-1, and S2-2 and agarose formulations at room temperature in 0.1 M K ₂ SO ₄ -H ₂ SO ₄ at pH 1.2 and 8.0.	105
4.30	Cumulative PCT release (in %) from thin films of the polymers S1-1 and S2-2 at room temperature in 0.1 M K ₂ SO ₄ -H ₂ SO ₄ at pH 1.2 and 8.0	107
4.31	Schematic representation of the possible behavior of drug release in the thick and thin hydrogel.	108

LIST OF FIGURES (Continued)

Figure		Page
4.32	Cumulative PCT release (in %) from PCT+agarose+chitosan hydrogel pellets at room temperature in 0.1 M K ₂ SO ₄ -H ₂ SO ₄ at pH 1.2 and 8.0.	111
4.33	Cumulative PCT release (in %) from PCT+agarose+S1-1 hydrogel pellets at room temperature in 0.1 M K ₂ SO ₄ -H ₂ SO ₄ at pH 1.2 and 8.0.	112
4.34	Cumulative PCT release (in %) from PCT+agarose+S2-2 hydrogel pellets at room temperature in 0.1 M K ₂ SO ₄ -H ₂ SO ₄ at pH 1.2 and 8.0.	113
4.35	Cumulative PCT release (in %) from PCT+chitosan+S1-1 thin films at room temperature in 0.1 M K ₂ SO ₄ -H ₂ SO ₄ at pH 1.2 and 8.0.	114
4.36	Cumulative PCT release (in %) from PCT+chitosan+S2-2 thin films at room temperature in 0.1 M K ₂ SO ₄ -H ₂ SO ₄ at pH 1.2 and 8.0.	115
4.37	Cumulative PCT release (in %) from PCT+agarose+chitosan+S1-1 and PCT+agarose+chitosan+S2-2 hydrogel pellets at room temperature in 0.1 M K ₂ SO ₄ -H ₂ SO ₄ at pH 1.2 and 8.0.	116
4.38	Display photographs of the electrical cable used as the precursor for Cu electrode fabrication.	118

LIST OF FIGURES (Continued)

Figure		Page
4.39	Amperometric H ₂ O ₂ calibration measurements via cathodic potential at an cable Cu disk electrode.....	120
4.40	Standard addition mode of H ₂ O ₂ quantification via cathodic amperometric at an electrical cable Cu disk electrode.....	121
4.41	Amperometric response of a Cu disk electrode in 0.1 M PBS (pH=7) to successive triplicate additions of 50 mM of analyte (H ₂ O ₂), interferents (ascorbic acid, AA and PCT) and analyte again.	122
4.42	Amperometric glucose calibration measurements with cathodic potential	124
4.43	Standard addition mode of glucose quantification via cathodic amperometric.....	125
4.44	Reproducibility of three separate GOx/Nafion-modified Cu electrode at cathodic peroxide detection potential.....	127

LIST OF ABBREVIATIONS

A	Ampere
AA	Ascorbic acid (Vitamin C)
BA	Butylacrylate
C60	Carbon-60
CE	Counter electrode
cm	centimetre
CNTs	Carbon nanotubes
CR	Controlled release
Cu	Copper
CV	Cyclic voltammetry
DC	Direct current
DDT	Drug dissolution testing
DET	Direct electron transfer
DPV	Difference pulse voltammetry
E	Potential
EC	Electrochemistry
ER	Extended release
g	gram
GCE	Glassy carbon electrode
GMA	Glycidyl methacrylate

LIST OF ABBREVIATIONS (Continued)

GOx	Glucose oxidase
I	Current
IR	Immediate release
L	Liter
M	Molar
mg	Milligram
mL	Milliliter
mm	Millimetre
mM	Millimolar
MWCNTs	Multiwall carbon nanotubes
Ø	Diameter
PCT	Paracetamol
RE	Reference electrode
SR	Sustained release
SS	Styrene Sulfonate
SWV	Square wave voltammetry
USP	United States Pharmacopeia
V	Volt
WE	Working electrode
µA	Microampere
µg	Microgram
µM	Micromolar

CHAPTER I

INTRODUCTION

A well-known quest of laboratories in the pharmaceutical industry is effective drug valuation assays. Related to this Analytical Chemistry issue, the objective of this Ph.D. project was the development of a convenient automated electrochemical scheme for the detection of drug release profiles as part of common drug dissolution testing. Good knowledge about the time course of the discharge of drug from, for instance, pressed tablets or lipid bilayers-surrounded liposomes or gel formulation is important for optimization of medical treatments of patients. The speed of drug dissolution in the body is a major contributing factor for the rate of the increase in concentration of the pharmaceutical agent in the body fluid to a maximum level and also of the length of time the therapeutically suitable body drug concentration is maintained. When normal, immediate-release tablets are completely dissolved, the internal drug metabolism and kidney function usually lead to a rather fast and efficient clearance of the active agent from the body fluid and, if disease symptoms remain, a new tablet dose has to be ingested to continue the healing process. To stretch the time between individual dose takings and to optimize the maintenance of curative drug level, the pharmaceutical industry focuses on the development of so-called extended or controlled release drug capsules. These modern forms of tablets store larger amounts of the drug than immediate release tablet; however, the dissolution of the drug is carefully adjusted by the physical and/or chemical design of the core and shell of the pill in a way that an overdosing via swift release of the full content is certainly avoided and a constant

therapeutic set point is preserved through slow but steady release over an extended period of time. Obviously, the adaptation of an extended/controlled drug release system is a tricky multi-parameter task and depends, for instance, on the chemical nature of the drug of choice, on the type of the release location in the body and on the chemical and physical identity of the capsule core and shell. Research and development of the novel advanced drug systems thus requires intense trials, and repetitive dissolution testing is one of the important complementary duties in pharmaceutical research for creating the data that support an understanding of the release behaviour of particular novel developments. Application of the knowledge is the basis for guided further design cycles that ultimately end with a product that is suitable for use with patients.

A large set of analytical techniques is available for the qualitative and quantitative determination of drugs including the major optical (spectroscopic) and electrochemical methodologies. For redox-active drugs, voltammetry is among the favored choices for application in drug analysis because it can be realized at low cost with cheap and compact instrumentation. Automated execution of drug electroanalysis is in the field highly desired as it (1) reduces time and costs per sample screen, (2) releases laboratory staff from monotonous labor-intensive duties for other activities and (3) reduces the risk for human error due to the move from manual one-by-one electrochemical measurements to automated non-manual execution. The need for automation is of course particularly true when large sample numbers have to be analyzed, and best example for this situation are the drug dissolution testing trials that are used in the Pharmaindustry in the course of the development of normal, extended/controlled, and hydrogel release drug formulations.

In the context of the above, as target of the Ph.D. thesis defined was the adaptation of an existing robotic workstation for electrochemical analysis to the needs

of a highly sensitive pharmaceutical compound determination and the assessment of sample libraries from drug dissolution tests. Important issues to accomplish in course of the study included the optimization of the working electrodes for most sensitive voltammetric detection of the drug of choice, the generation of special software scripts for programmed electrochemical drug detection and the design of the best protocols for the drug dissolution tests, for the sampling at desired pharmacokinetic release profiles ([drug vs. time curves]).

A thematically different second part of this thesis handled the construction of an advanced version of a glucose oxidases biosensor. (Oxidase) biosensors have the enzyme firmly immobilized on the solid electrode surface and they produce an analytical signal that is based on the specific enzyme/substrate reaction within the protein-entrapping matrix. The reason for the popularity of (oxidase) biosensors is their marked selectivity for important body fluid contents, in particular blood sugar. Furthermore, detection is achievable with simple electrode transducers and technically undemanding constant-potential detection of, for instance, hydrogen peroxide (H_2O_2), which is an electroactive by-product of the oxidase-catalysed substrate conversion. Commonly used electrode platforms are bare or chemically modified disks of platinum, gold, glassy carbon or carbon pastes, with active disk diameters on the nano- to millimetre scale and most common H_2O_2 detection mode is anodic amperometry at suitably high positive detector polarization. Anodic H_2O_2 detection in body fluids such as blood or urine has, however, the risk of interference problems, as physiological levels of ascorbic and uric acid, dopamine and/or consumed drugs (paracetamol would be an example) are electrochemically oxidized at the sensor surface as well and thus may contribute with unwanted portions to the analytically relevant H_2O_2 currents. A move from anodic to cathodic H_2O_2 quantification is a strategy to circumvent the mentioned

adverse influence of interferences and a number of electrocatalytic sensor surface modifications have been proposed for a facilitation of H_2O_2 measurement at negative electrode potentials. Know was at thesis start that the surface of copper electrode has electrocatalytic affinity for H_2O_2 reduction, however, the valuable feature was not explored use to establish oxidase biosensors with cathodic interference-free H_2O_2 quantification. Work with copper electrodes as oxidase biosensing platform with cathodic amperometric readouts was accordingly defined as a second major objective of this thesis study.

1.1 Research objectives

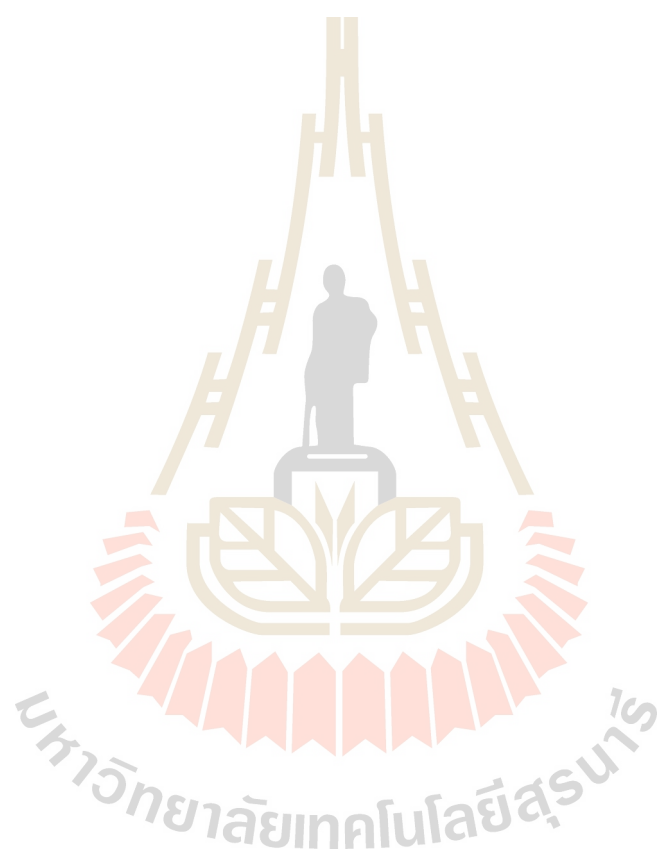
- (1) Adaptation of an existing robotic electrochemical device for reliable automated drug voltammetry in the 24-well microtiter plate format.
- (2) Tailoring the methodology of robotic microplate-based drug voltammetry that was established in (1) for the analysis of sample from pharmacokinetic drug release/dissolution testing. Tasks include optimization of the analytical performance for the detection of chosen drug targets, assessment of analytical figures of merits including sensitivity, linear range, reproducibility, detection limit, stability and recovery rate of the methodology. The widespread analgesics Paracetamol[®] was mainly worked with as easy and cheap to get model drug for most of the trials, though the system was also evaluated for use with other pharmaceuticals, e.g. doxorubicin, an expensive modern anticancer compound.
- (3) Application of the developed robotic voltammetry for prototype pharmacokinetic drug release profiling Proof of principle cases studies

were tackling two distinct paracetamol storage systems: (1) commercially available solid tablets formulations tailored for immediate or sustained (controlled) drug release-their inspection followed the standardized procedures of common pharmaceutical R&D with tablet dissolution and time sampling carried out in an initial step in a special dissolution container and released drug quantification in then aliquoted specimens performed independently later, and (2) research-level hydrogel and hydrogel/polymer composite drug storage matrices - release was here measured in-situ, with the drug gradually dissolving into the solution fillings of the microplate wells of the robotic electrochemical workstation. In either case the release profiles ([drug] vs. time curves) were constructed based on the collection of voltammetric raw data and then compared and interpreted in terms of time course of active compound liberation.

- (4) Establishment of cable-copper disk electrodes as cathodic transducer platform for glucose biosensing including proof of principle studies and sensor performance assessment.

In the following, an overview about the principles and background of drug development and drug dissolution testing, as conducted in the Pharmaindustry, will be provided. The need of analysis automation will be also be discussed, and the history, principles and advantages of 24-well microplate-based robotic electroanalysis presented, with special focus on some recent adaptations of the methodology for quantitative automated voltammetry. To prepare for the discussion of results of the second part of the Ph.D. thesis, actually copper electrode-based cathodic oxidase biosensor amperometry, the principles of (enzyme) biosensing will be introduced and

accompanied with a presentation of the already published options for a catalytically driven cathodic H_2O_2 detection at biosensor interfaces.



CHAPTER II

LITERATURE REVIEWS

2.1 State of the art of drug dissolution testing

Even when human health and well-being is well managed by appropriate diet and lifestyle, diseases cannot be avoided. In case of a disease appearance, drugs are useful therapeutic agents that, via interaction with cellular metabolic or other biological targets, support disease attack and body recovery to healthy status.

The drug development is significantly more expensive in terms of time and money than either lead discovery or drug design and many drugs will fall during the wayside. On average, for every 10000 structures synthesized during drug design, 500 will reach animal testing, 10 will reach phase of clinical trials and only 1 will reach the market place. Figure 2.1 shows overview the stage of a drug discovery in Pharmaceutical industry. The drug discovery as early steps of the target-based approach consist in target identification and validation of therapeutic targets. The drug design process occurs frequently, but not necessarily, by means of computational modeling approaches that are able to selectively interact with the identified target. Afterward, the development of a new drug requires were evaluated of non-clinical activity (efficacy) of a new drug candidate includes in vitro and in vivo assays that can be carried out throughout all stages of drug development. Finally, the new drug was required for therapeutic treatment and selling at drug store.

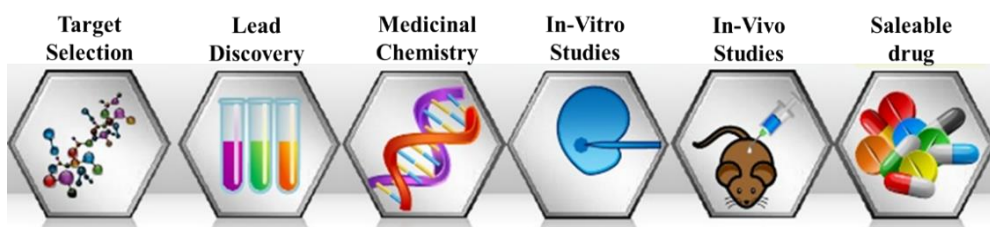


Figure 2.1 Steps in course of drug discovery and development. (Andrade *et al.*, 2016; Hughes *et al.*, 2011)

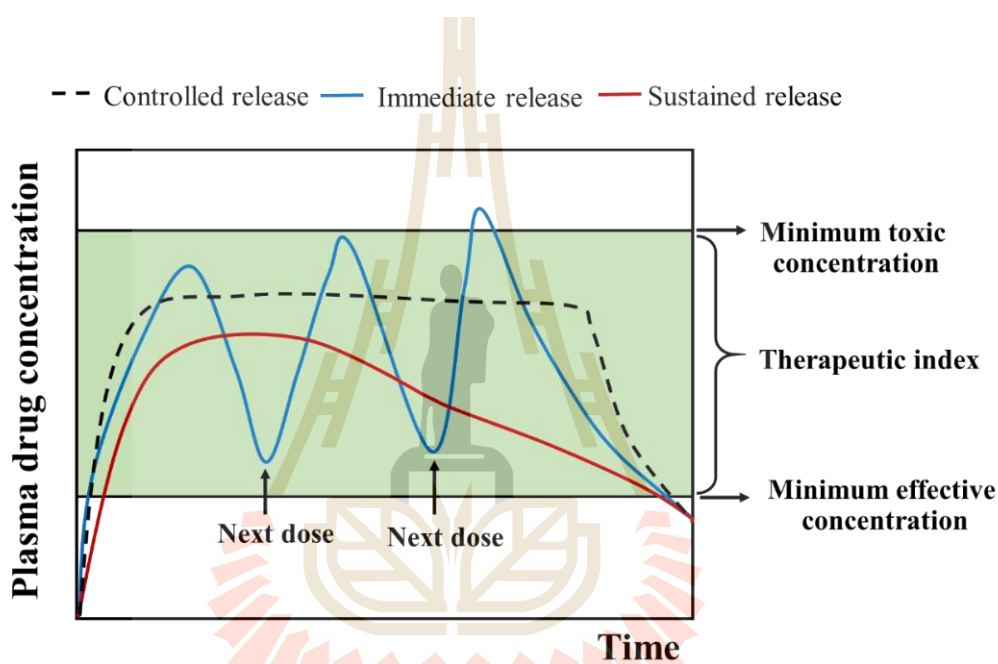


Figure 2.2 Time course of blood drug levels after uptake of immediate, controlled and sustained release tablets. (del Valle *et al.*, 2009; Siepmann *et al.*, 2011).

Most medicines are liquid or solid. Whether supplied as a liquid or solid, the drug uptake into the circulating blood system and the effective delivery to the target site of drug action is the most important issue to guarantee the success of the pharmaceutical treatment. After ingestion of a liquid or solid medicine the drug has to be dissolved, either already in the mouth/throat region, in the stomach or in the subsequent intestinal system. The blood drug level is accordingly increasing over time

before, as result of metabolic degradation and/or clearance via kidney function (filtration), the concentration in the blood decays gradually. Without further drug consumption body levels will reach zero after a time that depends on the type of drug and tablet structure. Then a new tablet uptake is needed to maintain the success of the healing process. The blue line in Figure 2.2 is a graphical display of the described time course of blood level of a drug in the body and informs about the various phase as well as about the requisite timed dose application for a patient. In Figure 2.2 the benefit of a sustained (red line) and controlled (black dash) drug release is demonstrated. As for the normal tablet it takes some time to reach maximum (effective) body level. In fact, a controlled release drug tablet is -by design- not emptied at that point in time and it is able to continue drug liberation. Therefore, the body level is maintained at constant level for an extended period of time because of the balance of metabolic drug destruction and continued provision via release. Accordingly, a tablet ingestion is, for instance, not needed as often as for the normal tablet option, which is for the patient consuming the advanced medicine more comfortable and a better treatment.

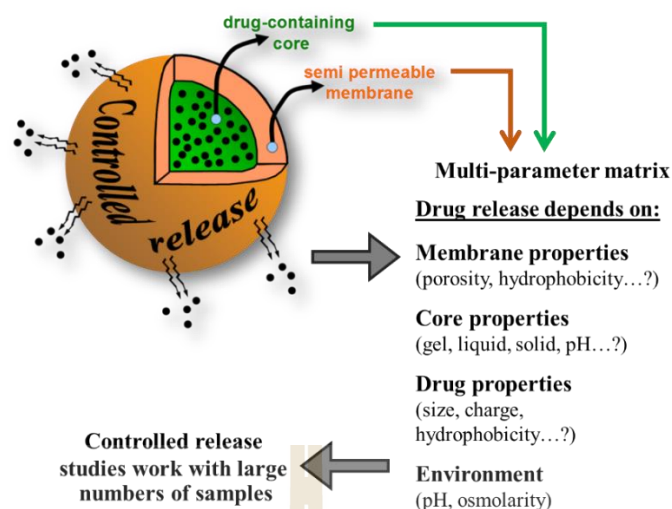


Figure 2.3 Controlled drug release out of macro-, and micrometric polymer capsules. Drug molecules in the core of the loaded containers diffuse through the membrane to get into the exterior, which in the body is the place where they should take their therapeutic action but in a release study may be the liquid medium of the drug suspension. The involved constituents are (1) the capsule core, (2) the capsule membrane, (3) the entrapped drug, and (4) the capsule environment. Their physicochemical properties have an impact on the efficiency of the molecular drug release and transmembrane trafficking. Analytical assessments of the multi-parameter process of drug release is thus associated with the need to work on large number of sample and high throughput assays are sought after to gain conveniently success.

As graphically illustrated in Figure 2.3, controlled release usually is established by membrane-bordered delivery systems such as capsules of macro-, micro- or nanometer dimensions, liposome or normal or reversed micelles. Detailed information on the general principals of the liberation of compartmented therapeutics is available in topical review (de Las Heras Alarcon *et al.*, 2005; Giannos *et al.*, 1995; Schroeder *et al.*, 2009), and books (Siepmann *et al.*, 2011; Wilson and Crowley, 2011) that cover the

subject. The development of advanced drug formulations demands a variety of analytical test trials that reveal an exact knowledge of the time course of the release of the pharmaceutically active compounds. One of the many strategies to study drug liberation from storage systems in vitro is drug tablet dissolution testing. Figure 2.4 shows the design of standardized in vitro dissolution testing as suggested in a publication by the United States Pharmacopeia (USP; <711> Dissolution) (Cohen *et al.*, 1990; Gray *et al.*, 2009). In well-defined manner a tablet is exposed in an optimized container to a dissolution medium while at distinct time points samples are taken for actual chemical inspection. Any analytical scheme that is sensitive to the drug of choice is suitable for quantitative visualization of the gradually increasing drug level in the dissolution medium. In the case the drug molecules under inspection are electroactive, e.g. they have redox center present in their chemical structure, they can be measured with the various schemes of voltammetry including cyclic and pulse voltammetry, amperometry and/or coulometry (see Figure 2.5).

Many drugs are well detectable through (stripping) voltammetry or other electroanalytical detection schemes because they possess in their structure electrochemically reducible or oxidizable chemical moieties and a number of review articles discussed in detail the role of modern voltammetric techniques as capable drug assay (Bobes *et al.*, 2001; Dogan *et al.*, 2009; Gupta *et al.*, 2011; Kauffmann *et al.*, 1996; Smyth and Woolfson, 1987; L. H. Wang, 2002). Classes of 'electroactive' drugs include analgesics, antibiotics, anticancer drugs, neuropharmaca and antidepressants, to name just a few. The conventional strategy of performing a voltammetry-based quantification of electroactive drug is based on manually operated electrochemical workstation and beaker-type electrochemical cells (refer to Figure 2.5); execution of all the individual steps of the analytical procedure (e.g. the electrochemical

conditioning/cleaning of the working electrode surface, subsequent accumulation of analyze species on top the working electrode and finally detection of accumulated analyze by means of e.g. differential pulse or square wave voltammetry) is performed by hand of the laboratory staff.

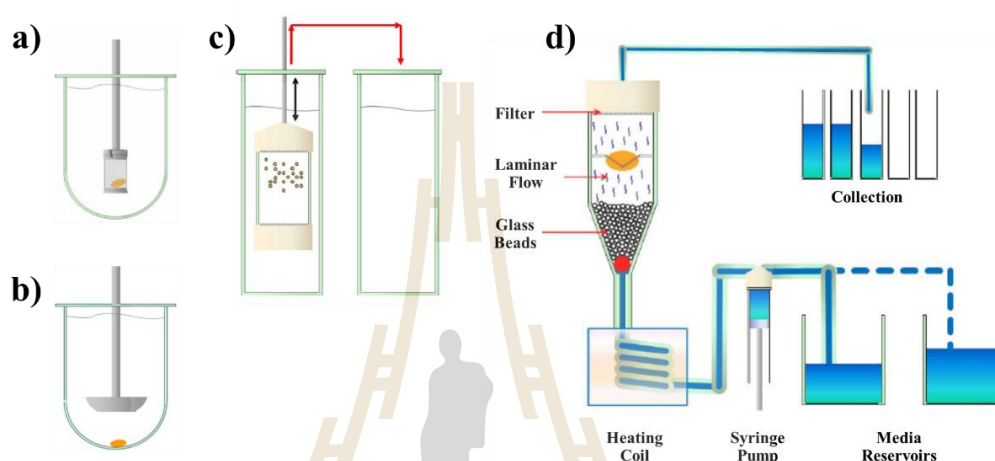


Figure 2.4 Schematic illustration of the apparatus for standardized in vitro drug dissolution testing. a) Basket (USP 1) and b) Paddle (USP 2) apparatus (Diebold, 2005), c) reciprocating cylinder apparatus (USP 3), and d) flow-through apparatus (USP 4) (USP 1 and 2: open-loop configuration; USP 3 and 4: closed-loop configuration) (Kostewicz *et al.*, 2014).

Manual drug voltammetry is acceptable with few samples but becomes tedious, time-consuming, and uncomfortable when dealing with larger sample collections. In addition, the likely appearance of manual operator errors in particular towards the end of a long working day may influence the accuracy and reproducibility of manual measurements more drastically, certainly under the pressure of increasing quantities of measurements. Robotic system will be a good alternative technique for overcoming the drawbacks of manual measurements in electroanalysis for drug detection and

quantification. One way to accomplish automation of drug electroanalysis to more or less extent is the integration of the related detection schemes into flow-based measuring systems that use computer-controlled flow of solutions. The flow-through electrochemical cell and tailored software were moduled to run the necessary procedures for the completion of data acquisition (Bobes *et al.*, 2001; Hanrahan *et al.*, 2004). An alternative way for the automation of electrochemical screening is the execution in a microtiter plate-based robotic system in which the plate wells act as small electrochemical cells. Well solutions are inspected electrochemically with a movable three-electrode assembly that is guided from well to well via a micropositioning device and used for assessments in the potentiostatic or galvanostatic mode. Such a robotic electrochemical system was first realized for high-throughput electrosynthesis and electroanalysis by Schuhmann, Speiser and co-worker (Erichsen *et al.*, 2005).

In this part, the aim was the adaptation of the existing setup for automated electrochemical measurements in 24-wells microtiter plates to the screening of profiling of drugs release. Paracetamol (PCT) were selected model sample drug which are commonly used as analgesics. In particular, for PCT tablets the dissolution testing performed using CNT as working electrode is a requisite. In addition, the natural and artificial polymers controlled the PCT drug release. Specifically, the robotic system was measured the profiling of drug release. The next section describes the state of the art of the instrumentation for robotic (automated) electrochemical measurements in sequentially addressable microtiter plates.

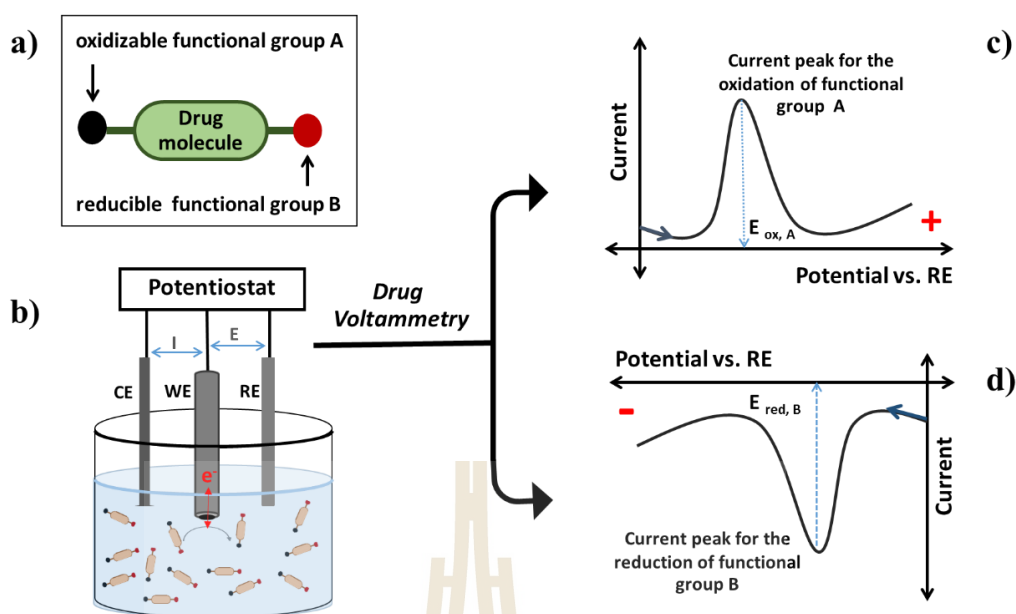


Figure 2.5 Identification of a drug molecule electro-activity for voltammetry. a) schematic of a drug molecule that has incorporated in its structure either an oxidizable (black circle, A) or reducible (red circle, B) functional group, or both, is shown. b) is shown a three-electrode electrochemical cell with a counter (CE), reference (RE) and working electrode (WE) in connection with a potentiostat. All electrodes are immersed into an electrolyte that contains dissolved drug molecules with group A and/or B and a supporting electrolyte. Such an arrangement represents the common beaker-type manual drug voltammetry. The current (electron flow) is recorded through a working electrode as a function of its potential with respect to the reference electrode. In the example the drug molecule oxidizes and, in an interfacial charge transfer reaction, hands over an electron to the electrode. Repetition of this electron exchange is the cause of current in the cell arrangement. To the upper as c) (lower as d)) are illustrated the voltammograms that would be recorded for an oxidizable (reducible) drug molecule during an anodic (cathodic) potential scan; a current peak is observed in the region around the apparent redox potential of the associated function group that causes electroactivity. The concentration-dependence of the peak current can be utilized for

the quantification of dissolved drugs, either by taking advantage of the calibration or by the standard addition method. Note: By international convention oxidizing (anodic) currents are plotted positive and reducing (cathodic) ones negative; negative potentials are on the x axes located to the left, while positive ones are to the right.

2.1.1 Automated electrochemistry

Electrochemistry is an alternative to separation, identification and quantification of chemical species to perform analytical detection and synthesis. In electrochemical procedures the electrons needed for redox reactions of a substrate are provided by an electric current supplied through electrodes. Within the family of electrochemical automation systems available for trace analysis are the automatic techniques of flow injection and microtiter plate. The principles of these individual schemes will be briefly explained in the following.

Electrochemical detection methods based on flow analysis system have been widely applied in various area, since its development (Furman and Walker, 1976). Some successful applications include: 1) determination of chloramphenicol in the standard chemical form, eye drops and milk sample on boron-doped diamond thin-film (BDD) electrode platform (Chuanuwatanakul *et al.*, 2008); 2) amperometric detection for morpholine determination in corrosion inhibitors (de Oliveira *et al.*, 2014); 3) simultaneous detection of adenine and guanine by differential pulse voltammetry (Thangaraj *et al.*, 2014); 4) determination of hydrogen peroxide (H_2O_2) by flow injection amperometric system (Reanpang *et al.*, 2015); and 5) monitoring of propofol in serum solutions (Rainey *et al.*, 2014). Figure 2.6 illustrates the schematic setup of a typical flow analysis electrochemical system.

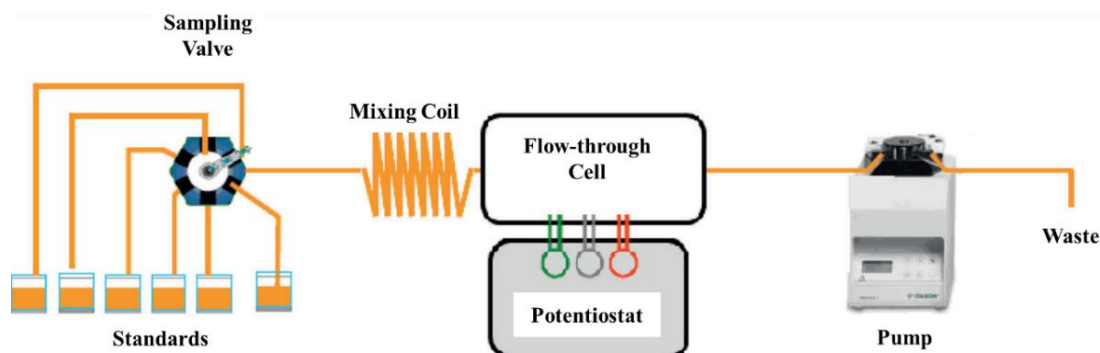


Figure 2.6 Simple schematic of flow-based electroanalysis of samples from drug release testing. (Rainey *et al.*, 2014).

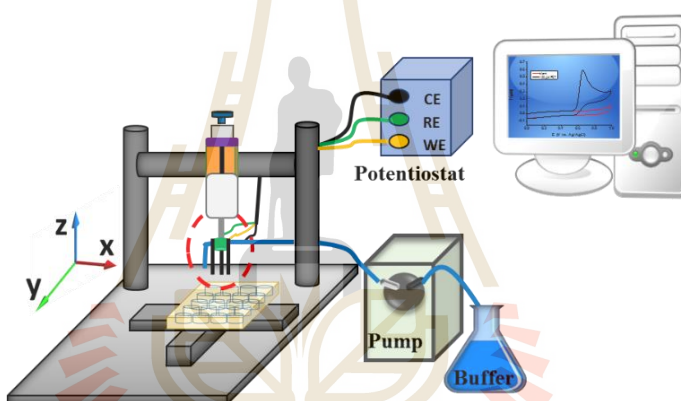


Figure 2.7 The device for automatic sequential electrochemistry in the wells of microtiter plate (Erichsen *et al.*, 2005). A computer-controlled EC workstation, an assembly of working, counter & reference electrode and an x, y, z micropositioning system are the central parts.

Elegantly, robotic electrochemical systems used were stepper motor-driven positioning stages in combination with flexible software to move specially designed electrode through the individual wells of the microtiter plates and to execute without operator intervention sequences of the requisite electrode actions for analytical measurements or electrosynthesis. In addition to the features allowing the automated

electrochemical measurements and/or synthesis, the system also incorporated tubes for solution dispensing and removal, a syringe pump establishing required microfluidics, and a special chamber design that allowed the supply of dry or wetted argon and thus the establishment of a controlled environment. A simplified schematic of the prototype workstation for automated (robotic) voltammetry is displayed in Figure 2.7. The electrode assemblies used for particular experiments are specifically designed to fit into the wells of the microtiter plate and their surface outfit adapted to the needs of the target analytical application. The automatic execution of sequences of measuring and positioning steps is used to address one well after the other and carry out in the well electrochemistry or electroanalysis.

Suitable electrode assemblies may, for example, incorporate as reference electrode a simple Ag/AgCl wire, a cylinder or disk-shaped metal or carbon macro- or microelectrode as the working electrode and a Pt wire spiral as the counter electrode. For the automation of voltammetric experiments in the individual plate wells, tailored software scripts have to be written that allow variation of the influential parameters of the motion of the electrode assembly and the measuring procedure as well as an easy data management. Additional features such as syringe pumps for solution delivery to the well, temperature control units for the well solutions, and a microtiter plate shaker may be added if needed. By one of the two inventing group, robotic electrochemistry in microtiter plates has been successfully used for an in-situ biosensor preparation and characterization (Diercks *et al.*, 2008; Erichsen *et al.*, 2005; Reiter *et al.*, 2004), nickel release measurements from corroding biomedical NiTi alloys (Ruhlig *et al.*, 2006) and the analysis of nitric oxide release from populations of endothelial cells that were fixed to the bottom of plate wells (Borgmann *et al.*, 2006). The other inventor focused more on application of the robotic electrochemical device for

microtiter plate-based electrocatalyst characterization (Reiter *et al.*, 2004) and electrosynthesis (Markle and Speiser, 2005; Markle *et al.*, 2005; Schwarz and Speiser, 2009). In recent work in our own laboratory the idea of microtiter plate electrochemistry robotic microtiter plate has been further developed towards qualitative and quantitative electroanalysis and the system has been made a convenient and sensitive automatic analytical assay for the measurement of ascorbic acid (Intarakamhang *et al.*, 2011) and total antioxidant (Intarakamhang and Schulte, 2012) capacities in fruit and plant extracts as well as pharmaceutical vitamin C tablets and herbal tea formulations, and heavy metals in waste and drinking water samples (Intarakamhang *et al.*, 2013). Robotic electrochemistry system for glucose estimation in model and real samples, utilizing enzyme modified pencil leads (PL) as effective electrochemical biosensors for robotic substrate quantification in 24-well microplates (Theanphonkrang and Schulte, 2017). Robotic electroanalysis of pharmaceutical formulations in microtiter plates was pioneered by S. Theanphonkrang and coworkers who used the technique for non-manual antibiotic measurements in dissolved tablet and spiked humans blood samples (Theanphonkrang *et al.*, 2015).

Until now, the electrochemical robotic approach in the microtiter plate format has not yet been applied for pharmaceutical, in particular not for the assessment of drug release proling. Application of robotic voltammetry in a microtiter plate to drug dissolution testing was thus made the first task of this thesis. In extension, the real-time monitoring of drug release from polymer carriers was defined as second target to be realized by the robotic electrochemical microtiter plate assay.

2.1.2 Robotic electrochemical for assessment of drug analysis

Electrochemical pharmaceutical analysis deals with a wide range of chemical compounds. Only requisite for the suitability of an electrochemical detection of pharmaceuticals is that the molecules are redox active through the presence of electroactive functional groups and phenol-, nitro-, quinone-, nitroso-, amine and thiol entities are just a few examples of the many existing electroreducible or oxidizable substituents. Meanwhile, an electrochemical evaluation of controlled drug release is not new but examples are still rare (Ensafi *et al.*, 2015; Fonseca *et al.*, 2015; Jara-Ulloa *et al.*, 2012; Mora *et al.*, 2009; Otarola *et al.*, 2016; Rodrigues *et al.*, 2016). Mora and coworker, (Mora *et al.*, 2009) for instance, demonstrated the use of manual voltammetric measurements, here in the square wave mode, for real-time monitoring of drug release kinetics from cancer drug-loaded liposomes. Otarola and coworker, (Otarola *et al.*, 2016) has been reported to determine the release profile of piroxicam, anon-steroidal anti-inflammatory drug, loaded in a drug delivery system based on nanostructured lipid carriers (NLCs). Base on the reported success case for the determination of the drug profiling release target analyte via non-robotic system. Aim of work was the implementation of drug electroanalysis into a workstation for robotic electrochemical measurements. To do this for the electroactive drugs would have been a study dirudissolution testing and for a proof of principle of the concept of robotic drug electroanalysis work was limited to a selection PCT.

Acetaminophen (N-acetyl-p-aminophenol or 4-acetamidophenol) also known as PCT is example of a drug that was target of electrochemical release studies. PCT is major ingredient in numerous cold and influenza medications and an agent in favor of the lowering of fever and the relief of pain associated with headache, toothache, backache, arthritis, migraine, neuralgia, muscular aches, menstrual cramps etc.

(Bessems and Vermeulen, 2001; Shiroma *et al.*, 2012). Generally, PCT does not exhibit any harmful side effects. However, abnormal level of PCT is believed to be associated with the formation of some liver and neurotoxic metabolites (Rowden *et al.*, 2006). The PCT has redox active functional groups and is thus an electroactive compound assessable by voltammetric detection (Figure 2.8). Worth mentioning is that the PCT electron transfer reaction in acidic solution irreversible; however, in neutral or alkaline solution reversibility may be gained.

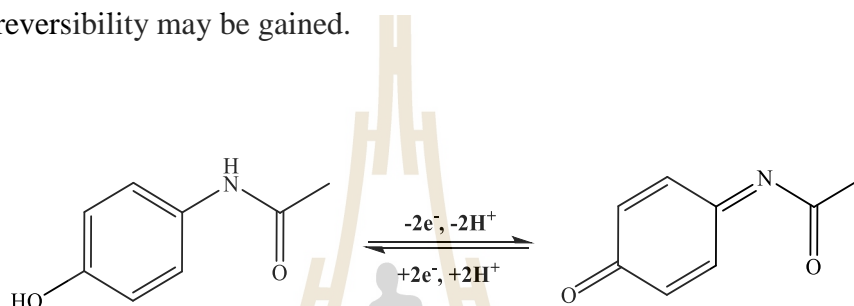


Figure 2.8 Chemical structure of paracetamol, PCT, and the reaction scheme for the redox reaction which may take place in interaction with an electrode via electron transfer across the solid-liquid interface (Fanjul-Bolado *et al.*, 2009).

Illustrative examples of electrochemical PCT determination with good performances work with porous pseudo-carbon paste electrode in differential pulse voltammetry mode (He *et al.*, 2009), with an implementation into a flow injection analysis and screen printed electrodes by carbon nanotube modification (Fanjul-Bolado *et al.*, 2009), and with square wave voltammetry at single wall carbon nanotube modified pyrolytic graphite electrodes (Kang *et al.*, 2010). Recently, nanoparticle modified electrodes have been proposed for the quantitative determination of PCT in pharmaceutical preparations including electrodeposited Au, Cu, Ru attachment of metal nanoparticles (Boopathi *et al.*, 2004; Ezhil Vilian *et al.*, 2014; Fanjul-Bolado *et al.*, 2009; Kutluay and Aslanoglu, 2014; Nair *et al.*, 2009) or C60 deposits (Brahman *et al.*,

2016) and already mentioned (Cheemalapati *et al.*, 2013; Fanjul-Bolado *et al.*, 2009; Hui *et al.*, 2014; Teng *et al.*, 2015) of electrodes, all offering high sensitivity with low detection limit. Hui *et al.* used organic–inorganic material (PNFCTs) were prepared with multi-walled carbon nanotubes (MWNTs) and a derivative of 3,4,9,10-perylenetetracarboxylic dianhydride (PTC-NH₂) via cross-linking. Then, PNFCTs were coated onto the surface of the glassy carbon electrode (GCE) and make a sensitive sensor for electrochemical PCT measurements (Hui *et al.*, 2014).

Based on the reported success case for the determination of the PCT target analytes. In thesis work, we have selected the electrochemical robotic device that provides a convenient electrochemical 24-well microtiter plate assay for automated the PCT drug dissolution testing characteristics of dosage forms in vitro models. The next subsection is dedicated to an introduction of PCT formulations and different type of profiling release will be described.

2.1.3 Drug dissolution testing of paracetamol tablet analysis

To improve the release behaviour of PCT tablet and make pain and fever treatment more convenient for patients in terms of dose repetition, there was a trend to move from normal quickly fully dissolving PCT formulations to options that offered a sustained release over an extended period of time. A typical “extended release” PCT tablet has the drug loaded both into an inner (core) and an outer (peripheral) zone (S. Yi *et al.*, 2011; S. J. Yi *et al.*, 2010). The core is designed to release the active compound slowly while the peripheral storage discharges PCT immediately on normal rate. An example of such an advanced PCT tablet is Tylenol[®], which has 650 mg of the acetaminophen equally distributed between the core and outer storage matrix. Upon ingestion, the 350 mg PCT in the outer zone are quickly released to raise the drug blood

level above the minimal effective level while the 350 mg in the core are then slowly supplied to the body to maintain therapeutic concentration over a longer stretch. Obeidat and coworkers (Obeidat *et al.*, 2010) demonstrated success with the use of spectrophotometric measurements for an assessment of the profile kinetics of PCT release from both, normal (immediate) and sustained release tablet variants. Figure 2.9 is a comparison of their drug release profiles and as expected the immediate release tablet emptied virtually 100% of its content in much shorter time than the special sustained release pills. Examples of manual electrochemical measurements of the time course of PCT release from the various tablets are the studies of Yang and coworkers (Morgan and Freed, 1981; Yang *et al.*, 2012). Electrochemical PCT determinations with a high quality of the corresponding voltammetric signal have been reported for carbon paste electrodes in differential pulse voltammetry mode (ShangGuan *et al.*, 2008), for glassy carbon electrodes (GCs) as cyclic voltammetry sensors (Daneshegar *et al.*, 2012; Tanuja *et al.*, 2017) and for differential pulse voltammetry (Keeley *et al.*, 2012). Apparently a carbon nanotube modification also tunes screen-printed carbon and noble metal electrodes well enough to gain a sensitive PCT voltammetry with low detection limit (Fanjul-Bolado *et al.*, 2009).

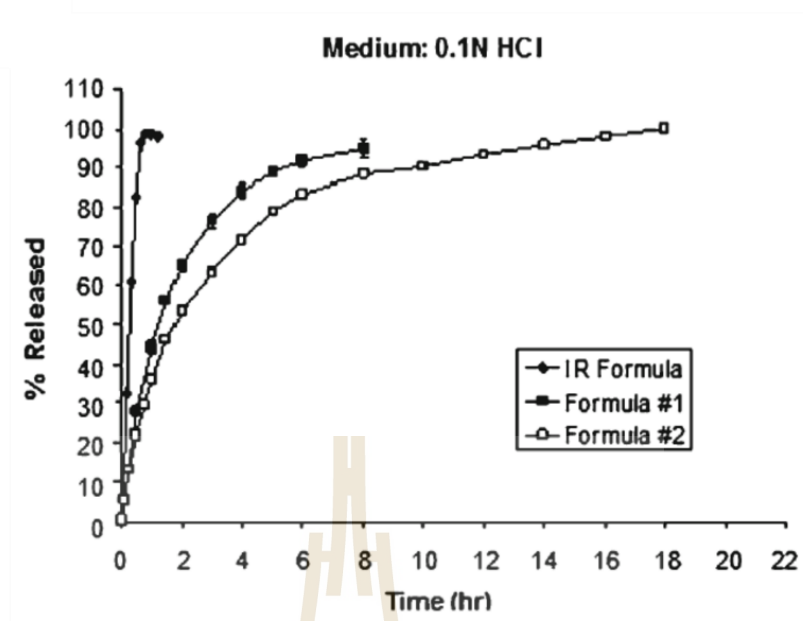


Figure 2.9 Drug release profiles of immediate release paracetamol formulation compared to the release profile from two sustained release formula in 0.1 N HCl pH 1.2 dissolution media (Obeidat *et al.*, 2010).

The success of manual PCT electroanalysis in revealing effectively the release kinetics of PCT drug tablets provided the motivation to approach with this part of thesis work a beneficial automation of the detection strategy, with carbon nanotube-modified working electrodes in charge as highly sensitive drug sensors and a microtiter plate-based robotic electrochemical device used for robotic trial execution on multiple samples in one plate run. The next subsection is dedicated to an introduction of natural and artificial polymers. It was covered the sample electroactive drug. The preparation of drug loading with polymer in microtiter plate-based robotic system will be described.

2.1.4 Drug release from polymer as a controlled drug delivery system

Polymers and copolymers have been widely used in extended release drug delivery systems. In fact, some polymers introduce the tunable properties for controlling drug release (Dai *et al.*, 2008; Kocak *et al.*, 2017). Moreover, such polymers respond to some environmental factors, such as changing in pH, light, temperature, solvent, ionic strength of the solution, electrical and magnetic fields, as well as introducing biomaterials and chemical agents (Kataoka *et al.*, 2012). Generally, the major obstacle to have a stable and capable drug delivering system is the uncontrolled condition during drug release. Therefore, the treatment of control drug release is still a great challenge in the pharmaceutical industry (Allen and Cullis, 2013; You *et al.*, 2016). Nowadays, many efforts have been made to obtain a more effective delivering system. Some researchers suggest that the combination system, which is created by combining two or more different responsive systems, is the most effective method to overcome these challenges (Gomez-Mascaraque *et al.*, 2014). With inspiration to the numerous design for polymers functional groups, a few polymers are being used extensively in controlled drug delivery. In this work, natural polymers such as agarose, chitosan, and artificial polymer for example, poly(Styrene Sulfonate-co-glycidyl Methacrylate-co-butylacrylate), P(SS-GMA-BA) are selected as the media for the controlled release of paracetamol. The characteristics of agarose, chitosan, and P(SS-GMA-BA) are described in the following paragraphs.

Agarose is a neutral polysaccharide extracted from the cell wall of certain Rhodophyceae algae, also known as agarophyte seaweeds. It consists of repeating units of alternating β -D-galactopyranosil and 3,6-anhydro- α -L-galactopyranosil groups (Millan *et al.*, 2002). Its chemical structure gives agarose the capacity to form very strong gels even at low concentrations. Gels of agarose provide a

moist environment and enhance the stability of the system when they are in combination with other polysaccharides. The easy-gelling ability and the thermoreversibility of the gel network have resulted in many applications of agarose in drug delivery systems. Both agarose alone and its blend with other polymers had been studied in these systems (Liu *et al.*, 2006; Niu *et al.*, 2017; Rossi *et al.*, 2015; Tunesi *et al.*, 2015; Zamora-Mora *et al.*, 2014).

Chitosan is a linear polysaccharide based on a binary co-polymer consisting of β -1,4 linked 2-acetamido-2-deoxy- β -D-glucopyranose (GlcNAc) units and 2-amino-2-deoxy- β -D-glucopyranose (GlcN) units whose proportions depend on the degree of acetylation of chitin (Khor and Lim, 2003). The chitosan polymer is insoluble in water but soluble under acidic conditions. Water-soluble chitosan is prepared by various deacetylation processes and it is susceptible to lysozymes, lipases and other enzymes. The products of chitosan degradation are non-toxic and chitosan has many useful properties. The chitosan is widely applied in wound healing, tissue engineering, drug delivery, and also for gene delivering in biomedical fields (Bhattarai *et al.*, 2010; S. J. Kim *et al.*, 2003) due to its biodegradability and biocompatibility. It can be easily processed into lots of formulations, such as hydrogels, microparticles, nanofibers, membranes, beads and scaffolds. Its application in hydrogel formulations for controlled drug delivery has been reported (S. J. Kim *et al.*, 2003; Park *et al.*, 2010; Puga *et al.*, 2013). Zamora-Mora (Zamora-Mora *et al.*, 2014) studied and developed composite chitosan/agarose gels, without chemical cross-linking, for applications in controlled drug delivery.

The P(SS-GMA-BA) was synthesized by mixing polymers including styrene sulfonate (sodium 4-vinylbenzenesulfonate, SS), glycidyl methacrylate (GMA), and butylacrylate (BA), via a free radical polymerization reaction with AIBN

as initiator. These composites have a combination of hydrogels' properties such as softness, high degree of hydration, high diffusivity of small molecules, electrical conductivity, pH sensitivity, crosslinking capability, water-solubility, and reversible redox properties. The SS has been applied in the development of drug delivery platforms such as lornoxicam drug encapsulation in layer-by-layer (LbL) polyelectrolyte self-assembled nanocapsules (Pandey *et al.*, 2015); doxorubicin loaded onto the poly(styrenesulfonate)-modified Ni-Ti layered double hydroxide film (Ge *et al.*, 2016); and dual-release mechanism of the KCl salt from the microspheres, which leads to the sustained release (Sui *et al.*, 2017). The GMA and BA have been used in drug delivery system by conjugating doxorubicin to the PEO-b-PGMA, poly(ethylene oxide)-b-poly(glycidyl methacrylate) micelles in a pH-responsive controlled release system (D. W. Kim *et al.*, 2017). Furthermore, the enoxacin and ethacridine lactate were loaded with semi-crystalline polymer networks from copolymerization of cooligoester-dimethacrylates and n-butyl acrylate for determining their capability as matrices for controlled drug release (Wischke *et al.*, 2010). The 5-Fluorouracil was encapsulated with poly(allylamine)-g-poly(t-butylacrylate) polymer nanocapsules and its capability of controlled drug release was evaluated (Sridaeng *et al.*, 2010).

Apparently, natural (agarose and chitosan) and artificial (P(SS-GMA-BA)) polymers work effectively in controlled release drug delivery system. Thus, in the context of this study, natural and artificial polymers were chosen as matrices to measure drug release under different conditions and hydrogel compositions/combinations in an electrochemical robotic system (combinatorial microelectrochemistry).

2.2 State of the art of electrochemical glucose biosensors based copper disk electrode

2.2.1 Electrochemical sensors

Enzyme-coupled electrochemical biosensors are based on the detection of an electric signal produced by an electro-active species, usually produced by an enzymatic reaction (Ronkainen *et al.*, 2010). The relatively simple layout consists of a bio-receptor layer of enzymes attached to a working electrode, which acts as a transducer (Figure 2.10). Measurable signal of amperometric enzyme biosensors based on oxidases have become widely used analytical tools over the past few decades, with applications in biotechnology, medicine and life sciences (Alkire *et al.*, 2011). The reason for the popularity of oxidase biosensors is their marked selectivity, achievable with simple electrode transducers and technically undemanding constant-potential detection of H_2O_2 , the by-product of the enzyme-catalysed reaction. However, amperometric enzyme biosensors have disadvantages when compared to electrochemical sensors, particularly when coupled to an enzymatic reaction. The essential challenge in developing these electrochemical biosensors has been overcoming the often inefficient electron transfer between the enzyme and the electrode surface (Marcus and Sutin, 1985). The major applications for electrochemical biosensors are in food and beverage quality control, security, environmental monitoring, bioprocessing, and most commonly in health care. For example, determination of glucose in blood continues to be the most dominant and most studied application of electrochemical biosensors and as such it is the most successful commercial application of enzyme-coupled biosensors (Ronkainen *et al.*, 2010). Furthermore, the assembly of functional amperometric oxidase based biosensors relies to a great extent on the application-oriented choice of electrode shape, size, material,

and the immobilization strategy. Commonly used electrode platforms are bare or chemically modified disks of platinum, gold, glassy carbon or carbon pastes, with active disk diameters on the nanometer to millimetre scale. For active redox protein immobilization, entrapment in thin films of natural or synthetic polymers and covalent oxidase bonding to functional groups on the electrode surface or to thin-film electrode surface modifications are feasible approaches. In addition, the amperometric (anodic) measurement of H_2O_2 at common working electrodes requires the application of a relatively high potential at which reducing species, such as ascorbic and uric acids and some drugs (e.g., acetaminophen), are also electroactive.

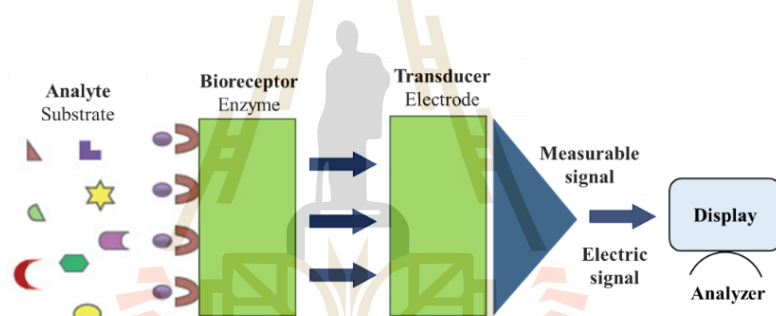


Figure 2.10 Schematic of the concept or design of biosensors (Putzbach and Ronkainen, 2013).

Part of thesis focuses on the use of the low-potential oxidase biosensor readouts. In addition, the methodology is employed on bare or chemically modified electrode platforms. First, a brief history of the evolution from first to third generation electrochemical biosensors is outlined, with glucose being used as an example of an analyte.

2.2.2 Evolution from 1st to 3rd generation biosensors

The first glucose biosensor was developed by Clark and Lyons of the Cincinnati Children's Hospital (Clark and Lyons, 1962). Their sensor used glucose oxidase (GOx) entrapped over an oxygen electrode by a semipermeable membrane to select for β -D-glucose in the presence of oxygen gas (O_2). The O_2 consumption as it reacted with protons and electrons to produce water was detected by the electrode as a change in potential.

In the 1st generation glucose biosensor, the trapped GOx would oxidize β -D-glucose to β -D-gluconolactone, with a simultaneous reduction of FAD to FADH₂ (Figure 2.11(A)) (Ronkainen *et al.*, 2010). Next, the FAD would be regenerated from FADH₂, using dissolved O_2 to produce H₂O₂. Finally, an applied voltage would induce oxidation of the H₂O₂ at the electrode surface, producing an electric signal.

The 2nd generation of biosensors addressed many of the 1st generation biosensor issues with the incorporation of a synthetic mediator as an electron shuttle molecule to replace dissolved O_2 in the production of H₂O₂ (J. Wang, 2008). Direct electron transfer is not possible without including some sort of mediators to facilitate the electron transfer because the FAD redox center of GOx is buried inside a thick protein layer, which slows the kinetic of the process (Zhu *et al.*, 2012). In the 2nd generation biosensor layout, the mediator_{ox} regenerates the FAD, with a simultaneous self-reduction (Figure 2.11(B)). Then the mediator_{red} is regenerated at the electrode surface, producing an electric signal. Ideal mediators react rapidly with the reduced enzyme, have low solubility in aqueous sample environment, are chemically stable in reduced and oxidized forms, are nontoxic, and have good electrochemical properties (i.e., low detection potential) (Zhu *et al.*, 2012).

The 3rd generation of biosensors involves wiring an enzyme to the electrode by co-immobilizing the enzyme and mediator directly onto the electrode surface or into an adjacent matrix such as a conductive polymer film (J. Wang, 2008). The immobilized mediators act as non-diffusion redox relay stations, effectively facilitating the transport of electrons from the enzyme active site to the electrode (Figure 2.11(C)). In some cases, direct electrical contact can be established between the enzyme and the electrode, thus greatly increasing the efficiency of the electron transfer. For these 3rd generation biosensors, immobilized mediators allow efficient electron transfer, resulting in a higher current density. Close proximity of the enzyme and the mediator to the transducer surface minimizes the electron transfer distance thereby resulting in faster response times. The applied electrode can operate at the desired voltage, eliminating background interference. This design also allows repeated and prolonged measurements because there are no reagents to replace. The evolution from 1st to 3rd generation reflects an effort to produce an efficient and selective transduction pathway. This pathway provides a rapid, amplified analyte signal and minimal background interference.

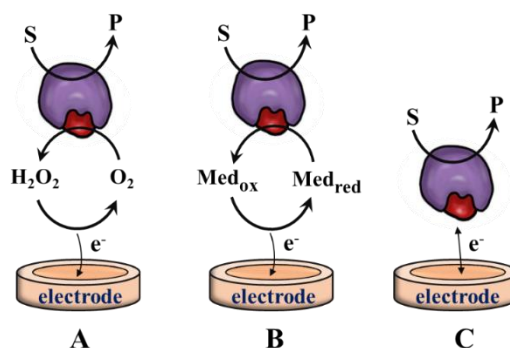


Figure 2.11 Three generations of amperometric enzyme electrodes for glucose based on the use of natural oxygen cofactor A), artificial redox mediators B), or direct electron transfer, C) between GOx and the electrode (J. Wang, 2008). The figure highlights modifications in the biosensor layout with each generation using glucose sensors as an example.

2.2.3 Electroactive interferences

The use of an unselective strong positive polarization for efficient H_2O_2 detection is a significant weakness of many oxidase-based biosensors, as it makes them susceptible to interference by electron transfer reactions involving redox active species other than the enzymically produced target. Unwanted contributions to the signalling current interfere sample quantification, particularly in complex samples containing only trace amounts of enzyme substrate. Body fluids, for instance, may contain detectable levels of anodically electroactive substances such as ascorbate and uric acid and, during medication, electro-oxidizable drugs such as PCT. Blood and urine electroanalysis with GOx based detectors in the routine anodic H_2O_2 detection mode is thus a good example of the need for protection against chemical interference with sensor signalling by other components of the sample. Detailed information on glucose biosensor signal interference and an introduction to the available strategies for elimination of such

interference are available in a recent review (Jia *et al.*, 2010). To summarize briefly, one option is to cover the immobilized enzyme with a coating that either is selectively permeable to the oxidase substrate but excludes interfering compounds (e.g. Nafion, with the advantage of charge repulsion), or incorporates oxidizing biocatalysts such as horseradish peroxidase (HRP) or ascorbic acid oxidase or other compounds (e.g. the metal oxides PbO_2 , MnO_2 , CeO_2) that remove interferents by oxidation before they reach the detector surface. Another approach is to reduce the detection potential of the electrode transducer to a value below that at which interference occurs. Tailored Prussian blue, metallized carbon and HRP sensor adaptations can, for instance, facilitate measurement of H_2O_2 by reduction, rather than oxidation, at a negative potential. It is also possible to use a synthetic redox mediator with a lower reduction potential, replacing the $\text{O}_2/\text{H}_2\text{O}_2$ couple as indicator of the enzymic reaction. The redox mediator, in its oxidized state, may be utilized as a dissolved species, like O_2 in aerated sample solutions, or integrated into the immobilization matrix as a functional part of a redox polymer.

Finally, the electrode potential of oxidase biosensors can also be reduced by exploiting direct electron transfer (DET) between the electrode platform and the immobilized enzyme, and measuring the (amperometric) current signal reacted to enzyme recycling, with a negative voltage stimulus close to the protein's formal potential, which is about -600 to -400 mV, depending on the experimental conditions (Baghayeri, 2015; Hu *et al.*, 2015; Palanisamy *et al.*, 2015; Terse-Thakoor *et al.*, 2015). The reported solutions for low-potential oxidase biosensor readouts often involve costly catalytically active micro- or nanomaterials and/or complex immobilization layer designs, so the methodology is still a subject of intense research activities in these field(s). However, copper and Cu-modified electrodes have not yet been explored as

low-potential signal transducers in oxidasebased biosensors. Their use as detectors in sugar chromatography is well established (Colon *et al.*, 1993; Kano *et al.*, 1996; Torto, 2009; Voegel and Baldwin, 1997), and they have also been used in the electroanalysis of amino acids and peptides (Ye and Baldwin, 1994), purines (Lin *et al.*, 1997), phenols (Kawde and Aziz, 2014), alcohols (Paixao and Bertotti, 2004) and heavy metal ions (Jovanovski *et al.*, 2015; Pei *et al.*, 2014). The motivation for the present work was a report of the successful use of Cu electrodes for cathodic amperometry of H₂O₂, which has not yet been exploited in oxidase biosensors (Somasundrum *et al.*, 1996). H₂O₂ has also been detected with noble metal or carbon sensors that had been chemically modified with copper micro- and nanomaterials (Deng *et al.*, 2015; Mani *et al.*, 2015; Selvaraju and Ramaraj, 2009).

Aims of this work first demonstrated that disk electrodes made of ordinary Cu wire, with no special micro- or nanoscopic surface modification, were capable of measuring H₂O₂ at low cathodic potentials. In a further exploration of this property, Cu disk electrodes were coated with a thin film of Nafion containing GOx. The film can convert cathodic H₂O₂ Cu sensors into sensitive biosensors for glucose with resistance to interference by other oxidizable substances.

CHAPTER III

RESEARCH METHODOLOGY

3.1 Experimental and methods

3.1.1 Materials and chemicals

Chemical	Supplier
Single-wall carbon nanotubes P3-SWNT	Carbon solution, Inc .California, USA.
Potassium chloride, anhydrous KCl	Carlo Erba ReagentiSpA, Rodano, Italy.
Monobasic potassium phosphate, KH_2PO_4	Carlo Erba ReagentiSpA, Rodano, Italy.
Hydrochloric acid, HCl	Carlo Erba ReagentiSpA, Rodano, Italy.
Nitric acid, HNO_3	Carlo Erba ReagentiSpA, Rodano, Italy.
Sodium hydroxide, NaOH	Carlo Erba ReagentiSpA, Rodano, Italy.
Sodium chloride, NaCl	Carlo Erba ReagentiSpA, Rodano, Italy.
Hydrogen peroxide, H_2O_2	Carlo Erba ReagentiSpA, Rodano, Italy.
Sodium phosphate dibasic anhydrous, Na_2HPO_4	Carlo Erba ReagentiSpA, Rodano, Italy.
Sodium phosphate monobasic monohydrate, $\text{NaH}_2\text{PO}_4 \cdot \text{H}_2\text{O}$	Carlo Erba ReagentiSpA, Rodano, Italy.
Sulphuric acid, H_2SO_4	Carlo Erba ReagentiSpA, Rodano, Italy.
Sodium 4-vinylbenzenesulfonate, $\text{C}_8\text{H}_7\text{NaO}_3\text{S}$	Sigma Aldrich, Kansas, USA.

3.1.1 Materials and chemicals (Continued)

Chemical	Supplier
butyl acrylate, C ₇ H ₁₂ O ₂	Sigma Aldrich, Kansas, USA.
Nafion [®] perfluorinated resin solution	Sigma Aldrich, Kansas, USA.
Agarose, C ₂₄ H ₃₈ O ₁₉	Sigma Aldrich, Kansas, USA.
Chitosan, C ₅₆ H ₁₀₃ N ₉ O ₃₉	Norgen Biotek Corp, Cannada
Glucose Oxidase, GOx (from <i>Aspergillus niger</i> type X-S, 136300 units/g)	Sigma Aldrich, Kansas, USA.
D-(+)Glucose, C ₆ H ₁₂ O ₆	Sigma Aldrich, Kansas, USA.
Ascorbic acid, C ₆ H ₈ O ₆ (vitamin C, AA)	Acros organics, New Jersey, USA.
Doxorubicin hydrochloride, C ₂₇ H ₂₉ NO ₁₁ ·HCl	Sigma Aldrich, Kansas, USA.
4-Acetamidophenol, 98%, C ₈ H ₉ NO ₂	Sigma Aldrich, Kansas, USA.
Paracetamol [®] (650 mg), C ₈ H ₉ NO ₂	Acros organics, New Jersey, USA.
Paracetamol [®] (325 mg), C ₈ H ₉ NO ₂	Janssen Korea Ltd., Korea.
Glassy carbon electrodes, GCEs	Edaq Pty Ltd, East NSW Australia.
Silver wire	Goodfellow, Huntingdon, UK.
Platinum wire	Goodfellow, Huntingdon, UK.
Cu disk electrode	Phelps Dodge Int. Corporation.
Ag/AgCl/saturated KCl	ALS Co., Ltd., Tokyo, Japan.

3.1.2 Instruments

- A function generator (Agilent[®] 3322A 20 MHz function/arbitrary wave form generator); for the electrophoretic deposition of carbon nanotubes on glassy carbon electrodes (GCEs) surface via constant DC voltage application to a 2-electrode cell.
- An electrochemical workstation from Gamry Instruments (potentiostat Model Reference 600[®], Gamry Instruments, Warminster, PA USA) was used for amperometric testing and calibration of Cu-based glucose biosensors.
- A robotic electrochemical workstation for automated voltammetry and amperometry in the vials of 24-well microtiter plates (Intarakamhang *et al.*, 2011). The system used an electrochemical potentiostat from PalmSens Instruments (Palm Instruments BV, Amsterdam, Netherland) for voltammetric experiments, sensor characterization, calibration measurements and electrochemical drug release profiling (as mentioned in section 3.3). Two variants of the robotic workstations were used throughout the laboratory work of the PhD study. The system employed in Thailand in the Biochemistry-Electrochemistry Research Unit was a more basic one without any automated well solution delivery and served for automated analysis of samples from drug tablet dissolution testing and first hydrogel release profile assessment. The equivalent system used during the RGJ-sponsored stay in the Schuhmann laboratory in Bochum had a syringe pump (Hamilton, Bonaduz, Switzerland) incorporated as additional device in favor of non-manual microplate well solution filling.
- A Denver balance TC 205, Denver Instruments, Colorado, USA.
- A common hot air laboratory oven, UNB, Memmert, Frankfurt, Germany.

3.2 Research methodology

3.2.1 Counter electrode (CE)

A Pt wire (5 cm in length, 0.50 mm \varnothing , GoodFellow, Cambridge Science Park, England) was coiled to a spiral at the bottom and soldered to a copper cable wire. Subsequently, the Pt and cable connection was sealed into a heat shrinking tube.

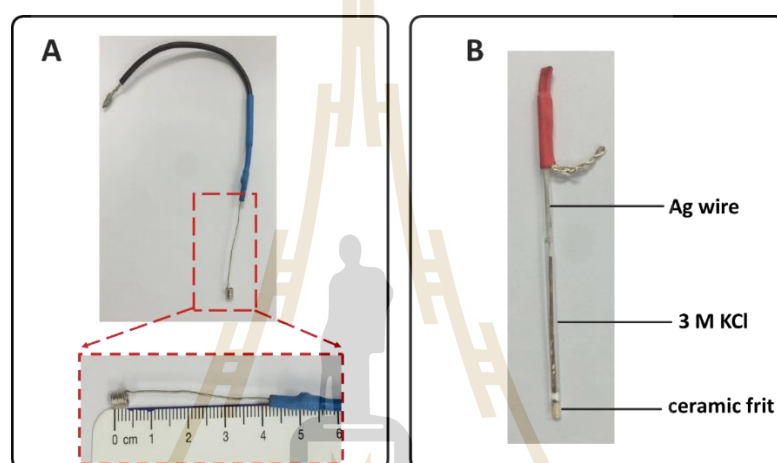


Figure 3.1 The photograph of a miniaturized A) Pt wire counter electrode, B) Ag/AgCl reference electrode.

3.2.2 Reference electrode (RE)

A homemade miniaturized pseudo Ag/AgCl reference is used as electrode. It is made by cleaning a silver wire with fine grade emery paper and subsequent rinsing with distilled water. Then, the 4 cm long part at the end of the wire to be AgCl coated is placed into a mixture of 0.1 M HCl and 3 M KCl. A potential of 10 volts is applied for about 10 minutes, using a platinum wire as a cathode. During the electrolysis a grey AgCl deposit is formed on the silver wire surface.

3.2.3 Working electrode (WE)

3.2.3.1 Bare glassy carbon electrodes

Commercial working electrodes disks are shard glassy carbon electrodes (GCEs 1 mm diameter) from Edaq Pty Ltd, East NSW Australia. At the beginning of the measurement, the bare GCE needs to be pretreated as follows:

- (1) polishing with 0.3 μm alpha alumina powder on polishing cloth.
- (2) sonication in DI water.
- (3) rinsing thoroughly with DI water.
- (4) pretreatment before further use by exposure to 50 cyclic potential ramps in 0.5 M H_2SO_4 at a scan rate of 0.1 Vs^{-1} from 0 to +1 V vs Ag/AgCl.

After that, GCE were rinsed with DI water at room temperature.

3.2.3.2 Preparation of CNT-modified glassy carbon electrodes

The electrodeposition of CNT on the GCE was described in detail by Boccaccini and coworker (Boccaccini *et al.*, 2006) and, for instance, in a recent article entitled 'Robotic voltammetry with carbon nanotube-based sensors: a superb blend for convenient high-quality antimicrobial trace analysis' (Theanponkrang *et al.*, 2015). Usually the procedure is carried out in a two-electrode electrochemical cell to attract carboxylated and negatively charged CNT filaments to the cathode. These filaments were than fixed on the cathode surface via van der Waals attraction. The steps for the preparation of CNT modified GCE are shown in Figure 3.2. At the beginning of the processes, the GCE needs to be pretreated as mentioned in section 3.2.3.1. The electrolyte for the electrochemical deposition of CNTs on the surface of the bare GCE was a of 20 mg/ml suspension of CNT in DI water. Deposits of CNTs on the GCE electrode surface were achieved by applying a positive DC voltage of 1 V for 10 minutes to the precursor electrode. The positive voltage initiates the anodic

electrophoretic attraction of the negatively charged carboxylated CNTs, which via van der Waals forces are kept finally in place at the carbon surface. Freshly CNT-modified GCE were dried after the deposition procedure at room temperature then rinsed with DI water. A thorough characterization of the working electrodes-modified CNTs was reported by Theanponkrang (Theanponkrang *et al.*, 2015) using a combination of voltammetry, impedance spectroscopy and electron microscopy.

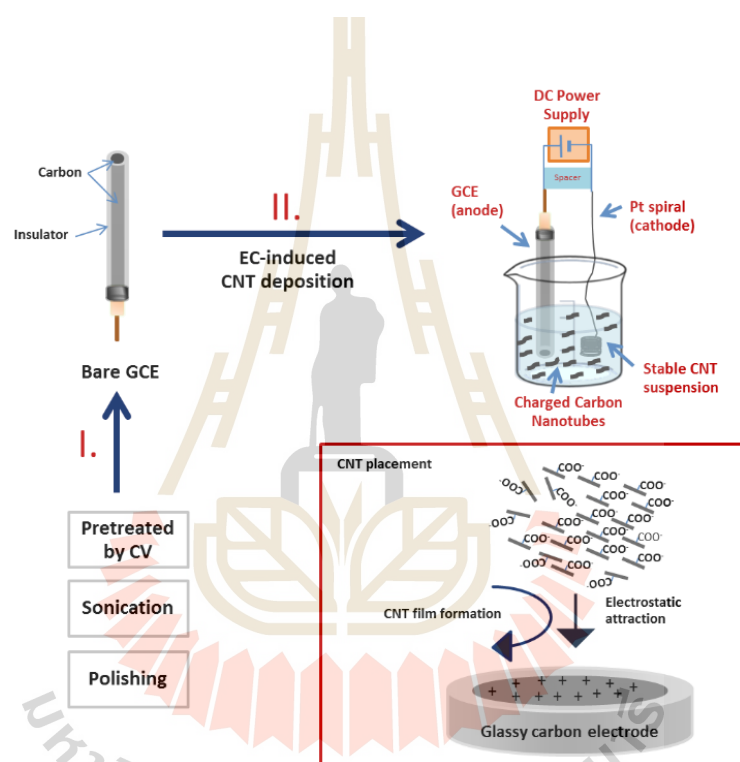


Figure 3.2 Schematic diagram of the procedure used for the preparation of CNT-modified GCE used in this study for drug measurements in the robotic electrochemical workstation.

3.2.3.3 Cu electrode and GOx immobilization

The starting material for Cu disk electrode manufacture was poly(vinyl chloride)-insulated electrical cable with a metal core of circular cross-section (Phelps Dodge Int. Corp., PD-THW 750 V PVC 708 TIS 11-2531). The plastic

insulation was stripped an approximately 5 cm length of cable and the bare Cu wire, of about 2 mm diameter, was then sealed with a two-component insulating epoxy resin (2-Ton Epox-Fix from Alteco Chemical Pte. Ltd., Singapore) into a glass tube of slightly larger inner diameter. Part of the Cu wire sticks at the top of the assembly in order to be used as electrical connection to the electrochemical amplifier, while at the bottom the glass rim and wire disk face were roughly aligned. After curing the epoxy resin overnight at room temperature, abrasion with rough emery paper was used to expose the embedded Cu disk. The disk and its surrounding glass/epoxy rim were then finely polished to a mirror-like appearance by continuous circular movements on increasingly fine emery paper. The same treatment was subsequently performed on a soft polishing pad soaked with alumina suspensions of 1-2 μm and then 0.4 μm particle diameter. The outcome at this stage was a glass/polymer-embedded Cu disk electrode of approximately 2 mm diameter (as shown in Figure 3.3) that could be used either for H_2O_2 amperometry or as the precursor in glucose biosensor construction.

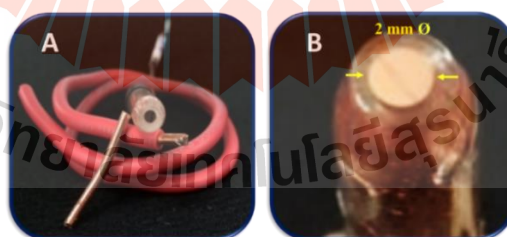


Figure 3.3 Digital photographs of A) the electrical cable used as the precursor for Cu electrode fabrication B) a completed Cu disk electrode.

To demonstrate the suitability of bare Cu electrodes as cathodic platforms in oxidase-based biosensors they were modified with a surface deposit of polymeric Nafion blended with the enzyme GOx. Figure 3.4 shows the precursor

preparation of the electrodes. The Cu electrode of the active layer was constructed by simple drop-and-dry application of a mixture of equal volumes of 20 mg/mL GOx stock solution and commercial 10% aqueous Nafion dispersion. 10 mL of this mixture were dropped onto the disk surface and complete solvent evaporation was allowed to take place. Dried electrodes with the enzyme/Nafion top coat were carefully rinsed with distilled water and then their glucose response was checked by amperometric calibration measurements.

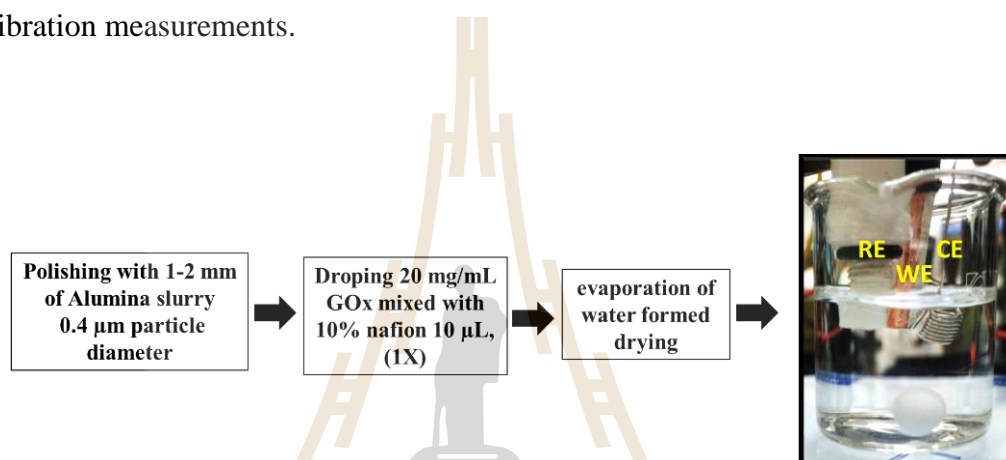


Figure 3.4 Digital photographs of modification of cable Cu disk electrodes via coating with a GOx-immobilizing Nafion thin film and the electrochemical cells set up.

3.3 Robotic electrochemical workstation

The hardware and software for the robotic electrochemical device were purchased from Sensolytics GmbH, Bochum, Germany. The two computer-controlled linear measuring stages are responsible for precise horizontal (x/y) movements of a standard 24-well microtiter plate. A third linear measuring stage of the same type controls the vertical (z) positioning of an assembly of the working electrode, counter electrode, and reference electrode. All electrochemical experiments were carried out through the operation of a three-electrode electrochemical sensor assembly small enough to be immersed into the microtiter plate well without damage. The computer,

in combination with custom made Sensolytics software, controlled the automatically performed positioning electrochemical procedures and was it used for data acquisition and analysis. Figure 3.5 represents the robotic electrochemical system in a photo. The three-electrode assembly with a working, counter, reference electrode incorporated in special holders is shown in close up view.

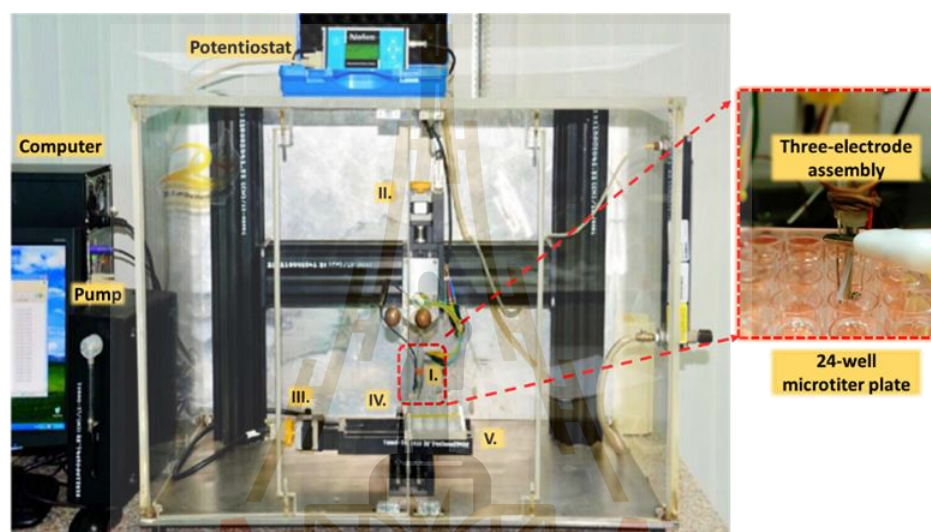


Figure 3.5 Photo of the robotic electrochemical system: I) electrode holder with working, counter, and reference electrode; II) z-positioning for vertical movement; III) and IV) x-, and y-positioning for container movement; V) 24-well microtiter plate base. Close up view of three-electrodes fixed to the holders and moved in a container of the 24-well microtiter plate (Erichsen *et al.*, 2005).

3.4 Robotic voltammetry for drug tablet dissolution testing with CNT modified glassy carbon electrode

For voltammetric measurements in the robotic device, a three-electrode assembly composed by working, counter, and reference electrode incorporated in a solid plastic holder was used. Disk glassy carbon electrodes (GCEs 1 mm diameter)

modified with CNTs were used as WEs. The Pseudo-RE was an Ag/AgCl wire and the CE was a Pt spiral. The microtiter plate of the analyzed sample used was the employed 24-well. All measurements were performed at room temperature using aerated 0.1 M $K_2SO_4-H_2SO_4$ mixed with 0.1 M KCl solutions as supporting electrolyte. The PCT commercial tablet drugs were selected model sample dissolution testing.

3.4.1 Differential pulse voltammetry of PCT

Differential pulse voltammetry (DPV) is an extremely useful technique for measuring trace levels of organic and inorganic compound species. A fixed magnitude pulse, superimposed on a linear potential ramp, is applied to the working electrode. The current is sampled twice, just before the pulse application and again later in the pulse life. Then the first current is subtracted from the second and this computed current difference is plotted against the applied potential. The resulting differential pulse voltammogram consists of current peaks, the height of which are directly proportional to the concentration of corresponding analytes. The peak potential is a characteristic feature of the related compound. Moreover, the DPV is more sensitive technique than CV techniques. Accordingly, the DPV was selected for analysis and the peak currents were used for the construction for calibration curve. This calibration curve was then used for the monitoring of drug released profile.

From the cyclic voltammetry study, an oxidation peak occurred at 600 mV vs. Ag/AgCl. The DPV measurements were conducted with the CNT-modified glassy carbon electrode. The parameter of DPV used potential scan from 0.3 to 0.9 V, potential step 5 mV, potential pulse and time pulse 25 mV, and 0.07 s, respectively.

3.4.2 Calibration curve for drug via robotic DPV in 24-well plate

The parameters used for the calibration trial were mentioned above. The load of a microtiter plate with model drug solution of concentration ranging from 0-1800 μM is illustrated in Figure C1 (Appendix C1). The script for the employed robotic DPV is provided in the Appendix C2.

3.4.3 Reproducibility for drug quantification via robotic electrochemical measurements

These experiments test two concentration of model drug solutions: 10 and 80 μM PCT. In the wells sample testing were all spiked with 10 μM PCT or 80 μM PCT. The experimental conditions and the robotic script commands are listed in Appendix C3.

3.4.4 Robotic DPV for drug profiling measurements in drug tablets

Robotic DPV was used to carry out PCT measurements in the commercial drugs tablets as difference formulations including immediate release and extended release tablets. The PCT immediate release and extended release tablets are 325 mg/tablets and 650 mg/tablets, respectively. However, the collected drug dissolution testing from home-made basket method was treated with a USP Dissolution Apparatus.

3.4.4.1 In vitro drug dissolution testing with the basket method

The strategy of vitro drug dissolution testing via the basket method is shown in Figure 3.6. The dissolution set up is including the beaker for the dissolution medium, a tea ball strainer used to keep the drug tablet in place in the dissolution medium, and a magnetic bar. The dissolution medium is 0.1 M H_2SO_4 -

K_2SO_4 solution with a pH of 1.02, which is about the acidity of stomach fluid in which the tablet usually is degraded in course of treatment. 300 mL of the dissolution medium was used as volume for the dissolution test. 20 samples were collected during a tablet dissolution test at time period of 9 hours. In triplicate analysis trial thus 60 samples, however to be dealt with, either in conventional manual or in robotic (automated) manner. The stirring speed is variable but at normally trials 100 rpm was recommended for standard dissolution testing by the United States Pharmacopeia (UPS) (Levy and Nelson, 1961). 15 μ L samples were taken at the beginning the tablet commercial releasing ($t=0$) and then at time points, as for instance shown in Figure 3.7.

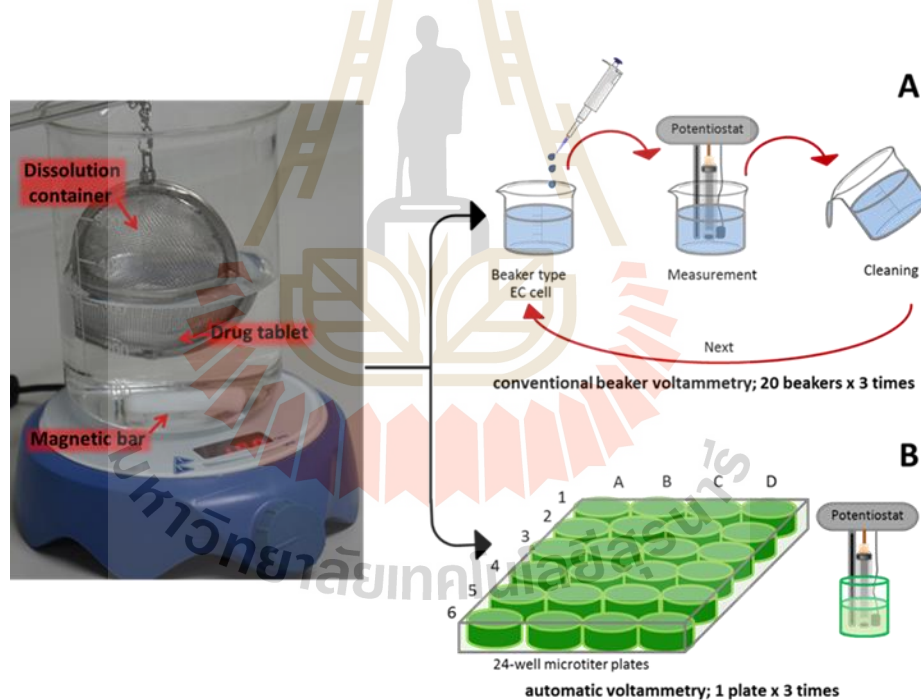


Figure 3.6 Drug dissolution testing via standardized “basket” method as suggested and standardized by the United States Pharmacopeia (USP). Manual sample analysis A), robotic sample analysis B).

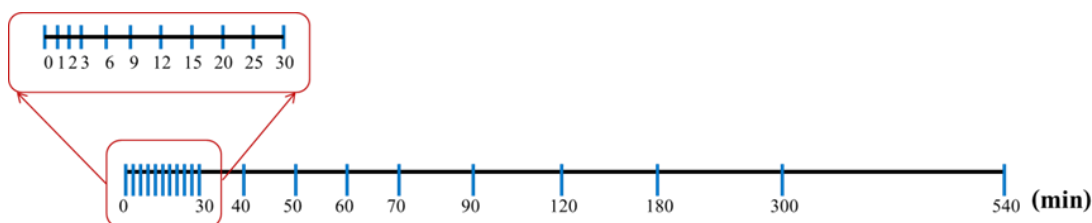


Figure 3.7 Display of the schedule for sample collection within a PCT tablet dissolution test.

3.4.4.2 Dissolution testing of PCT drugs used DPV via robotic measurements in calibration curve mode

The calibration curve method was chosen for the quantification of paracetamol releases in the 24-well microtiter plate. In a 24 well microtiter plate a set of 19 samples were placed in the well except for in the #1 well of the A, B, C, and D columns, and in the #2 well of the A, water and blank solution, respectively. The script for the employed robotic DPV is provided in the Appendix C4.

3.5 Robotic microtiter plate based drug voltammetry and controlled released from hydrogel drug formulations

This part of the thesis was carried out under the guidance of Prof. Dr. Wolfgang Schuhmann in Analytische Chemie Electroanalytik & Sensorik, Department of Chemistry and Biochemistry, Ruhr-University Bochum, Bochum, Germany. The three electrodes in electrochemical cells are WE, the disk bare glassy carbon electrodes. The RE was used an Ag/AgCl wire and the CE was a Pt spiral. All measurements were performed at room temperature using aerated 0.1 M K_2SO_4 - H_2SO_4 mixed with 0.1 M KCl solutions as supporting electrolyte. PCT drug were selected model sample of controlled release from hydrogel drug formulations.

3.5.1 Square wave voltammetry of PCT

Square wave voltammetry (SWV) is a large-amplitude differential technique in which a waveform composed of a symmetric square wave, superimposed on a base staircase potential, is applied to the working electrode. The current is sampled twice during each square-wave cycle, once at the end of the forward pulse and once at the end of the reverse pulse.

The SWV measurements were conducted with a step potential: 7 mV, potential amplitude: 25 mV, frequency: 100 Hz. The experimental conditions and the robotic script commands are listed in Appendix D1 and D2.

3.5.2 Stability of the working electrode

Six-hour long measurements in 200 μM PCT analyte were performed in the SWV mode in a well of a microtiter plate. These solutions were analyzed and stored every 5 minutes. The resulting traces were compared for judgments on the stability of electrode and analyte. Then the calibration curve was plotted using short linearity range from 5 μM to 600 μM PCT standard solutions. This calibration curve was used to calculate the concentration of analyte, and to check the stability of the working electrode. The microtiter plate loading used for PCT quantification in calibration mode of robotic measurement using, the 24-well microplate formatting stability test with the PCT concentration of 200 μM is shown in Figure 3.8.

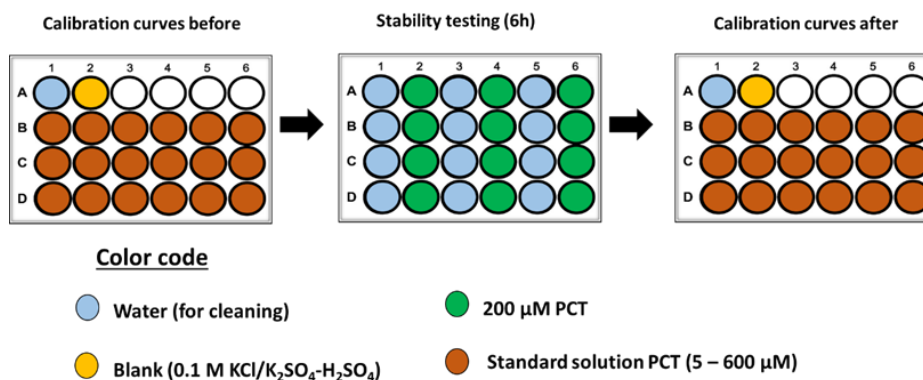


Figure 3.8 The microplate layout for response stability tests with a 200 μM PCT sample.

3.5.3 Robotic SWV for drug release from agarose natural hydrogels

The concentration of drug released was measured via SWV using the robotic monitoring system. The PCT release from the agarose hydrogel was evaluated at room temperature at pH conditions of 1.2 and 8.0.

3.5.3.1 PCT drug loading with agarose hydrogel in microtiter plate

The agarose hydrogel was prepared dissolving 2 g of agarose in 100 ml of DI water and heating the mixture to 70 °C until the agarose was completely dissolved. The agarose solution was then cooled down and maintained at room temperature. The PCT drug solution was prepared by dissolving it in DI water, with concentration of 1 mM, 2 mM, 4 mM, and 8 mM. The hydrogel drug loading in microtiter plate was prepared by mixing 150 μL of 2% (w/v) agarose solution with 150 μL of PCT stock solutions in order to change the drug concentrations while keeping the concentration of agarose hydrogel constant (i.e. 1% agarose drug loading in bottled of well equal 300 μL). After the addition, the solution was maintained at room temperature for 1 hour for the gelification process (Figure 3.9). The percentage drug release was calculated by the following equation:

$$\text{Cumulative of PCT released (\%)} = C_i/C_o \times 100$$

Where C_i and C_o are the concentration of PCT released and loaded with hydrogel, respectively. To investigate the influence of pH on the drug release behavior, the water content of the hydrogel was determined by using the robotic electrochemical system automated suction buffer in the wells sample of different pH values. The pH of the buffer solution was adjusted with 0.1 M H_2SO_4 and 0.1M K_2SO_4 .

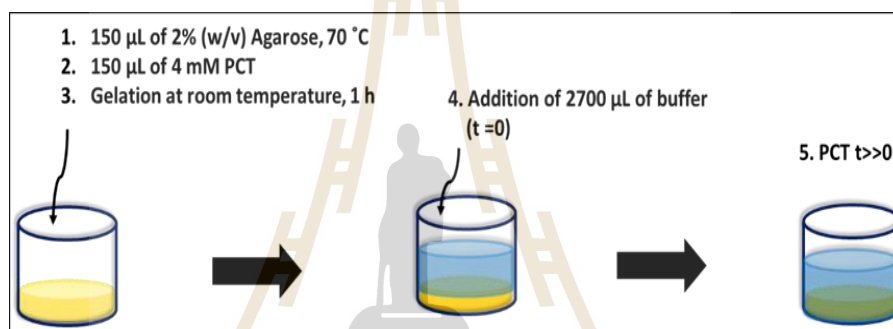


Figure 3.9 Scheme of the preparation of PCT-loaded agarose hydrogels in individual wells of microplates.

3.5.3.2 Robotic voltammetry determination of PCT release from agarose hydrogels in 24-well microtiter plate

The calibration curve method was chosen for the quantification of profiling paracetamol release in the 24-well microtiter plate. The robotic system controlled the buffer solution suction in the microtiter plate and/or the electrode movements. The experimental conditions and the robotic script commands are listed in Appendix D2 (Table D.2). Rows A1 and A2 indicate the wells used for the cleaning and for the blank, respectively. The drug release from PCT/agarose hydrogel was measured in triplicate as shown in red colour wells in row A3-A5. The rows B-D show

six different known PCT concentrations in triplicate that were used for plotting pre- and post-calibration curve.

3.6 Drug release from natural and artificial hydrogels by means of the electrochemical robotic system

This part of the thesis was carried out under the guidance of Prof. Dr. Wolfgang Schuhmann. The Poly(Styrene Sulfonate-co-glycidyl Methacrylate-co-butylacrylate), P(SS-GMA-BA) is an artificial polymer. It was synthesized by Dr. Adrian Ruff at Analytische Chemie Electroanalytik & Sensorik, Department of Chemistry and Biochemistry, Ruhr-University Bochum, Bochum, Germany. The copolymers P(SS-GMA-BA)-S1 (or S1-1) and P(SS-GMA-BA)-S2 (or S2-2) reveal nominal compositions of 50 mol% SS, 30 mol% GMA, 20 mol% BA (S1) and 80 mol% SS, 10 mol% GMA, 10 mol% BA (S2), respectively. The synthesis and characterization of polymer S2-2 was described earlier by Lopez et al, (Lopez *et al.*, 2017). Polymer P(SS-GMA-BA) was prepared analogously with the respective composition of comonomers. Synthesis of S1-1 and S2-2 were described in appendix A1. Figure 3.10 illustrates the molecular structure of the artificial immobilization matrix P(SS-GMA-BA) and its nominal composition.

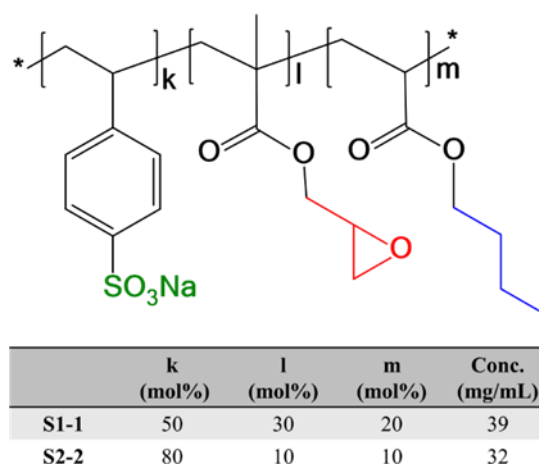


Figure 3.10 Molecular structure of the artificial immobilization matrix P(SS-GMA-BA) and nominal composition.

3.6.1 The application of robotic SWV for drug release from artificial and natural hydrogels

The agarose, chitosan, and P(SS-GMA-BA) polymers were selected for the controlled drug release. The drug release concentration was measured via SWV using the robotic monitoring system. The PCT was selected as a model drug to evaluate its release from the agarose hydrogel at room temperature at pH conditions of 1.2 and 8.0.

3.6.1.1 PCT drug loading in one-component hydrogel in microtiter plate

The concentration of sample drug was 2 mM PCT completely loading in to component polymers. The agarose hydrogel was described in the above sections. Figure 3.11 displays the necessary steps for the preparation and loading of the drug in chitosan, a natural polymer and artificial polymer. The chitosan films in microtiter plate wells were prepared with fixing 0.3% (w/v) chitosan solution containing 1% (v/v) of acetic acid. The 200 μ M drug sample was loaded as chitosan film. These samples produced a 300 μ L drug loading at bottom of microtiter plate wells.

After that, the solution was kept for 72 hours at room temperature to allow the evaporation of water and the formation of films. Meanwhile, the P(SS-GMA-BA) film was prepared by mixing 150 μL of 39 mg/mL S1-1 or 32 mg/mL S2-2 polymer with 150 μL of 4 mM paracetamol in the microtiter well. This final mixture was kept for 72 hours at room temperature for the evaporation of water and thus the formation of films.

3.6.1.2 PCT drug loading in two-component hydrogel in microtiter plate modelling

Figure 3.12 illustrates the step to loading the drug samples with the blend polymer hydrogels including the two-component part such as, agarose+chitosan, agarose+S1-1, agarose+S2-2 polymers.

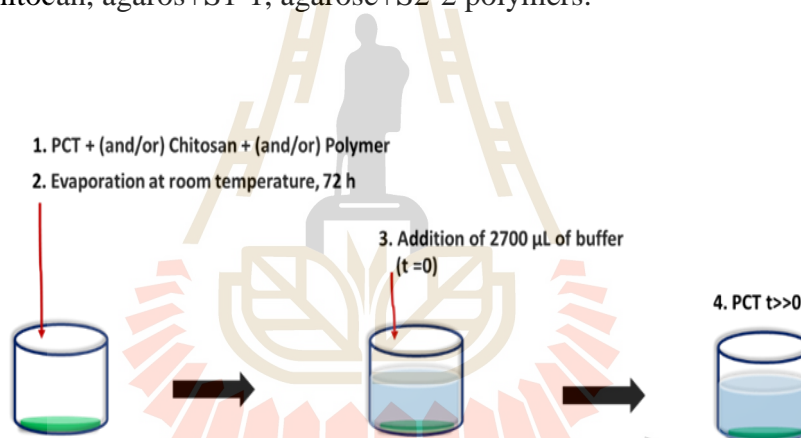


Figure 3.11 Scheme of the preparation of PCT-loaded chitosan or P(SS-GMA-BA) films in individual wells of microplates. The plate layout was used to measure three samples loading and six different concentration of PCT calibrations.

Composite agarose+chitosan hydrogel in microtiter plate wells were prepared with mixing the 0.3% (w/v) chitosan solution containing 1% (v/v) of acetic acid and 1% (w/v) agarose. Solutions with a higher chitosan concentration were not used, because they have a high viscosity, which is not suitable for microfluidic emulsion. The drug samples were loaded as chitosan+agarose hydrogel 200 μM in

finally solutions. After completion of the addition, maintained overnight at 4 °C to allow the mixtures to gel.

Composite chitosan+polymer (S1-1 or S2-2) film in microtiter plate wells were prepared with mixing 150 μL of 39 mg/mL S1-1 or 32 mg/mL S2-2 polymer with 0.3% (w/v) chitosan solution containing 1% (v/v) of acetic acid. The PCT drug loading was 200 μM . After mixing the polymers and paracetamol solutions, the final mixture was kept for 72 hours at room temperature to let the water evaporate and thus the formation of films.

Composite agarose+copolymer (S1-1 or S2-2) hydrogel in microtiter plate wells were prepared with mixing 150 μL of 39 mg/mL S1-1 or 32 mg/mL S2-2 polymer with 1% (w/v) agarose. The final concentration of the drugs in the agarose+polymer hydrogel was 200 μM . After completion of the addition, the solution was maintained overnight at 4 °C to allow the mixtures to gel.

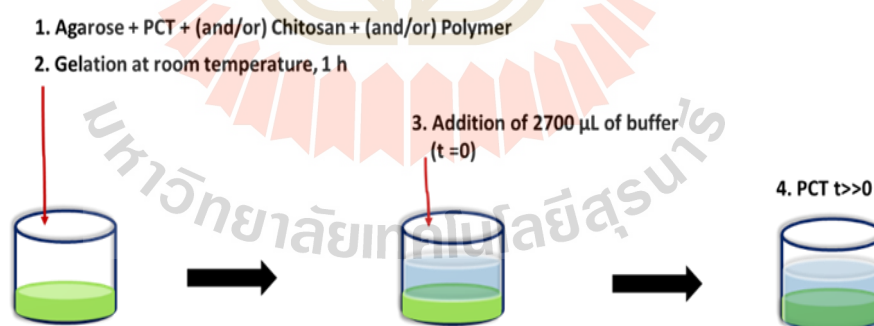


Figure 3.12 Scheme of the preparation of PCT-loaded two- and three-components hydrogel/polymer formulations in individual wells of microplates. The plate layout was loaded three samples and six different concentration of PCT. The calibrations mode was measured.

3.6.1.3 Drug loading in three-component hydrogel in microtiter plate

Three-component hydrogels were the composition the agarose+chitosan+polymer (S1-1 or S2-2) hydrogels in microtiter plate wells were prepared with 150 μL of 39 mg/mL S1-1 or 32 mg/mL S2-2 polymer with 1% (w/v) agarose mixed with 0.3% (w/v) chitosan solution containing 1% (v/v) of acetic acid. After the addition 300 μL of solution mixing in the wells of microtiter plate, the solution was maintained overnight at 4 °C for the gelification process.

3.7 Cathodic H_2O_2 analysis with electricity cable Cu disk electrodes as Oxidase biosensor platforms

Amperometry measurements were performed in the conventional beaker. A three-electrode held together as an assembly was identical in design to the one used for the hydrogen peroxide and for the glucose analysis. All were performed at room temperature using 0.1 M PBS solution pH 7.0 and 200 rpm as stirring rate.

3.7.1 Calibration curve of H_2O_2 with Cu disk electrode

A cathodic working potential of -0.15 V vs. Ag/AgCl/saturated KCl reference electrode was identified as suitable to reduce H_2O_2 at diffusion-limitation conditions. The current response at this potential was measured for a blank 0.1 M PBS buffer solution and for the buffer after sequential additions of 20 μM (10 times), followed by additions of 100 μM (8 times), and finally 200 μM (20 times) H_2O_2 stock solution. The amperometric current was recorded and used to construct a calibration curve. Calibration graphs can be plotted as the current response of the working electrode vs concentration of H_2O_2 .

3.7.2 Cu disk electrode testing interference in amperometric method

For the interference test, 50 μM hydrogen peroxide, ascorbic acid, and paracetamol were added 0.1 M PBS buffer solution (pH 7). The experimental conditions were mentioned above section.

3.7.3 Determining ability of Cu disk electrode to determine H_2O_2

For this trial, the H_2O_2 was evaluated by the common standard addition method via conventional beaker type amperometry. The model sample was adjusted 100 μM H_2O_2 in the solution. The model sample was spiked with the addition of H_2O_2 standard solution to raise the concentration to 100, 200, and 300 μM . The model sample concentrations were computed using the standard calibration method from plots of the background-corrected peak currents as a function of added H_2O_2 . To check on the accuracy of the developed assay, recovery rate experiments were performed on samples with a known amount of pure hydrogen peroxide. The recovery of the added H_2O_2 was calculated by comparing the concentration obtained from spiked samples with the actual added concentration.

3.7.4 Calibration curve of glucose biosensor via Cu disk electrode at cathodic potential

Commercial sensors based on glucose oxidase (GOx) were the prototypes used as examples. The cable Cu disk was coated with a GOx-containing polymeric Nafion layer which converted the Cu disk electrode to a glucose biosensor. The biosensor can operate at negative potential for cathodic detection of H_2O_2 produced by enzymic substrate oxidation. For amperometric experiments were performed with a controlled the potential of -0.15 V relative to the reference, in 0.1 M PBS pH 7.0, and

with aliquots of stock glucose solution added sequentially. The current response at this potential was measured for a blank 0.1 M PBS buffer solution and for the buffer after sequential additions of stock glucose solution. The additions increased the level of glucose from 20 μM to 2000 μM . The amperometric current was recorded and used to construct a calibration curve. Calibration graphs can be plotted as the current response of the working electrode vs the concentration of glucose. Of note, analysis of the raw I/t recording were processed with Origin software.

3.7.5 Determination of the glucose with GOx/Nafion-modified Cu disk electrode

The amount of glucose was evaluated by the common standard addition method using the amperometric technique on GOx/Nafion-modified electrical cable Cu disk electrodes. The glucose content was calculated from the current response of the amperogram using the standard addition method for determining the interception at x axes. The amount of added glucose and the degree of recovery were calculated for each sample.

CHAPTER IV

RESULTS AND DISCUSSION

Starting point for the attempts of this PhD thesis in establishing a methodology for non-manual voltammetric acquisition of drug release profiles was a robotic electrochemical workstation that was specially designed for the execution of the various voltammetry and amperometry detection schemes in the individual wells of 24-well microtiter plates. The basic device plus operational software was available; however the system's hardware and software and the working electrodes had to be tailored for the task of repetitive drug measurements in reliable and accurate manner. Main electroanalytical tool of the robotic voltammetry/amperometry setup was a movable three-electrode assembly with integrated working counter and reference electrodes (Refer to Figure 2.7, Chapter II). Counter electrode for the work of this study was a coiled Pt wire while the reference electrode was either a Ag/AgCl pseudo-reference system or a miniaturized version of a fritted Ag/AgCl/3M KCl electrode. The working electrode was a carbon nanotube-modified glassy carbon electrode (GCE) for the applications of robotic voltammetry to tablet dissolution testing, but a bare GCE when using the methodology for drug release from agarose hydrogels, thin polymers films and agarose hydrogel/polymer composite structures. The robotic electrochemical analyzer used three computer-controlled positioning devices (Linear Measuring Stages, Limes, Owis, Staufen, Germany) for precise vertical (z) positioning of the three-electrode assembly and for synchronized horizontal (x/y) movements of a standard 24-well microtiter plate. All electrochemical experiments of this chapter were carried out

through the operation of the specified three-electrode assembly via a PalmSENS3 electrochemical sensor interface (Palm Instruments, BZ Houten, The Netherlands). A personal computer in combination with tailored commercial software (Sensolytics GmbH, Bochum, Germany) controlled the automatically performed positioning and electrochemical procedures and organized the data acquisition and analysis.

In the following sections the requisite adaptations of the existing robotic voltammetry setup to the task of automated drug release measurements will be described. Also all details of the protocols for computerized runs of the three-electrode assembly through pre-loaded microplates for data acquisition will be explained. And the analysis of the acquired sets of voltammograms and their processing into the desired drug release profiles will be outlined and discussed for the cases of drug tablet dissolution and drug liberation from hydrogel and/or polymer films.

In line with the chronology of the PhD work done, next will be the presentation of all experiments regarding the analysis of drug dissolution from solid tablets, following the principles of standardized drug dissolution testing (DDT, refer to Figure 2.4, Chapter II).

4.1 Robotic voltammetry as convenient tool for analysis in course of tablet dissolution testing

4.1.1 Required methodological adaptations and consistency verification

Aim of the work of this chapter was to establish robotic microtiter plate-based voltammetry as alternative analytical tool for convenient since non-manual assessments of the many samples that are repeatedly faced when using the common strategy of drug dissolution testing in the format of the standardized official United

States Pharmacopeia basket method for drug release profiling (refer to Figure 3.6 in Chapter III for an illustration of the methodology). As model system for the proof-of-principle trials used were two different formulations of the pain and fever killer Paracetamol[®] (PCT), namely immediate and an extended release tablets. The immediate release version had 325 mg of the analgesics stored uniformly in a quickly disintegrable pellet. The extended release table had, in clear contrast, 325 mg of the drug more firmly stored in a difficult to break core region for slow release and another 325 mg placed in a quickly disintegrable outer shell layer (See Figure 4.1). Published release profiles for the two types of solid PCT formulations were available and their one- and biphasic appearance could serve as reference for the ones acquired with the novel electrochemical procedure developed in this PhD thesis.

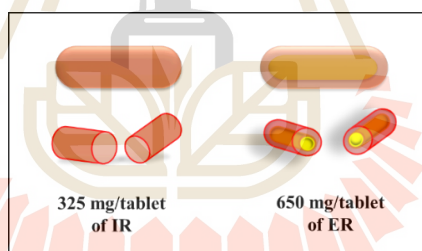


Figure 4.1 Schematic illustration of paracetamol drug tablets in the immediate-release (IR) and extended-release (ER) release form.

As PCT tablets were the chosen model for the establishment of sample analysis from DDT trials it was particularly important that the working electrode of the three-electrode assembly was well sensitive for the drug and able to measure the compound stably and accurately at least for the time of one complete run through all samples in a 24-well microplate. Working electrode for the trials of this subsection were actually carbon nanotube-surface modified GCEs. They offered indeed the desired

good quality PCT voltammetry. Figure 4.2 is a display of a typical example of a DPV that was at a CNT/GCE-WE recorded in a solution of 100 μM PCT in 0.1 M $\text{K}_2\text{SO}_4\text{-H}_2\text{SO}_4/\text{KCl}$ solution, which is a mixture recommended in the field of drug dissolution testing as artificial stomach solution. Also part of Figure 4.2 is, for comparison, the DPV of a bare GCE in the same measuring electrolyte. Well visible is that the modification of the carbon surface of the GCE with a nanoporous CNT thin film is going along with a favorable enhancement of the DPV signal related to PCT detection, expressed actually as significant increase in the height of the PCT anodic current peak. For all trial of samples from basket-type tablet dissolution testing the CNT-coated GCE version was therefore made the detecting sensor.

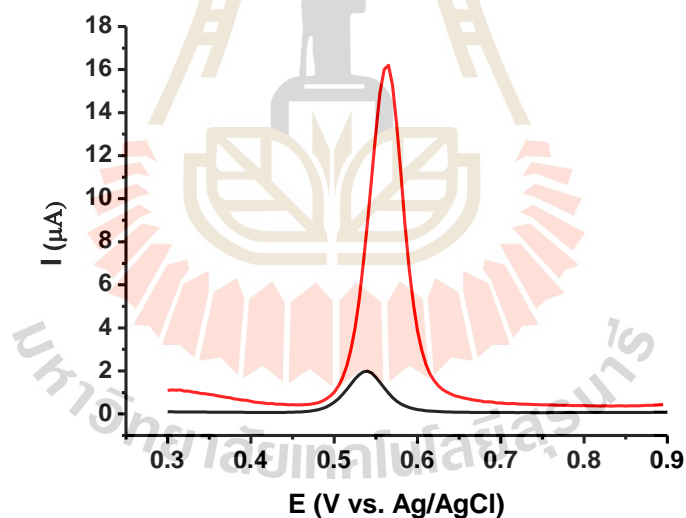


Figure 4.2 Differential pulse voltammograms of 100 μM PCT in 0.1 M $\text{H}_2\text{SO}_4\text{-K}_2\text{SO}_4$ mixed with 0.1 M KCl (pH 1.02) at a bare (black) and a CNT-modified (red) GCE. Pulse voltammetry was performed using E_{pulse} of 25 mV, E_{step} of 5 mV and t_{pulse} of 0.07 s.

The analytical performance of a CNT/GCE working electrode was further evaluated in automated calibration trials, with the analyte concentration varied from low (4 μM) to high (1400 μM) PCT levels in the measuring electrolyte. The actual microplate load for an automated calibration trial is illustrated in Figure 4.3(a). In fact, well A1, B1, C1, and D1 were all loaded with water and well A2 was filled with bare supporting electrolyte, here artificial stomach solution pH 1.02, respectively. Artificial stomach solution was chosen as electrolyte for the DPV measurement because it is a model of the environment in which paracetamol tablet degrade and release their drug content after a consumer ingested the medication. All other wells (A3-A6, B2-B6, C2-C6, and D2-D6) were filled with PCT/measuring buffer mixtures of increasing drug level. Figure 4.3(b) is then displaying the collection of DPV voltammograms as they were acquired by the robotic EC workstation automatically in course of the computer controlled sequential movement of the three-electrode assembly through the individual containers of the microplate. As expected, the peak height of the set of PCT DPVs increased progressively with increased PCT concentration. Exact measures of the individual peak heights were taken and plotted as function of known (since adjusted) PCT well levels. The obtained calibration curve is offered in Figure 4.4. A linear relationship became evident between the anodic current peaks, I_{pa} , and the concentration of PCT in the range from 4 μM to 1400 μM . The linear range regression equation for the particular example in Figure 4.3 is $y = 0.0475x - 0.4539$, with the R^2 value settled at good 0.9973. From the data of triplicate repetition of the calibration trials, the average value for the sensitivity of CNT/GCE working electrode against PCT was revealed as $0.048 \pm 0.01 \mu\text{A}/\mu\text{M}$ ($n=3$). The detection limit (3σ) of robotic PCT voltammetry was found to be 1.15 μM .

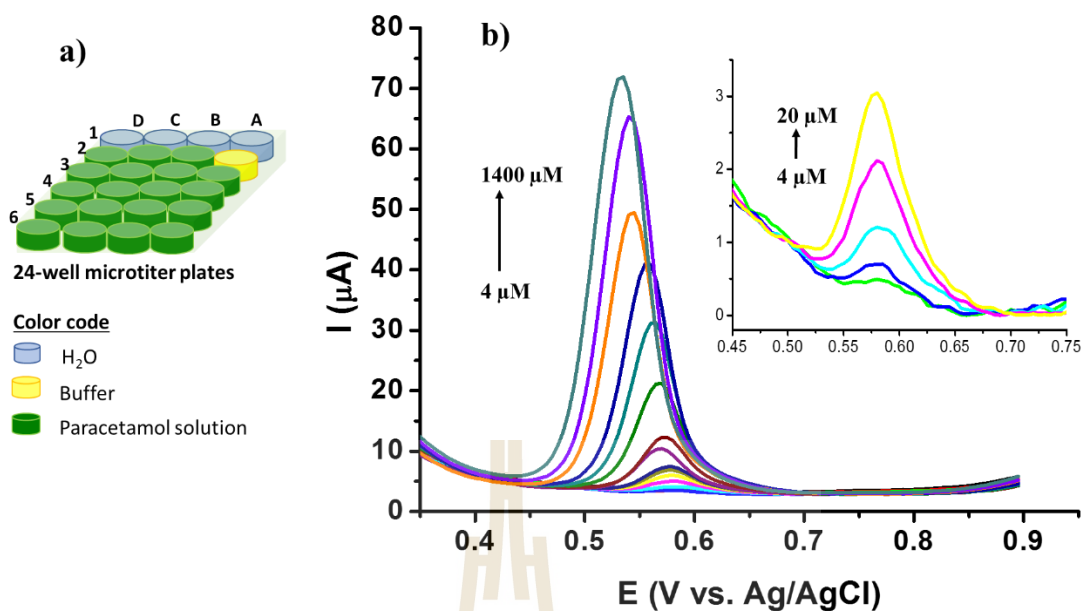


Figure 4.3 Robotic PCT calibration measurements with a CNT/GCE working electrode in sequential action in the containers of a pre-loaded 24-well microtiter plate. a) The load of the 24-well microtiter plate for PCT. b) Automatically recorded differential pulse voltammograms (DPVs) for analyte solutions of 4-1400 μM ; inset: a zoom of the DPVs for PCT levels of 4-20 μM . (Measuring electrolyte: 0.1 M H₂SO₄-K₂SO₄ mixed with 0.1 M KCl (pH 1.02); pulse voltammetry parameters: E_{pulse} of 25 mV; E_{step} of 5 mV; t_{pulse} of 0.07 s).

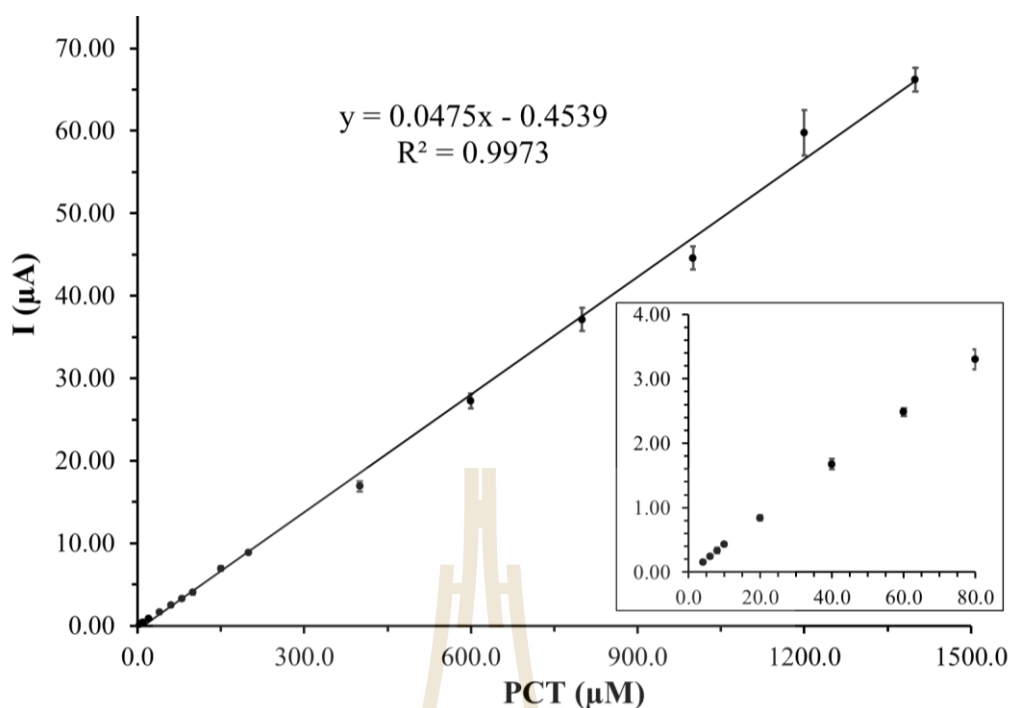


Figure 4.4 Calibration plot for robotic PCT DPV with a CNT/GCE working electrode in sequential action in the containers of a pre-loaded 24-well microtiter plate. Plotted peak represent the average values derived from triplicate plate runs as illustrated in Figure 4.3. Linearity stretches from 4-1400 μM PCT; the inset is a zoom of the calibration curve for PCT levels between 4 and 80 μM .

The reasonable quality of a non-manual gain of PCT calibration curves was a first valuable accomplishment of the targeted robotic drug (here: PCT) analysis. However, it had also to be shown that robotic PCT voltammetry is stably delivering accurate signals over the period of a full plate run, which may be between tenths of minutes or up to a several hours, depending on sample number in the plate and the setting of the software or hardware protocol for execution of the I/E experiments. Repetitive robotic DPV was thus executed in microtiter plate wells with PCT model samples of known concentration.

A first stability test trial was completed with a 10 μM and another with 80 μM PCT sample loading. The design of the plate load was actually such that every second well was water-filled and the wells in between were charged with sample. Microplates with such a layout were in a kind of a stability test subjected to DPV acquisition in the robotic mode. Figure 4.5 is the display of the set of DPVs of the stability tests, together with the plot of the DPV peak currents as function of time. Individual stability test plate runs took about 60 minutes. For both tested PCT levels, 12 bell-shaped I/E curves were obtained with the current maximum settled at about +0.56 V relative to the reference electrode. Visibly, for a particular PCT level the set of recorded DPVs were well superimposed. Apparently, neither a decrease nor increase of the peak currents happened, which evidenced stable drug detection at the CNT/GCE working electrode. Statistical analysis of all peak currents revealed virtually constant values ($0.58 \pm 0.02 \mu\text{A}$ ($n=12$), %RSD were 2.84 for 10 μM PCT and $4.20 \pm 0.06 \mu\text{A}$ ($n=12$), %RSD were 1.45 for 80 μM PCT).

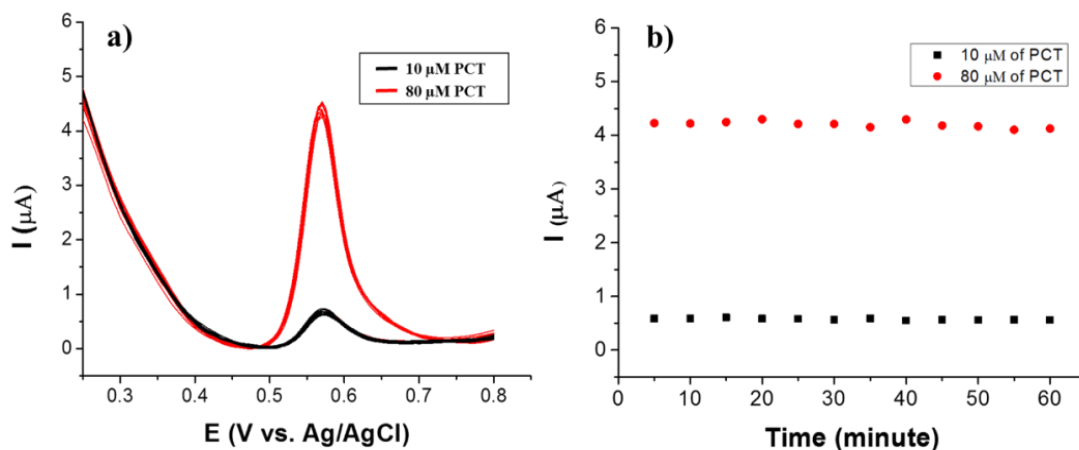


Figure 4.5 Robotic PCT differential pulse voltammetry in 24-well microtiter plates: Stability test I. a) Overlay of the acquired 12 PCT DPVs for analyte levels of 10 (black) and 80 μM . b) Plot of the peak currents (extracted from the DPVs behind graph a) versus the time of acquisition; 10 μM (black) and 80 μM (red) PCT concentration. Measuring conditions: CNT/GCE working, Ag/AgCl reference and a Pt-wire counter electrode. Differential pulse voltammetry: E_{pulse} of 25 mV; E_{step} of 5 mV; and t_{pulse} of 0.07 s. Electrode positioning and voltammogram execution was programmed for the measurement of one trace every 5 minute for a period of 1 h. Supporting electrolyte: 0.1 M H_2SO_4 - K_2SO_4 mixed with 0.1 M KCl (pH 1.02).

A second stability test trial was accomplished with the more challenging microplate load that is displayed in Figure 4.6(a). Addressed via robotic voltammetry analysis were now samples with 20, 40, 60 and 80 μM PCT levels in artificial stomach solution. In row A and B of the microplate the four liquids were ordered in the wells with number 3-6 from low to high and high to low concentrations, respectively. Row C and D of the same microplate had in the wells with number 3-6 fillings with a random distribution of the four chosen PCT levels. A microplate with such a layout had therefore the individual PCT levels four times included and they were subjected in

triplicate repetition to the established DPV acquisition in the robotic mode, to gain good statistics. One of the robotic plate runs took about 60 minutes and Figure 4.6(b) shows the three sets of four original DPVs per chosen PCT level of the complex trial. In general, the recorded I/E curves were nicely bell-shaped and the four DPV traces for a particular level were within one run well superimposed. Furthermore, the peak heights appeared also well reproducible among the three repetition of robotic microplate analysis. The calibration data of the CNT-modified GCE working electrode of the trial (refer to Figure 4.6(c) for the details) could be used to convert all obtained individual well DPV peak currents from the triplicate automated sample analysis run into actual sample PCT concentrations (refer to Figure 4.6(d)) for recovery rate calculations. Obtained for the 20, 40, 60, and 80 μM PCT levels were actually average recovery rates of 100.6 ± 7.1 , 102.1 ± 5.4 , 102.8 ± 9.5 , and 102.9 ± 4.8 , respectively. This was a satisfactorily sound performance of robotic microplate DPV in the quite complex stability test trial bearing in mind the many hours of continuous sensor operation during an entirely non-manual data acquisition.

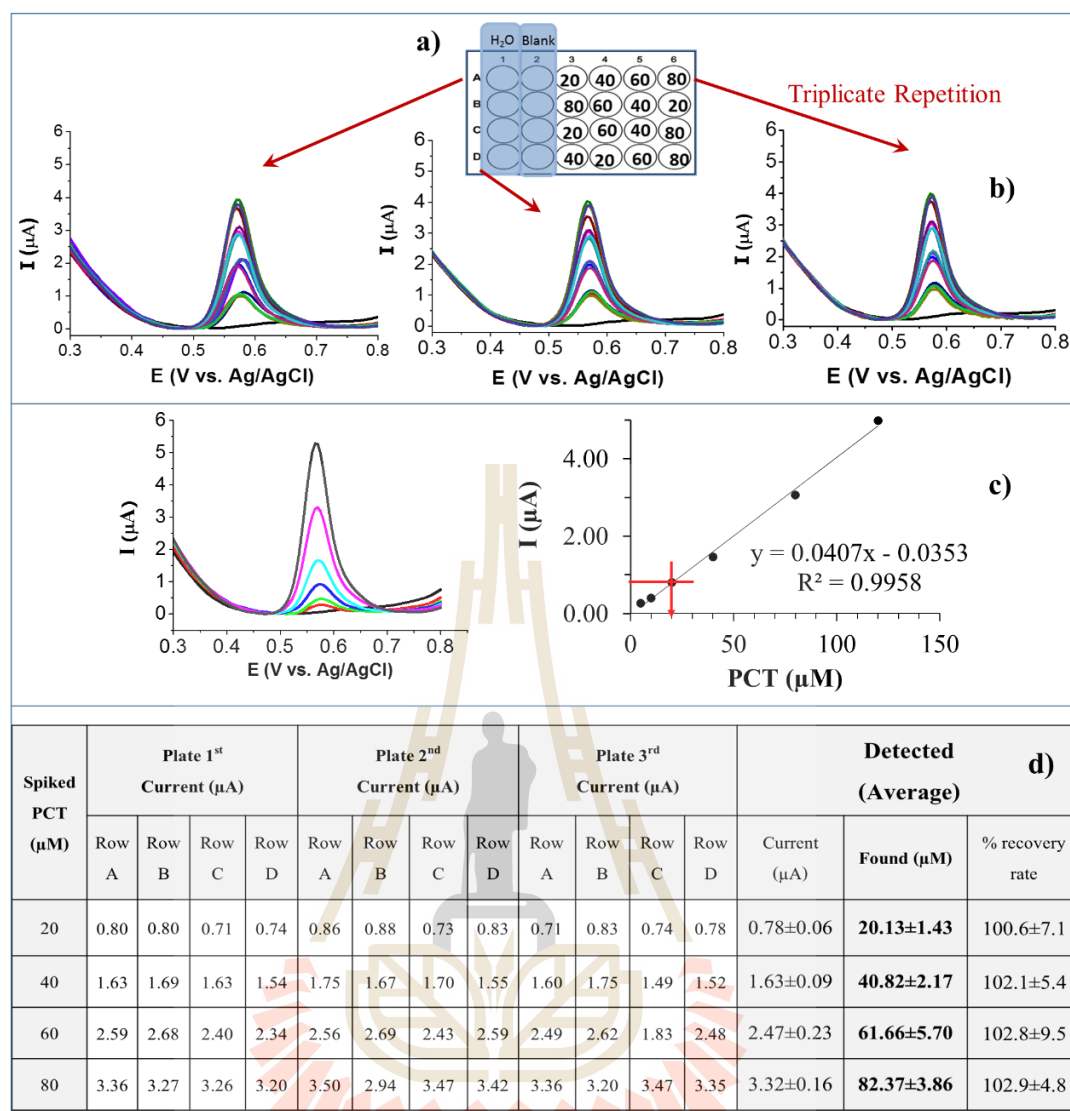


Figure 4.6 Robotic PCT differential pulse voltammetry in 24-well microtiter plates: Stability test II. a) The microplate load distribution of the 20, 40, 60, and 80 μM PCT model samples addressed in the triplicate quantification trial. b) The 3 sets of 4 DPVs per PCT level acquired in course of the triplicate plate runs. c) The DPV set (left) and linear regression plot (right) for the calibration of the particular CNT/GCE sensor responsible for all recordings in b). d) Table summarizing the results of stability test II and listing the average recoveries for the 20, 40, 60, and 80 μM PCT model samples. Measuring conditions: Same as for stability test I in Figure 4.5.

The observations of above stability tests I & II suggested that CNT-modified GCE sensors on an about hourly timescale were save against adverse electrode fouling. Accordingly, robotic voltammetric PCT quantification via computer-controlled analytical runs through sample-loaded microplate wells seemed to be practical. The system in the specified technical configuration was thus applied with confidence in the further work for (1) assessments of model samples (for recovery rate performance tests) and (2) PCT samples from immediate and extended release drug tablet dissolution testing (for PCT release profiling).

The recovery rate trials were actually carried out on samples with known 20 μM PCT levels in both the standard addition and the calibration mode. Figure 4.7(a) is a display of the microplate layout for automated standard addition analysis of PCT model samples. A representative set of DPVs corresponding to the measurements in well with a particular model sample and in three wells with PCT standard additions is shown in Figure 4.7(b). And the computed standard addition plot for the particular run is provided in Figure 4.7(c). From the appearance of the standard addition plot the PCT level was computed as 19.9 μM compared to the adjusted (expected) level of 20 μM . Accordingly, the recovery rate for this specific robotic standard addition voltammetry run was 99.4%. Table 4.1 is offering the summary of the outcome of robotic DPV in the standard addition mode for 4 samples in a microplate, which was approached once. The average recovery for the total of 4 determinations was a good $99.9 \pm 6.2\%$. Earlier stability test II disclosed for model samples with 20 μM PCT the average recovery rate of robotic DPV in the calibration mode as $100.6 \pm 7.1\%$ (n=12) (refer to Figure 4.6(d)).

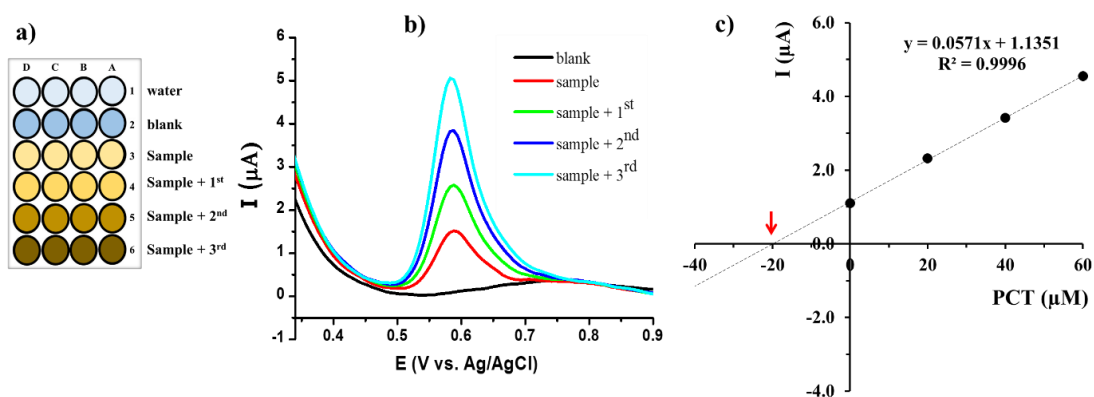


Figure 4.7 Quantification of PCT in a model sample with an adjusted 20 μM level by the standard addition method. a) 24-well microtiter plate loading as used for robotic voltammetric PCT quantifications in model samples, with CNT-modified glassy carbon disks as working electrode and the standard addition method for analysis. b) Set of difference pulse voltammograms (DPVs) acquired in a robotic voltammetry run through bare electrolyte, model sample, and model sample with drug supplementation. Differential pulse voltammetry parameters: E_{pulse} of 25 mV; E_{step} of 5 mV; and t_{pulse} of 0.07 s. c) Standard addition plot and linear regression plot/extrapolation to $y = 0$.

Table 4.1 Recovery rate performance of robotic PCT voltammetry in the standard addition method.

Microtiter plate rows	Detected concentration		
	Adjusted (μM)	Found (μM)	% recovery rate
A	20	19.5	97.5
B		21.7	108.6
C		19.9	99.4
D		18.8	94.2
Total (n = 4)		19.9 ± 1.2	99.9 ± 6.2

A direct comparison of the recovery rate performance of robotic PCT voltammetry in the standard addition and calibration mode is offered in Table 4.2. Obviously, both procedures had an about equal quality in verifying model sample PCT levels and thus both would meet the requirements of an analytical strategy for the analysis of samples from drug dissolution testing. However, for an analytical plate run in the standard addition mode the sample number is restricted to a maximum of 4 while in the calibration mode up to 20 samples, including a run in bare buffer, can be approached in one go. Choice for the automated quantification of the many samples from tablet dissolution testing/release curve profiling was thus the latter strategy with exploitation of a calibration of sensors prior and/or after sample plate rounds.

Table 4.2 Comparison of the recovery rate performance of robotic PCT voltammetry in the standard addition and the calibration method.

Method	Detected concentration		
	Adjusted (μM)	Found (μM)	% recovery rate
Standard addition	20	19.9 ± 1.2 (n=4)	99.9 ± 6.2
Calibration		20.1 ± 1.4 (n=12)	100.6 ± 7.1

4.1.2 Tablet drug dissolution testing with microplate-based robotic voltammetry sample analysis

As mentioned already before in the introductory thesis part, drug dissolution testing is in pharmaceutical industry commonly used for collecting valuable *in-vitro* information about the time course of the release of a drug, both for quality control purposes during tablet production and as guidance for the developments of new formulations. A pelleted solid drug is actually allowed to gradually liquefy into a solvent to yield the corresponding drug solution. The analytical task is time-dependent

detection of actual drug levels in solution, which here was proposed to be performed automatically through use of the robotic electrochemical screening technique. The PCT tablet dissolution test followed the approved protocols recommended for the standardized approach of the pharmaceutical industry. However, instead of a certified commercial dissolution basket used in this prototype studies as a cheap alternative was a tea ball strainer in which paracetamol tablets were kept in place in the solution supportive of tablet degradation and of active ingredient dissolution in controlled manner (refer to Figure 4.8(a)). Medium for dissolution testing of this study was actually a buffer simulating the strongly acidic stomach settings. It was prepared as proposed in literature in form of a 0.1 M mixture of $\text{H}_2\text{SO}_4\text{-K}_2\text{SO}_4$, with the pH value adjusted to physiological 1.02. Constant values of pH, temperature, agitation, and medium composition were maintained during ongoing tablet dissolution.

Over a period of 9 hours a collection of 1-mL samples was withdrawn from the dissolution medium in course of the drug release experiment and replaced by bare measuring buffer, first just shortly after immersion of the tablet-containing tea strainer into the dissolution medium, and then at defined time points until termination of the trial (refer to Figure 4.8(d)). 15 μL aliquots of the collected specimen were later, at a time of convenience, pipetted into designated containers of 24-well microplates with 2995 μL volumes of a 0.1 M mixture of $\text{H}_2\text{SO}_4\text{-K}_2\text{SO}_4/0.1$ M KCl, pH 1.02 as supporting electrolyte for voltammetry analysis. The plate load design for the robotic dissolution sample assessment was similar to the earlier described calibration trials, but with the dissolution samples of unknown concentrations filled into the wells A3 to A6, B2 to B6, C2 to C6, and D2 to D6 instead of adjusted calibration solutions (refer to Figure 4.8(b) or Figure 4.3(a); wells A1 and A2 of the microplate carried DI water for the electrode cleaning and bare buffer).

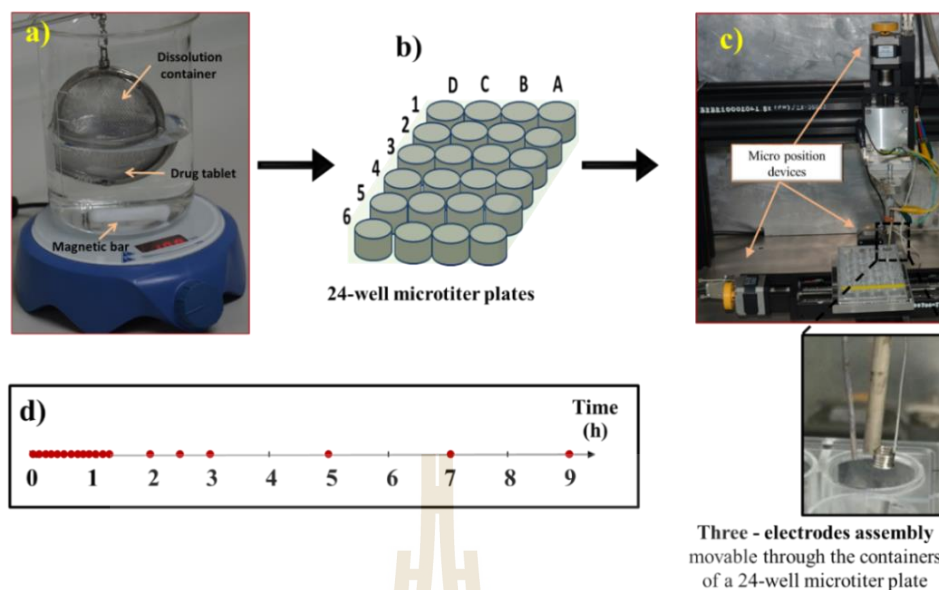


Figure 4.8 Illustration of the in vitro Paracetamol[®] tablet dissolution testing with the basket method and subsequent sample analysis via robotic voltammetry. a) Photograph of the dissolution of PCT tablets in a stainless steel tea strainer, immersed on a magnetic stirrer into artificial stomach solution as dissolution medium. This system resembled the standardized basket-type dissolution testing approach as approved by the USP and European Pharmacopoeia (refer to Figure 2.4 in Section II for details). b) 15 μL of the 1 mL samples from various stages of dissolution were added to 2985 μL into 24-well microplates and screened at 200 times dilution for their actual drug content via robotic DPV. c) Photographs of the workstation for robotic voltammetric drug sample analysis in the 24-wells microtiter plate format and of the three-electrode assembly above a particular microplate well. d) Schematic diagram of the schedule of sampling with sample aliquots being withdrawn over a period of up to 9 hours, at higher rate during the initial phase of solvent exposure and less frequent at later stage.

Operation of the robotic electrochemical workstation on sample-loaded microplates delivered within a period of about 90 minutes for every sample plate well the desired finger-print pulse voltammogram from which the peak height could be determined and, with the aid of calibration data, being used for the purpose of drug concentration determination.

Each robotic electro-analytical plate run on samples from dissolution testing for release profile acquisition was accompanied by the pre-calibration of the freshly cleaned determining CNT-modified GCEs, via robotic voltammetry in microplate wells with known PCT solution loads. A graphical illustration of the plate load and the protocol of the measurement sequence are shown in Figure 4.9(a) and Figure 4.9(b). The about 2h-long automated pre-calibrations 1, 2, and 3 allowed peak current-to-concentration conversion. A comparison of the characteristics of the last pre-calibration, namely number 3, with the final post calibration, 4, evidenced, on the other hand, yet again the previously observed voltammetric response integrity of the working electrode for the duration of a plate run and confirmed the requisite reliability of repetitive PCT electroanalysis in the robotic workstation.

The strategy depicted in Figure 4.9 was used for the construction of the drug dissolution profile of an immediate- and an extended release PCT tablets as shown in Figure 4.1. Both formulations were exposed to dissolution testing (as shown in Figure 4.8(a)), 1 mL samples were withdrawn at certain times (as shown in Figure 4.8(a)), 15 μL aliquots of the takes loaded with 2995 μL buffer into the designated wells of a microplate (as shown in Figure 4.10(a)), and the robotic acquisition of 'in-well' PCT-DPV measurements with precalibrated sensors was triggered.

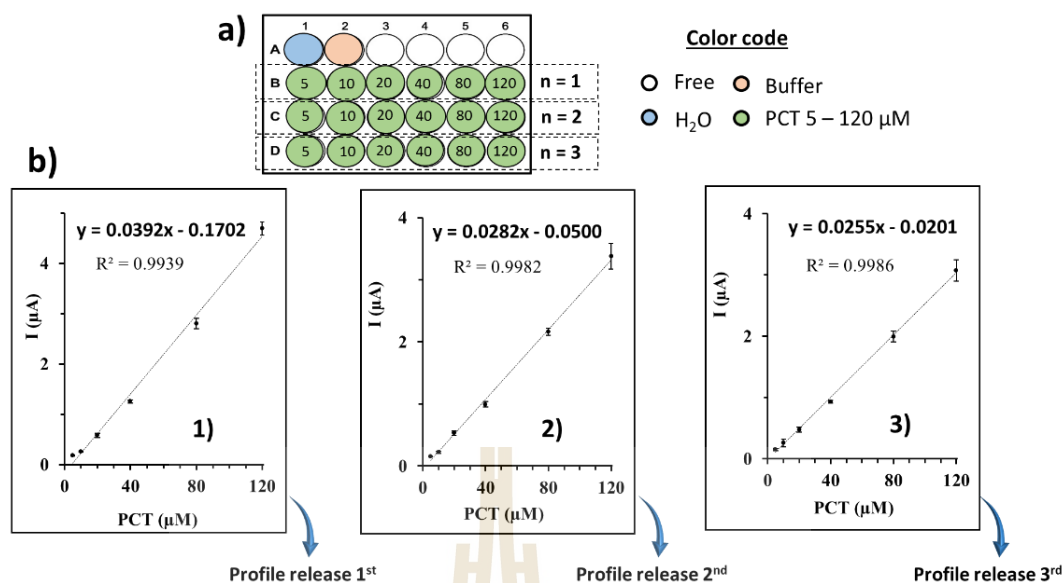


Figure 4.9 Illustration of the protocol for the analysis of samples from Paracetamol® tablet dissolution testing with the methodology of robotic voltammetry in 24-well microplates in the calibration mode. a) The 24-well microtiter plate loading used for working electrode pre-trial calibration. b) Calibration plots from an example trial obtained before and after assessments of real samples from dissolution testing.

Figure 4.10(b) is a display of the 20 DPVs that came up one after the other in cause of the robotic run of the working electrode assembly through all samples from a dissolution test with the ‘immediate release’ version of a PCT tablet. Figure 4.10(c) is then the plot of the extracted DPV peak currents vs. time while Figure 4.10(d) has all peak currents with aid of calibration data for the working electrode of the test translated into actual PCT concentrations at specific time points after dissolution onset. The recorded release profiles, whether expressed as I vs. t or $[PCT]$ vs. t , both pictured nicely the expected quick, uni-phasic delivery of PCT to the measuring buffer through liberation of the compound from the solid tablet. From a look to the insets of Figure 4.10(c) and Figure 4.10(d) it is obvious that all stored PCT in the tablet actually got

already dissolved in the initial 30 minutes exposure to the artificial stomach solution, which reflects correctly the established pharmaco-kinetic dissolution characteristics of this particular fast release-type of commercial PCT formulation.

Note that in the dissolution testing related to the trial of Figure 4.10 the complete discharge of the 325 mg PCT of the immediate release tablet into the 300 mL dissolution medium is lifting the final PCT concentration in the liquid of the dissolution container to about 7.17 mM PCT. A 15 μ L aliquot of this solution introduced into 2985 μ L microplate well measuring buffer refers to a 200 times dilution and an about 35.8 μ M PCT level is thus in this case the target level of screening on samples of the dissolution test and maximum expected level in the release profiles. This is very well confirmed in the electrochemically acquired release profiles of Figure 4.10(d) where the final PCT sample level is reaching the desired target level.

The robotic voltammetric plate runs leading to the release profile shown in Figure 4.10(d) were actually carried out in four-fold repetition, to get an idea about the reproducibility of the non-manual electrochemical methodology for drug release curve profiling. Figure 4.11(a) has all resulting four release profiles for the inspected immediate release PCT tablet presented in one [PCT] vs. t plot. The deviations between the individual curves are insignificant and all four disclose correctly the expected time course of drug liberation as the speedy, uni-phasic process that is aimed at by their formulation design for as quick as possible reach of a curing effect in case of pain or fever.

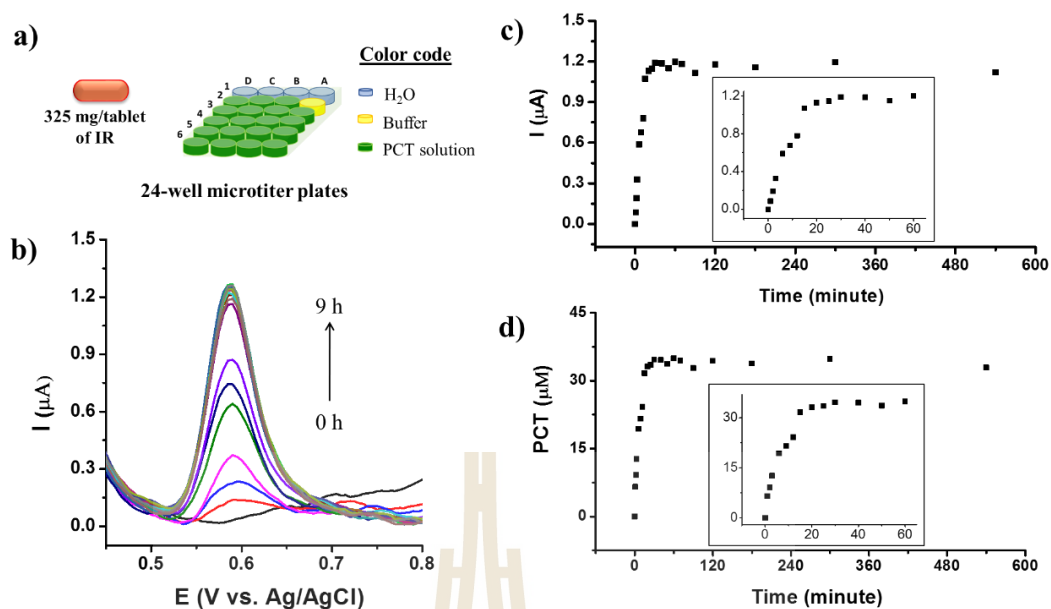


Figure 4.10 Robotic voltammetric quantification of PCT in samples from PCT tablet dissolution testing. Inspected object was here an ‘immediate release’ tablet with 325 mg active drug stored in a solid pellet; dissolution medium was artificial stomach solution. a) The 24-well microtiter plate loading of the trial. b) Representative set of 20 PCT differential pulse voltammograms as acquired in course of the automated run of the three-electrode assembly through the microplate wells (DPV parameter set: step E_{pulse} of 25 mV; E_{step} of 5 mV; and t_{pulse} of 0.07 s). c) Plot of DPV peak current vs. dissolution time, and d) PCT level vs. dissolution time (the common ‘release profile’).

In a copy of the procedure described in detail for the immediate release PCT tablet its extended release equivalent was inspected with dissolution testing/robotic voltammetry trials for an exposure of the specific release characteristics. Figure 4.11(b) displays the obtained four [PCT] vs. t plots for the extended release tablet. Again the four individual traces do not deviate significantly from each other, indicating acceptable reproducibility of the analytical assay for release profiling. Expected from the 2-layer extended release tablet design with a 350 mg slow-releasing

core and a 350 mg fast-releasing peripheral layer was a markedly different the release profile than the one that was exposed for the immediate release PCT tablet with just a simple pelleting of the drug into a solid matrix.

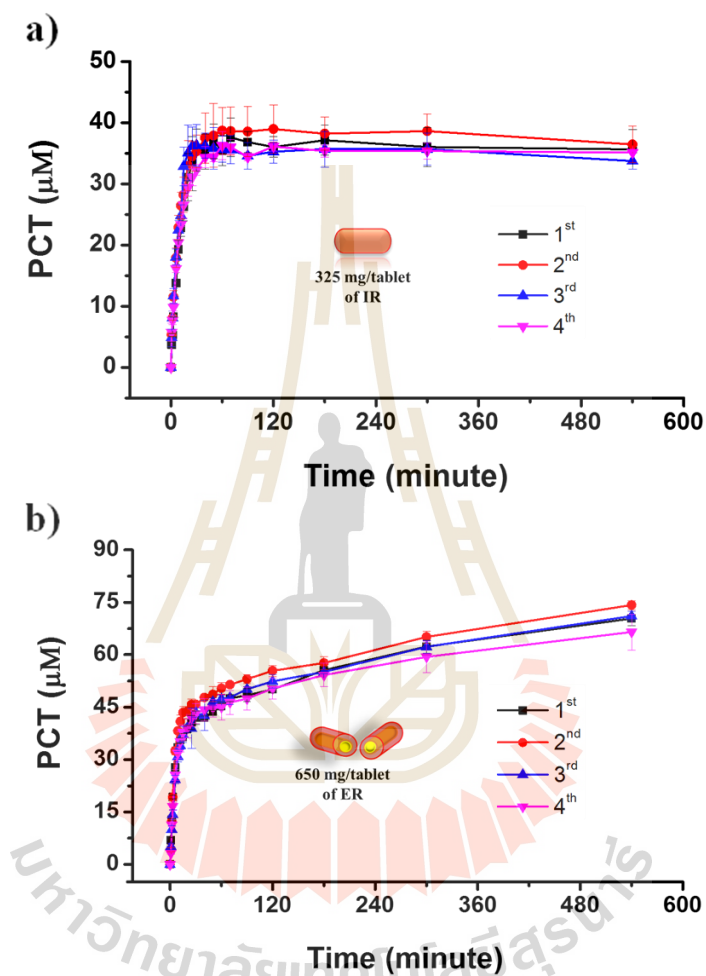


Figure 4.11 Time course of PCT release from a) an immediate-release (IR) formulation with 325 mg drug content per tablet ($n=4$, at room temperature) and, b) an extended-release (ER) formulation with 650 mg drug content per tablet (325 mg in the core and 325 mg in the periphery, $n=4$, at room temperature). Data points in the individual plots a) and b) represent the mean values of three separate microplate-based sample measurements, and the error bars symbolize the standard deviation.

And this difference is indeed well confirmed by the comparison of the corresponding voltammetrically assessed release profiles in Figure 4.11(a) and Figure 4.11(b). While the immediate release PCT tablet is obviously related to a one-phase discharge process the extended release PCT tablet goes visibly through an initial quick discharge process related to PCT dissolution from the outer tablet zone and then moves on to a much slower gradual ejection of the PCT from the tablet interior. The rates of drug dissolution from the extended release periphery and the immediate release tablet body (= slopes of the release curves) are visibly about the same and the related drug load of 325 mg is fully freed within the order of about 30 minutes. Discharge of the extra 325 mg PCT load in the tablet core of an extended release tablet needs, however, nine hours, as indicated by the reach of the expected about 72 μM final drug concentration in a microplate well with sample from the dissolution testing at this point in time.

The measured distinct differences in the dissolution characteristics of immediate and extended release PCT formulations are very nicely pictured when displaying their [PCT] vs. t profiles in one graph (refer to Figure 4.12(a), for an example).

Figure 4.12(b) is finally a graphical illustration that is more common in the field of pharmaceutical research, as it displays the cumulative release (in % of the total drug load) as function of time. This plot was for the trial of this study constructed from the initially acquired trace in Figure 4.12(a) by normalizing for each time point the actually measured PCT content to the known amount of drug, as listed on the package of the particular commercial medication.

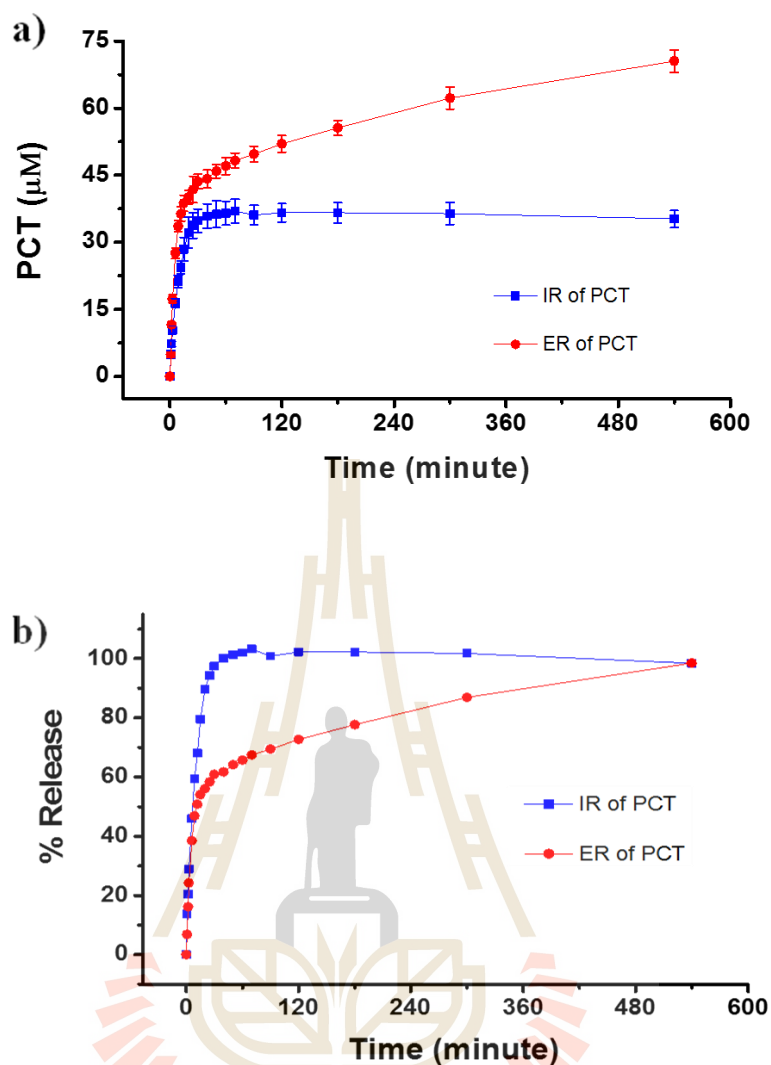


Figure 4.12 A comparison of the averaged drug release profiles of an immediate (blue-line) and an extended (red-line) release PCT tablet. Of note, each curve is the result of 12 robotic microplate voltammetry measurements ($n=12$) at room temperature. Individual data points represent mean values and error bars symbolized the standard deviation. a) Expression of the release profiles in b) as plots of % cumulative PCT release vs. time, for both types of PCT tables.

Finally, in order to further validate the suitability of the proposed non-manual electrochemical procedure for sample analysis from tablet dissolution studies, the temperature dependence of the release of PCT from an immediate release tablet was

monitored with the robotic voltammetric assay, at room temperature of 25 °C and at about body temperature of 37 °C. The obtained two release profiles are shown in Figure 4.13.

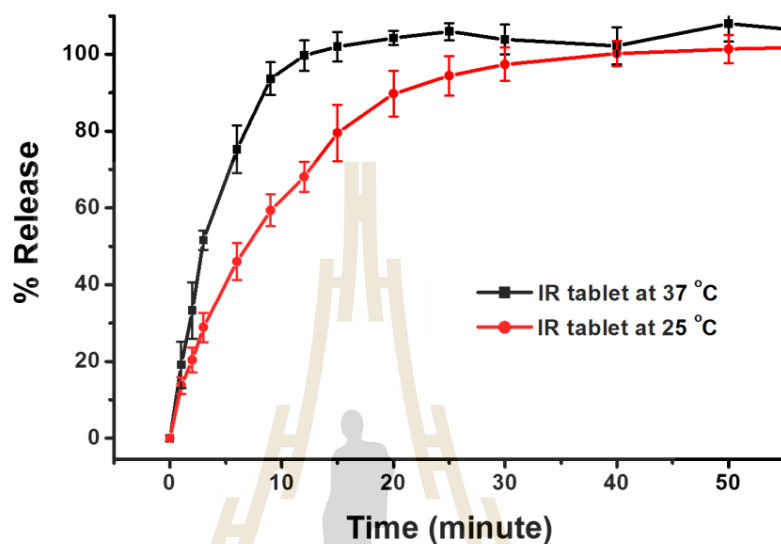


Figure 4.13 Shows comparison of averaged drug release profiles different temperature as body (black line) and as room (red line) of the dissolution medium at pH 1.02 with the immediate release formulation (data points represent the mean concentration and error bars the standard deviation).

For otherwise identical conditions, the release of PCT, was correctly identified as speedier at the elevated temperature, which was predictable due to the expected positive impact of temperature rise on molecular mobility of the stored drug molecules and possibly molecular matrix degradation, too.

According to above presented results, it can be concluded that the microplate-based robotic voltammetry assay is an adequate alternative for tracking the paracetamol drug release in the samples from tablet dissolution testing. The comparison of the release profiles of two types of PCT formulations in Figure 4.11 is the outcome

of 480 measurements. Individual voltammogram acquisitions (2 tablet systems, 4 tablet tested for each system, triplicate quantifications of 20 samples per tablet), not including the about 60 voltammograms for triplicate working electrode pre-calibration. Assuming a 4-5 minutes span for the acquisition of a voltammogram in one sample, the total time needed for barely manual sequential execution including electrochemical cell assemblage, measurement and cell cleaning and rearrangement would be about 1920 to 2400 minutes (32 to 40 hours), with no single break allowed at all. A similar total time is needed for the completion of the 480 measurements in the robotic electrochemical workstation. However, since the immense task of 480 individual voltammetric quantifications is then carried out non-manually through the computerized operation of a sensing tool in microplate wells the paramount benefit of the established methodology is the gain of convenience, freeing of laboratory staff for the execution of other duties and the exclusion of human errors otherwise at risk because of mindnumbing repetition of manual voltammetric measurements. Success of the application of the procedure was verified for model pharmaceutical formulations, actually two PCT tablets of different release behavior. However, a lot of other already established drugs and not yet explored synthetic or natural organic compounds show pronounced redox activity and could potentially be screened via voltammetry-based electroanalysis. A fruitful extrapolation of the established novel robotic voltammetry assay for dissolution testing of novel drugs and/or novel immediate, extended or controlled tablet formulations in industrial or academic research settings is thus easily imaginable as tool that offers simplicity, reliability and convenience just through the sound technical automation of an electroanalytical strategy.

4.2 Application of robotic voltammetry in 24-well microtiter plates as screening tool for drug release from agarose-based hydrogels matrices and polymer thin films

In the previous section robotic PCT differential pulse voltammetry was shown to be a successful analytical practice for quantification of the drug in samples from commercial pharmaceutical tablet dissolution testing. Here, the application of the methodology was further extended to direct measurements of the model drug of this study, PCT, from thick agarose hydrogel layers that have been formed at the bottom of microtiter plate wells with a variable level of the drug inside. Motivation was the plethora of published studies regarding the exploitation of drug-loaded hydrogel as advanced pharmaceutical formulation with potential to function as ‘smart’ matrix for stimulated extended (‘sustained’) and/or controlled compound release. Obviously, the immense activity on the subject is associated with the availability of analytical assays that, in convenient, reliable and cost-effective manner, deliver for the hydrogel targets the data for release profile construction. Microtiter plate-based voltammetry as introduced in Chapter 4.1 for sample analysis from dissolution tests combined the desired convenience/ease of use with a satisfactory assay accuracy/cheapness. The strategy thus would, in an appropriate adaptation, be a promising alternative to the (manual) electrochemical and (manual or automated) optical options used so far for drug quantification in samples from hydrogel release trials, assuming that the drug of choice is redox active and quantifiable via voltammetry. In the following the technical adaptations of microplate-based robotic voltammetry for the specific task of PCT release measurements from model agarose hydrogels will be described and the outcome of a series of test trials be presented and discussed to prove functionality of the proposed

approach. First proof-of-principle experiments used bare agarose layers on microplate well bottoms as model matrices. However, direct voltammetric in-the-well release measurements were also carried out for PCT that was trapped on/at or in thin polymer films on individual well bottoms, and for a number of composites of synthetic polymer and agarose. Obvious became indeed throughout the inspections the distinct suitability for assessing the pharmacokinetic release characteristics of hydrogel/polymer model matrices via automated voltammetry in prepared microplates. Next is the system and measuring protocol description for direct, in-the-well voltammetric drug release measurements on hydrogel pellets and (bio-) polymer films.

Figure 4.14 shows the electrochemical robotic apparatus that was used for the automated voltammetric PCT release monitoring from agarose/polymer drug storage systems. In principle the setup is the same as for previous work on samples from dissolution testing. Again, a three-electrode assembly but now with a bare GCE-based working, an Ag/AgCl/3 M KCl reference electrode, and a platinum spiral counter electrode was the tool enabling sensitive PCT square wave voltammetry (SWV). However, wells had to be approached by the electrode assembly in dry state, without electrolyte filling to avoid PCT release from matrices at the well bottoms prior to assembly arrival. A tube was therefore added as new element to the holder of for the WE/RE/CE. The tube was through a suitably sized computer-controlled syringe pump connected to a reservoir for measuring buffer solution (e.g. artificial stomach solution, PBS of desired pH etc.). With the electrode set the buffer-delivering tube could thus be maneuvered from well to well, with the specially arranged software scripts in charge of coordinated sequential approach of individual wells, time of rest in the containers, pump times and volumes, and execution of the voltammetric measurements plus data storage. The microtiter plates were prepared such that selected wells were equipped at

their bottom with drug-loaded hydrogels, films of synthetic polymers or hybrids of the two polymeric materials.

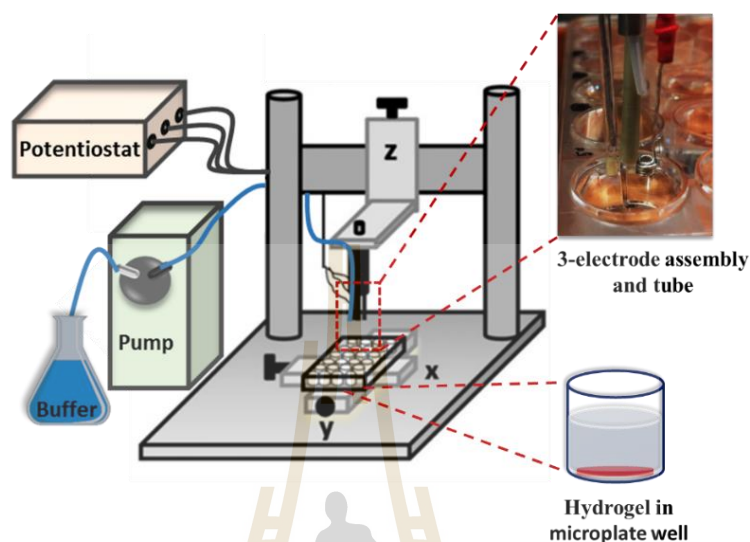


Figure 4.14 Schematic of the robotic electrochemical workstation as used for voltammetric drug release measurement from drug-loaded hydrogels, thin films of synthetic polymers or hybrids of the two polymeric materials in individual containers of 24-well microplates. Important extra elements, as compared to the system used for samples from drug dissolution testing (refer to Figure 4.8), are (1) a syringe pump and (2) a thin plastic tube addition to the holder of the working/reference/counter electrodes, which in joint use allowed controlled electrolyte delivery to initially dry wells with subsequent immediate trigger of voltammetry recording.

For all following automated release measurements from hydrogel and polymer PCT storage matrices square wave voltammetry at the bare glassy carbon electrodes was used as analytical scheme and again the release trials were performed in acidic artificial stomach solution. Shown in Figure 4.15(b) is the collection of the square wave voltammograms (SWVs) as gained in a typical robotic SWV calibration run of the

electrode assembly through a microplate with suitable load (Figure 4.15(a)). The electrode assembly was actually cleaned in well A1 in DI water before the SWV in bare solution was recorded in well A2. The sequence continued with cleaning in A1, first PCT SWV in well A3, washing in A1, second PCT SWV in well A4 and so on until the SWV was recorded in well D6.

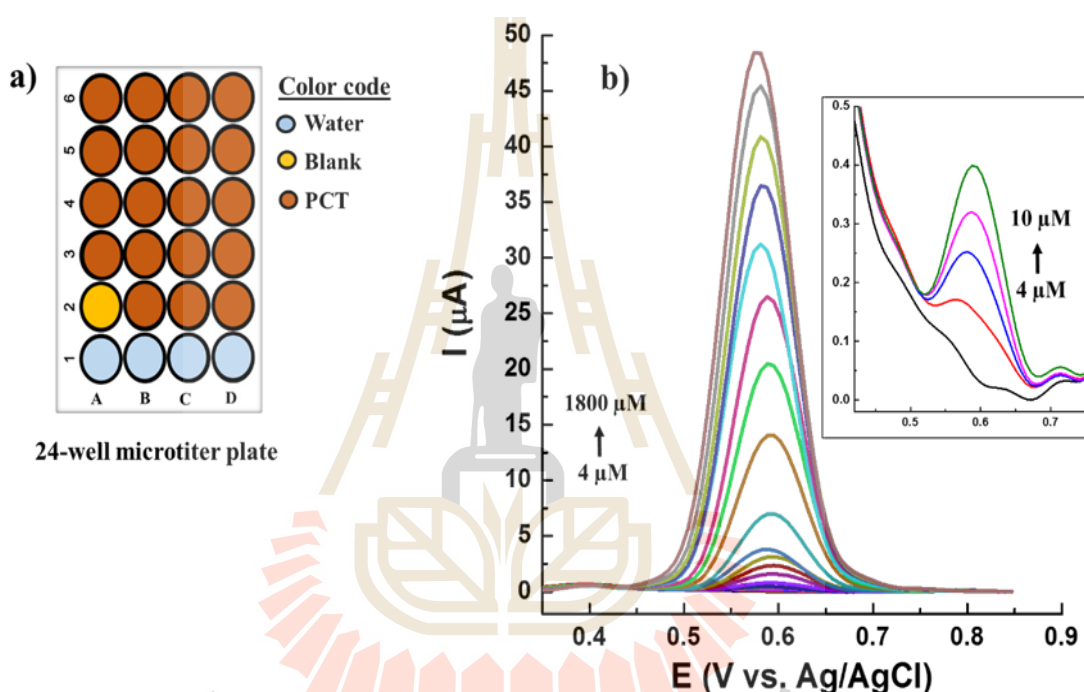


Figure 4.15 Calibration of a bare GCE working electrode in the robotic SWV mode. a) Related 24-well microplate load. b) Representative set of PCT SWVs in H_2SO_4 - K_2SO_4 buffer/0.1 M KCl, (pH 1.2) for PCT levels from 4 μM to 1800 μM . The inset is a zoom into the graph for drug concentrations between 4 μM and 10 μM . Parameters of square wave voltammetry: potential step: 7 mV, potential amplitude: 25 mV and frequency: 100 Hz.

Figure 4.15(b) is a display of a representative set of SWVs of the calibration trial while the corresponding calibration plot is offered in Figure 4.16. The linear

regression equation was $I_{pa} (\mu\text{A}) = 0.2750 + 0.0302c (\mu\text{M})$ ($R^2 = 0.9986$). Practical detection limit for the assay was on the order of about $0.5 \mu\text{M}$.

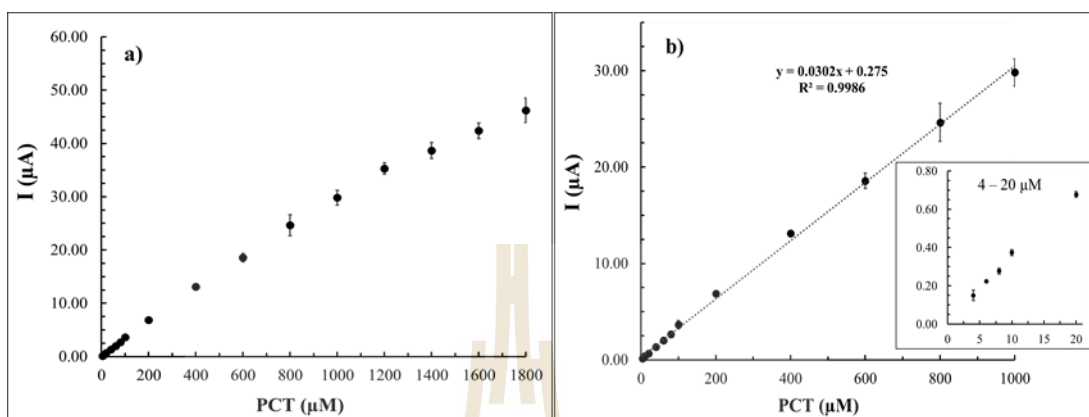


Figure 4.16 Display of the plot of the peak height of PCT SWVs displayed in Figure 4.15(b) as a function of the PCT concentration. b) Zoom into the plot in a) with demonstration of linearity of the voltammetric response up to $1000 \mu\text{M}$. The inset is a further zoom into the calibration plot for PCT levels of $4 \mu\text{M}$ to $20 \mu\text{M}$.

The response stability of robotic SWV at bare GCEs toward PCT was determined in robotic SWV via a non-stop 6-hour-long run of a WE/RE/CE electrode assembly through 12 microplate wells with ultrapure water (for rinsing) and 12 wells with solutions of $200 \mu\text{M}$ PCT (for repetitive quantification). The plate load of this stability trial is displayed in Figure 4.17(a). Note that before and after the stability test calibration plate runs were carried out. A typical pair of two of the acquired calibration plots is displayed in Figure 4.17(b) and a good match was observed between two the linear regions of the two data sets.

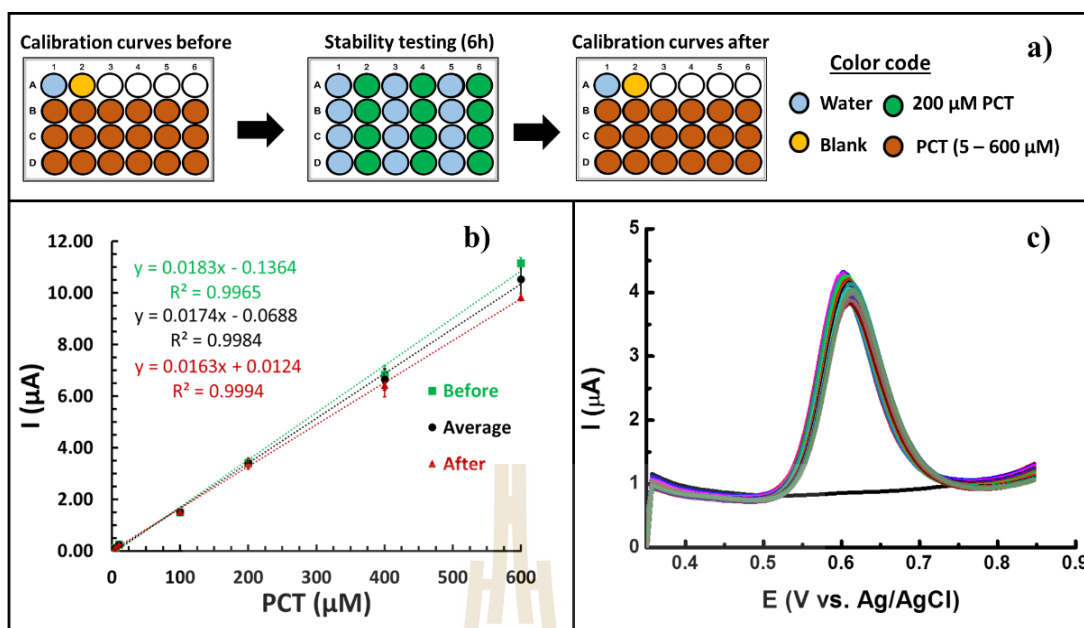


Figure 4.17 Response stability of robotic SWV at bare GCEs toward PCT. a) Illustration of the trial outline with the stability test microplate run sandwiched between pre- and post-calibration. A SWV was measured every 5 minutes for the period of 6 hours. b) The pre- and post-calibration plots (data points were measure in triplicate, errors bars - if visible - represent standard deviation) and their statistical average. c) Compilation of the 72 SWVs from six robotic voltammetry microplate runs with twelve 200 μM PCT samples per plate. Measuring solution was 0.1 M KCl/K₂SO₄-H₂SO₄ (pH 1.2) and the SWV parameter set included a step potential of 7 mV, potential amplitude of 25 mV, and frequency of 100 Hz.

In course of the continuous 6 hours of automated sensor operation 6 complete moves from first well A1 to last well D6 were possible and thus (6x12) SWVs were acquired and stored. The entire set of 72 SWVs of the stability test is visualized in Figure 4.17(c). Appropriately all I vs. E curves were obtained as reasonably well superimposed traces and the peak SWV peak currents strayed with only small deviation around average ($3.29 \pm 0.16 \mu\text{A}$, n=72). Taking advantage of the available sensor

calibration data, the 200 μM of PCT in the well solution was measured as 187.2 ± 8.5 μM , $n=72$), which refers to an acceptable average recovery of 93.6 ± 4.3 μM , $n=72$) and adverse electrode fouling with loss of sensitivity could be excluded on the time scale of the trial.

As CNT-modified GCEs did for DPV bare GCEs offered in the robotic electrochemical workstation stable PCT electroanalysis in the SWV mode. The trustful performance extended long enough to allow completion of automated hour-long microplate voltammetry runs on samples distributed through the available plate containers. Robotic PCT-SWV was therefore applied with confidence for the assessments of the PCT release characteristics of PCT-loaded hydrogel pellets or polymer films that are summarized in the next sections.

4.2.1 24-well microtiter plate voltammetry as convenient screening tool for drug release from hydrogel drug formulations

The chemical and physical versatility offered by the many available hydrogel systems made this type of smart biocompatible material a prime choice for applications as drug carrier with an ability to release stored pharmaceuticals on demand and on extended time scale. The enormous R&D activity on the subject is nicely reflected by the appearance of more than 3,700 publications within the time span of the last five years that relate in a 'Web of Science' topic search to the terms 'drug release' and 'hydrogel'. For just agarose as one of the many biological hydrogels the Web of Science search combination with 'drug release' still delivers more than 100 articles for 2017-2013. A significant number of the covered scientific communications include inspections of the release kinetics of the studied drug-loaded hydrogel materials. It is thus clear that the need of well-working and convenient analytical schemes for the

completion of that interesting task stimulates a vibrant activity in advanced sensor design, automation of measuring sequences and setup simplification.

Since agarose hydrogels are easy to make and handle they have been chosen as model material of choice in this dissertation for trials that had the aim to proof the suitability of robotic voltammetry in 24-well microplates to serve as high-quality analytical tool for the quantification of drug release from this special type of storage matrix. Figure 4.19 illustrates the microplate load (a) and the protocol of well approach/activity (b) of a typical robotic voltammetry quantification trial of the release of PCT from agarose. The wells of the microplate, namely well A3, A4 and A5 were equipped on their bottom with identical PCT-loaded agarose pellet, for triplicate assessment on a particular condition. The PCT/agarose 'formulation' was created in the three well through the placement of a warm PCT/agarose solution and allowing gelation to take place via slow cooling to room temperature. Transparent hydrogel pellets were gained, firm enough to peel them out of the well for photographic documentation (refer to Figure 4.18). No electrolyte was in the 'agarose' sample wells until a software trigger from the workstation computer initiated syringe pump action and delivery of the desired volume of, for instance, artificial stomach solution. And only then the acquisition of SWVs in just electrolyte-filled wells was launched and repeated at programmed time points.

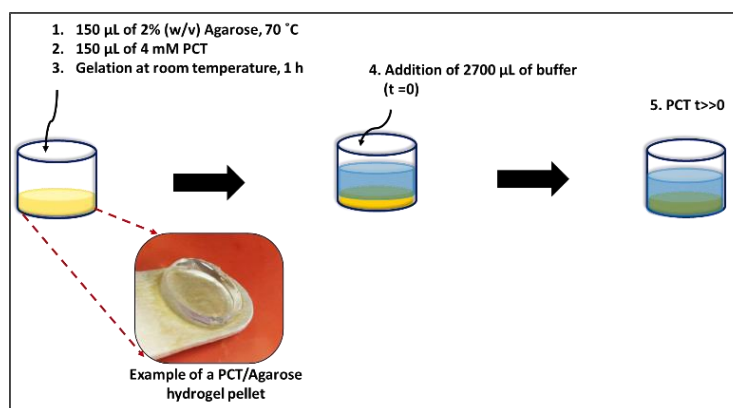


Figure 4.18 Illustration of the charging of microplate wells with transparent PCT-loaded agarose hydrogels that after gelation completion can be inspected via microplate-based robotic voltammetry regarding their drug release characteristics.

Microplate wells A1 and A2 carried purified water for electrode assembly rising in between measurements and bare measuring electrolyte for the acquisition of the SWV of a blank. The microplate wells in the row B were charged with six PCT solutions of increasing and known concentrations and this ‘standard’ load was repeated in the rows C and D to facilitate triplicate repetition of sensor calibration. The software script for robotic hydrogel release profiling was tailored to the guidance of the electrode set through all the wells, in the following order: A1, electrode assembly rinsing; A2, blank SWV acquisition; B1-B6, SWV acquisition for 1st calibration; A1, electrode assembly rinsing; A2, blank SWV acquisition; C1-C6, SWV acquisition for 2nd calibration; A1, electrode assembly rinsing; A2, blank SWV acquisition; D1-D6, SWV acquisition for 3rd calibration (completion of the triplicate pre-calibration run); A1, electrode assembly rinsing; well A2 blank SWV acquisition; A3, pump activation & electrolyte filling, instantly after first SWV acquisition (t=0); move of electrode assembly to A4, pump activation & electrolyte filling, instantly after first SWV acquisition (t=0); move of electrode assembly to A5, pump activation & electrolyte

filling, instantly after first SVW acquisition ($t=0$); movement of electrode assembly back to A3, recording second SVW ($t=5$); further to A4, recording of second SVW ($t=5$); further move to A5, execution of second SVW ($t=5$); sensor return to A3, recording of third SVW ($t=10$); move to A4, recording of third SVW ($t=10$); travel to A5, recording of third SVW ($t=10$); repetition of the movement/SVW acquisition cycle in wells A3-5 for $t=15, 20, 25, 30, 45, 60, 75,$ and 90 minutes; A1, electrode assembly rinsing; A2, blank SWV acquisition; B1-B6, SWV acquisition for 1st calibration; A1, electrode assembly rinsing; A2, blank SWV acquisition; C1-C6, SWV acquisition for 2nd calibration; A1, electrode assembly rinsing; A2, blank SWV acquisition; D1-D6, SWV acquisition for 3rd calibration (completion of the triplicate post calibration run). The details of script responsible for the processes of computer-controlled pump activation and electrolyte filling (e.g. pumped volume (unit; μL), pump speed (unit; $\mu\text{L/s}$) and the timing of electrode assembly movement are described in Appendix D2 (as Table D2).

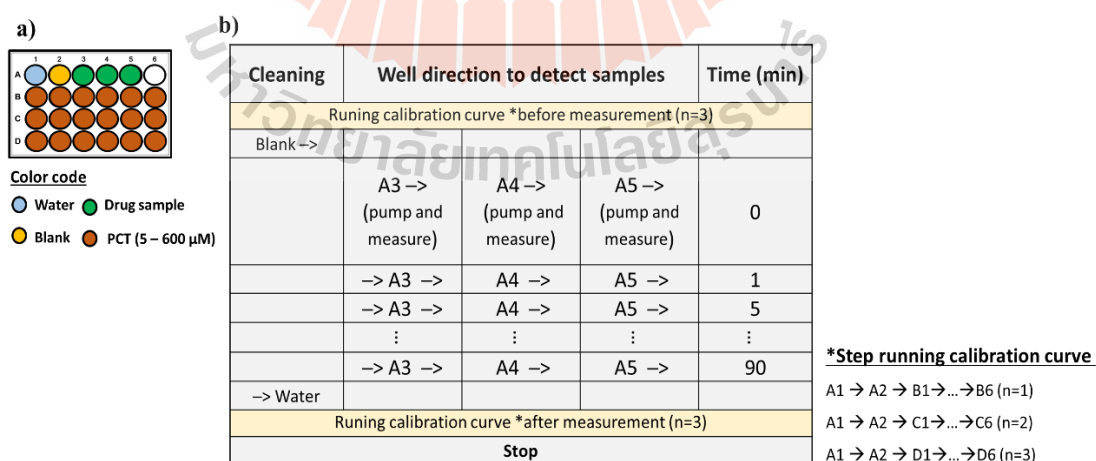


Figure 4.19 The microplate load a) and the protocol (event sequence) of well approach/activity b) of a typical triplicate robotic voltammetry quantification trial of the release of PCT from gelled agarose.

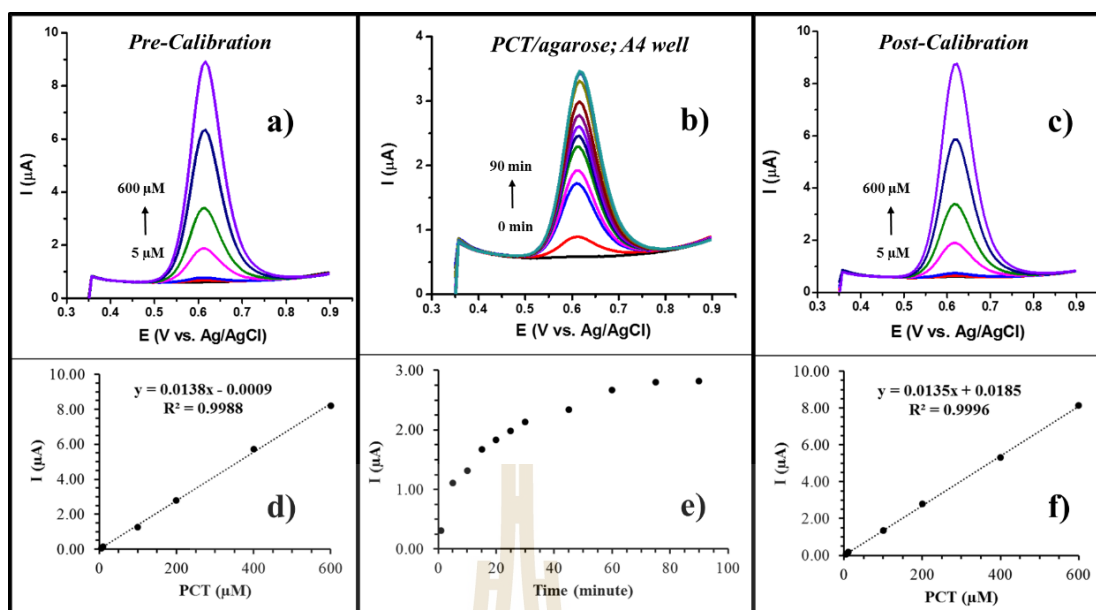


Figure 4.20 Typical data of a robotic voltammetry quantification trial regarding the release of PCT from 1% agarose hydrogels in a microplate well. a) SWV set for pre-calibration, b) SWV set acquired in the agarose well in course of drug discharge, and c) SWV set for pre-calibration, d) pre-calibration curve constructed from data in a), e) Plot of SWV peak currents in b) vs. time, f) post-calibration curve constructed from data in c). Trial buffer was 0.1 M KCl/K₂SO₄-H₂SO₄ (pH 1.2), SWV step potential: 7 mV, SWV potential amplitude: 25 mV, SWV frequency: 100 Hz.

With above outlined robotic voltammetry the release of PCT from the natural 2% agarose hydrogel pellets at room temperature was evaluated in buffer solutions at high (8.0) and low (1.2) pH. Figures 4.20(a) to Figures 4.20(c) display three representative sets of PCT SWVs as they were collected in a trial in course of the pre- and post-calibrations and the dissolution run on the 1% agarose hydrogel pellet with 2 mM PCT load in artificial stomach solutions of pH 1.2. The corresponding pair of pre- and post-calibration plots is shown in Figure 4.20(d) and Figure 4.20(f), respectively. Apparently, a good linearity was observed for both calibrations and the sensitivity of

the used GCE working electrode with a deviation of just 2% almost identical. Figure 4.20(b) is the offer of the set of PCT SWVs that was acquired with the GCE sensor in between the calibrations in 4.20(a) and c in the well with the drug-loaded agarose hydrogel. As expected the peak currents increased in course of the 90 minutes trial due to the diffusion-driven gradual leakage of PCT out of the storing hydrogel matrix into the covering electrolyte solution. Figure 4.20(e) summarizes the trend with the display of a plot of the determined peak currents as function of time. This plot is actually reflecting the raw version of the release profile for the specific hydrogel/PCT formulation. With the aid of the data from pre-calibration, for instance, the y-axes (here: current) were converted into actual PCT solution levels, resulting in a plot as shown in Figure 4.21. Now the values on the y-axes directly stand for the measured PCT concentration. The bend of the curve informs then on the change in PCT in the microplate well over time and is thus the more genuine form of the PCT release profile. Common practice in the pharmaceutical science is a further conversion of the [drug] vs. t plot into so-called plots of cumulative release plots which have the actually drug level at given time points normalized to the concentration that can be computed from the known drug load in the formulation and the volume of the solution into which release takes place

$$\text{Cumulative PCT release (\%)} = \frac{[\text{Released PCT}] \text{ at a given time point}}{[\text{PCT}] \text{ based on the adjusted hydrogel drug content}} \times 100 \quad \dots\dots (1)$$

Figure 4.21 is example of a plot of the cumulative release of PCT from a 1% agarose hydrogel pellet as it was computed with the data of a robotic trial as depicted in Figure 4.19, with a bare GCE completing three sets of PCT SWVs in all

three hydrogel-charged wells of a prepared microplate. Just after placement of the dissolution buffer into the hydrogel-containing well the rate of PCT liberation is very fast, reaching substantial 40% of cumulative release in just 5 minutes of dissolution activity. Then the drug ejection slows considerably down to reach full discharge of the PCT hydrogel load at about 75 minutes.

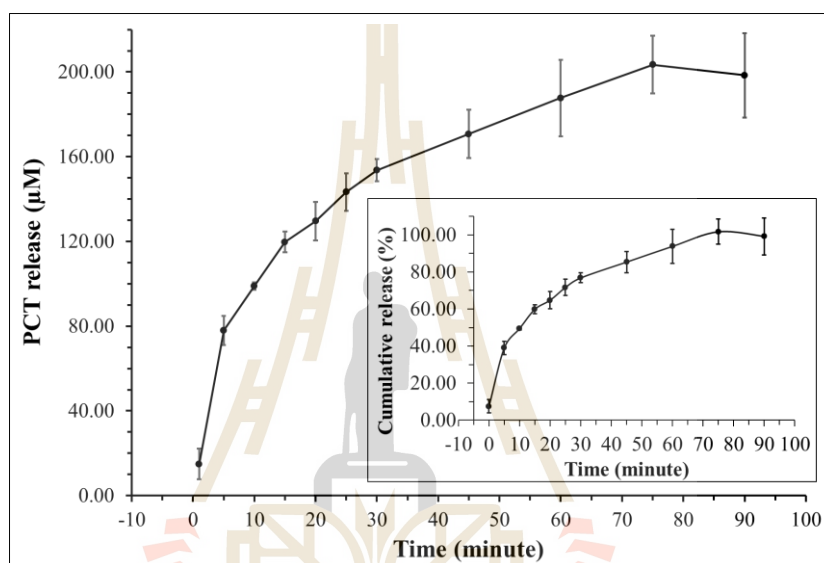


Figure 4.21 Time dependence of PCT release from a 1% agarose hydrogel as assessed with a robotic trial as outlined in Figure 4.19 and with data from triplicate repetitions of measurements as shown in Figure 4.20. The inset is a graphical illustration that considers the transformation of the original dissolution curve into a cumulative release profile. Single data points in the graph represent the average of the three SVW peak heights at a given stage of release and the error bars symbolize the calculated standard deviation of the measurements.

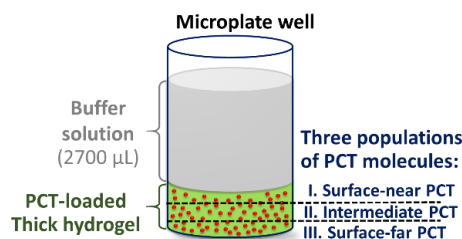


Figure 4.22 Distribution of PCT within a 0.3 mm thick hydrogel pellet in a microplate well. In the simple model three zones are suggested, with PCT present in surface near, central and bottom locations. The obvious path length for a diffusion from the inner of the hydrogel into buffer solution relate to two stages of release, namely the fast one liberating quickly all surface near PCT, and a gradually slowing one for the discharge of the deeper buried drug molecules.

The release of PCT from the hydrogel into the dissolution buffer is a diffusion-driven process, directed by gradient between the PCT level in the hydrogel (initially equal to the adjusted load) and the concentration in the neighboring solution (initially equal to zero). Accordingly, the characteristic profile of PCT release from a hydrogel pellet may be explained by the presence of drug molecules in different zones of the storing matrix, as compared to the hydrogel/buffer interface (refer to Figure 4.22). Surface-near PCT molecules will have it easy to leave the hydrogel environment and their discharge into the electrolyte will be speedy and responsible for the fast reach of a significant solution level of the drug. As deeper the location of PCT molecules in the hydrogel pellet is as longer they have to diffuse through the polymer gel structure to finally enter the buffer. PCT from the core and bottom of the hydrogel pellet are thus expected to need longer to be release, which explains the gradual decay in the speed of liberation (= flattening of the release curve with clear slope decrease happening past the onset release period).

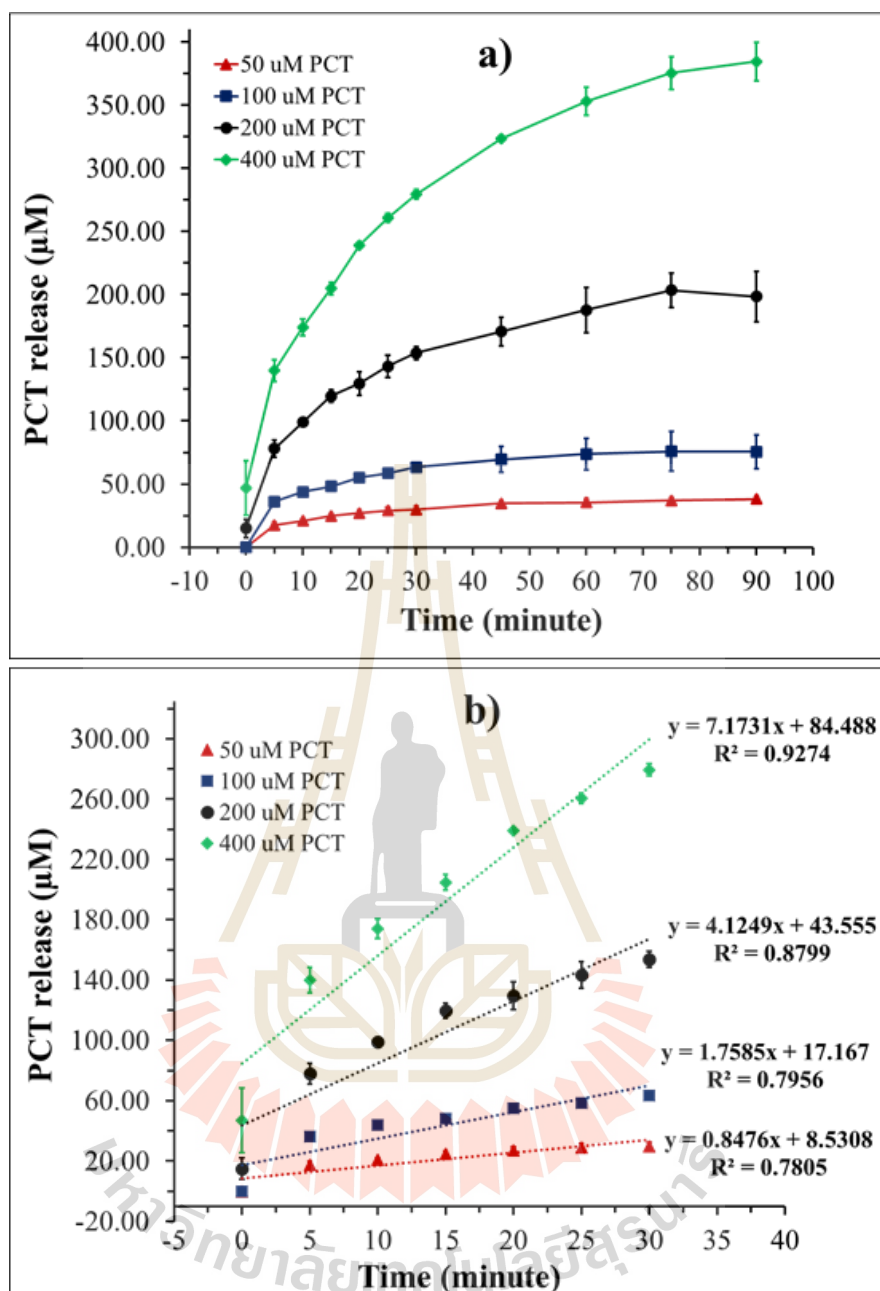


Figure 4.23 PCT release profiles as constructed with data from a triplicate comparative robotic voltammetry release trial at room temperature for 1% agarose hydrogels with 4, 2, 1, and 0.5 mM PCT load. a) Entire plot from test start to 90 minutes of voltammetric inspection, b) Zoom into the first 30 minutes of curve a). Each data point in the graphs represents the mean concentration, and the error bars represent the standard deviation. The measuring conditions were as specified before, for the tests related to Figure 4.20 and Figure 21.

That the release of PCT from an agarose hydrogel in simplest form indeed is a diffusion-driven process is nicely visualized by a comparative robotic voltammetry release trial at room temperature on a set of four 1% agarose hydrogels with different amount of the drug in the polymer structure. Inspected were actually pellet loads of 4, 2, 1, and 0.5 mM, (which refer to 400, 200, 100, and 50 μM to measure solution concentrations, for full release).

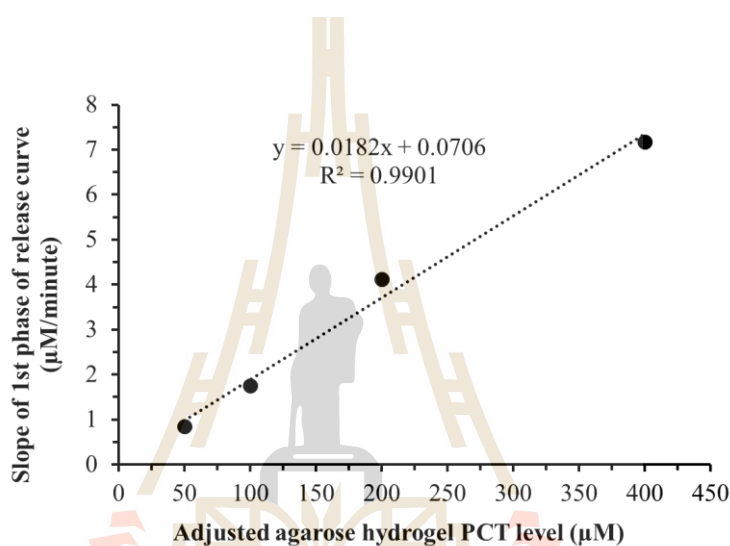


Figure 4.24 Triplicate comparative robotic voltammetry release trials at room temperature for 1% agarose hydrogels with 4, 2, 1, and 0.5 mM PCT load. Slope of the initial phase of drug liberation (from Figure 4.23(b)) was plotted versus the accustomed drug levels.

Figure 4.23 summarizes the trial outcome as a comparison of the four PCT release curves that have been constructed from an analysis of the acquired SWV sets. The plots for all four drug load settings displayed the already discussed distinct biphasic release characteristic of the preceding trials, with a fast release of surface-near PCT and a gradually decelerating liberation when the surface-distant drug follow.

Slopes were extracted from 4.23(b) for the initial release stage (0 to 30 minutes) and their comparison revealed, for instance, an about 4 times faster release for the hydrogel sample with highest PCT content, as compared to the one with lowest. In addition, a draw of the determined slope against the adjusted hydrogel PCT levels expressed well the linear dependence of diffusional PCT move out of the formulation into dissolution medium that was expected from the straight proportionality to the concentration gradient (Figure 4.24) as driving force for the process.

In a final set of robotic voltammetry dissolution trials the characteristics of at room temperature PCT release from bare 1% agarose hydrogels were determined verified for either strongly acidic, pH 1.2, or slightly alkaline, pH 8.0, buffer solutions. The corresponding cumulative release profile constructions are displayed in Figure 4.25. It can be observed that profile that is valid for pH 1.2 is not significantly different to the one measured at pH 8.0. Apparently, the intensity of PCT molecule liberation from its storage place was about the same for the two conditions. Behind this may be that the hydroxyl groups of acetaminophen are related to a pKa of 9.5 (Prescott, 1980) and PCT is protonated and thus uncharged at both pH settings of the trial. Furthermore it has been reported that the solubility of PCT in aqueous media is not noticeably varying with acidity/alkalinity (Tasic *et al.*, 1992). The congruence of the PCT/hydrogel release curves is therefore a sign that the drug species is stable in properties with influence power on movement speed in an entrapping polymer matrix and at the same time confirms that agarose as primary storage gel does not change much for a move from pH 1.2 to 8.0 in its capability to entangle PCT.

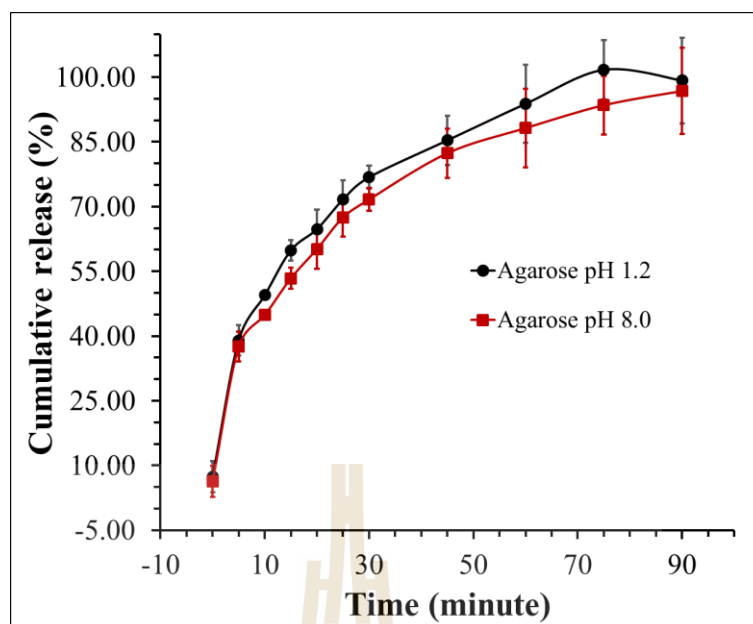


Figure 4.25 PCT release profiles as constructed with data from triplicate comparative robotic voltammetry release trials at room temperature for 1% agarose hydrogels with a 2 mM PCT load at pH 1.2 (black curve) and 8.0 (red curve). Each data point in the graphs represents the mean concentration, and the error bars represent the standard deviation. The measuring conditions were as specified before, for the tests related to Figure 4.20 and Figure 21.

The results of this part of thesis work are convincing evidence that the established robotic microplate PCT SWV voltammetry is a well-working and convenient analytical approach for studying drug release from hydrogel-type polymer formulations. The assessment of the drug discharge is basically happening at real-time, with no operator involvement after robotic trial start. Strength of the automated screening technique is its convenience, which will be particularly valuable when - in course of advanced drug delivery system development large numbers of samples/formulations have to be worked on for design optimization. To further outline the potential of the methodology the extension of an application to inspections of paracetamol release from

thin films of two synthetic and one biological polymers, blends of those, and their composites with agarose gels will be described and discussed.

4.2.2 Robotic microplate-based voltammetry as screening tool for drug release from synthetic and natural polymer thin films and their blends with agarose hydrogels: A comparative case study

In the preceding sections, robotic PCT DPV and SVW were evidenced as successful analytical practice for the quantification of model drug PCT in samples from pharmaceutical tablet dissolution testing or for the drug release profiling of bare agarose hydrogels. Described in this chapter is a further extension of the methodology to an accurate evaluation of the liberation of PCT from thin films of two synthetic and one biological polymer, as well as from blends of these the two materials with each other and with agarose hydrogels.

The tested biopolymer was chitosan, the deacetylated version of the structural component of the chitin shells of, for instance, marine crustaceans and insects (refer to Figure 4.26). The two synthetic polymers, here abbreviated as polymers S1-1 and S2-2, were acrylate-based macromolecules that combined in their structure as ribbon linear carbon chains with three different building block attachments: (1) a sulfonic acid moiety on a benzene ring, (2) an epoxy entity as ester side group of a carboxylic acid attachment and (3) an aliphatic multiple carbon chain as ester side group of another carboxylic acid functionality (refer to Figure 4.27). Polymers S1-1 and S2-2 were actually part of a large-number polymer library that was in the laboratory of the external RGJ host at the Ruhr-University of Bochum, first and foremost prepared for advanced biosensor fabrication. The polymer collection served in this context as valued tunable starting material for the smart synthesis of redox polymers that then, for

instance, could be exploited in advanced (enzyme) biosensor designs to directly chain the biocatalytic protein to electrified solid interfaces (Lopez *et al.*, 2017; Ruff *et al.*, 2017). Here they were kindly supplied by Prof. Schuhmann and his group member, Dr. Adrian Ruff for the purpose of PCT release testing. Worth mentioning that changes in the molar ratios of the sulfonic acid, epoxy and carbon chain building blocks actually allowed to create polymers with various degrees of hydrophilicity/hydrophobicity and cross-linking character, respectively. The materials that were trialed via microplate robotic voltammetry regarding the time course of PCT release of stored PCT are listed and categorized in Table 4.3. 4 one-, 5 two- and 2 three-component PCT formulations were inspected in triplicate at room temperature and pH 1.2 and 8 and then linked with their particular PCT release profiles.

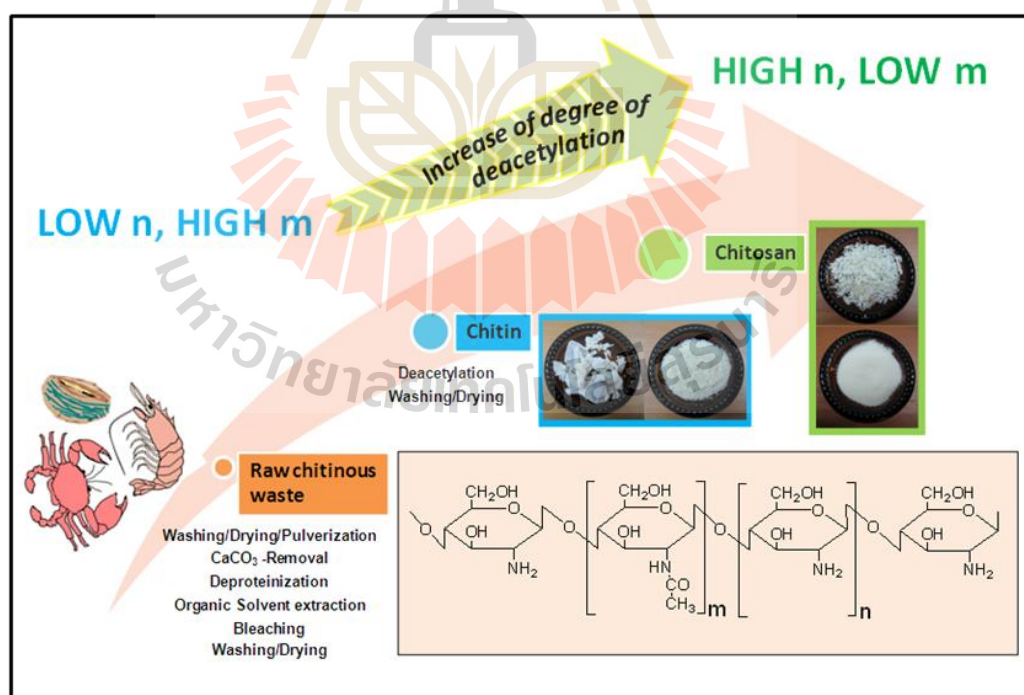


Figure 4.26 Origin and molecular structures of the biopolymer chitosan, which is product of a deacetylation of chitin, the material of the shells of marine crustaceans and insect skin (Suginta *et al.*, 2013).

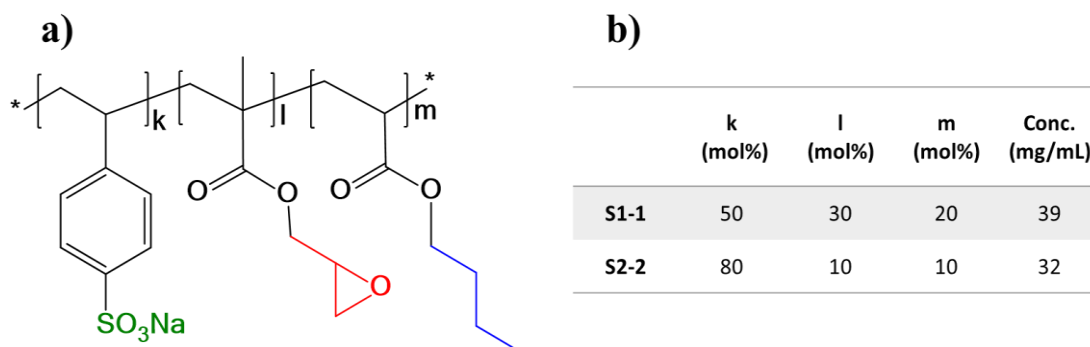


Figure 4.27 Molecular structures of polymers S1-1 and S2-2. a) Fundamental ribbon is an acrylate-based polymer chain with attached styrene sulfonic acid, epoxy and aliphatic carbon side chains. b) Stoichiometric molar ratios (in %) of the 3 units in P(SS-GMA-BA)-S1 (or S1-1) and P(SS-GMA-BA)-S2 (or S2-2). The epoxy group in the S1-1 and S2-2 structure allows individual polymer strings to crosslink.

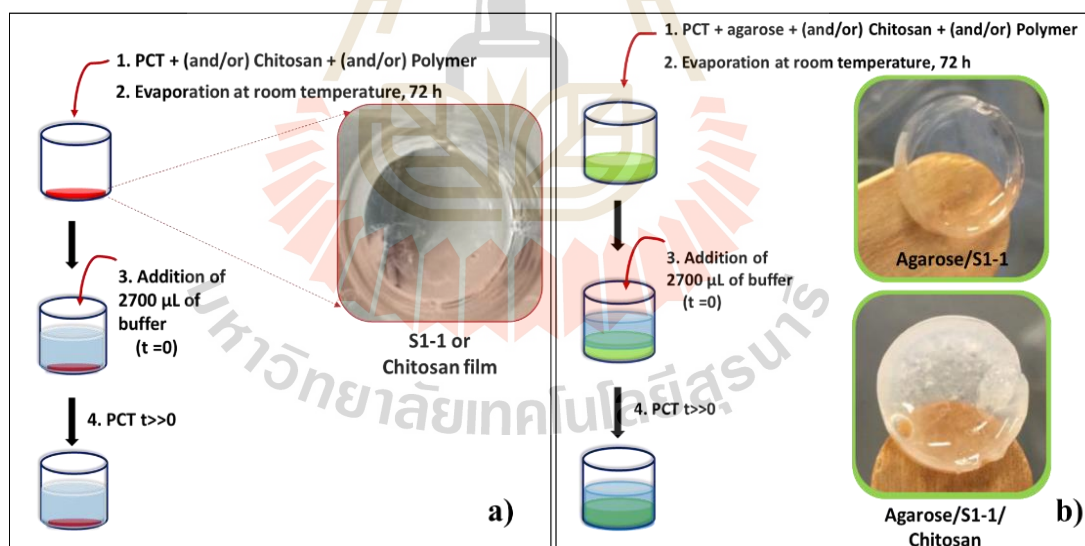


Figure 4.28 Schematic and photographs of the preparation of PCT-loaded chitosan+S1-1 or S2-2 blends with agarose hydrogels and pure chitosan, S1-1, or S2-2 films with PCT charge in 24-well microtiter plate containers. The photos in a) a typical PCT+polymer film is shown. The photos in b) compare a bare PCT+agarose hydrogel with an PCT+agarose+S1-1+chitosan equivalent.

Table 4.3 Materials trialed via microplate robotic voltammetry as to the time course of their PCT storage properties. The PCT concentration for all listed systems was maintained at 2 mM.

Category	Material	Physical form
One-component	Agarose	Gel
	Chitosan	Film
	Polymer S1-1	Film
	Polymer S2-2	Film
Two-component	Agarose + Chitosan	Gel
	Agarose + S1-1	Gel
	Agarose + S2-2	Gel
	Chitosan + S1-1	Film
	Chitosan + S2-2	Film
Three-component	Agarose + Chitosan + S1-1	Gel
	Agarose + Chitosan + S2-2	Gel

S1-1 or S2-2 films with PCT load were prepared by mixing 150 μ L of 39 mg/mL S1-1 or 32 mg/mL S2-2 polymer with 150 μ L of 4 mM paracetamol in the microtiter plate wells No.A3, A4, and A5 and allow solvent evaporation to take place, as explained in the previous section for PCT+agarose hydrogel samples. For chitosan 90 μ L of a 1% solution of the biomaterial was blended in plate wells No.A3, A4, and A5 with 60 μ L of 10 mM PCT stock and 150 μ L of water and solvent disappearance was waited. Robotic SVW analysis of the PCT release speed in wells with target systems was carried out at room temperature in buffer solutions with the pH values of 1.2 and 8.0 in the same manner as described for the automated measurements on bare

agarose hydrogels. Through the usual SVW peak current determination and value transformation into accumulative PCT levels the related cumulative release profiles for the 11 formulations were constructed. Following will be the presentation of the obtained information on the drug release behavior of the 11 polymer and polymer+agarose systems and a comparison of particular cases will be used to underline the identified remarkable distinctions. The cumulative PCT release from bare agarose (Figure 4.25) was used as sort of reference.

4.2.2.1 Release characteristics for the film-like one-component chitosan, S1-1 or S2-2 PCT formulations

The obtained cumulative drug release profiles for the film-like one-component chitosan, S1-1 or S2-2 PCT formulations at pH 1.2 and 8.0 are shown in the Figure 4.29, in comparison to the equivalent curve of bare agarose. The character of the release profiles of the four drug storage materials got through the comparative robotic electroanalysis trials disclosed as markedly different. At pH 1.2, about full release of charged PCT was, for instance, reached for chitosan already after about 15 minutes, for agarose it took with 75 minutes much more time, polymer S2-2 used 105 minutes and on the timescale of the trial (150 minutes) polymer S1-1 did not get to full discharge at all.

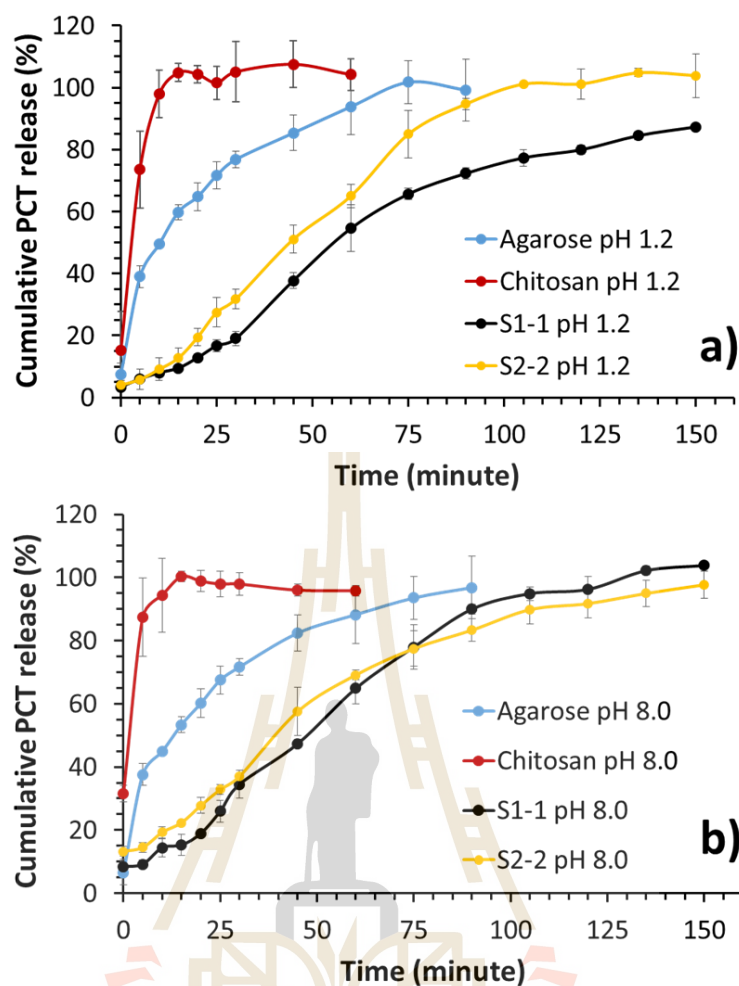


Figure 4.29 Cumulative PCT release (in %) from chitosan (red), S1-1 (black), and S2-2 (yellow) and agarose (blue) formulations at room temperature in 0.1 M K_2SO_4 - H_2SO_4 at pH 1.2 a) and at slightly alkaline buffer at pH 8.0 b). Each data point represents the average value of a triplicate repetition and the error bars represent the associated standard deviation.

At pH 8.0, the time needed for release completion is about the same for chitosan but slightly stretched for the bare agarose (75 → 90 minutes) and the polymer S2-2 (105 → 135 minutes) storage systems. And at the moderately alkaline condition also the polymer S1-1 becomes capable to expel about its entire PCT content after 150 minutes of buffer solution exposure. In fact, the agarose hydrogel and chitosan

(refer to Appendix D.3 as Figure D.1 and D.2) PCT release profiles as a whole did not vary much with a pH change for the dissolution buffer from acidic to weakly alkaline settings. PCT release profiles of S2-2 thin film followed the agarose and chitosan example and were pH independent while S1-1 thin films seemed to be easier freed at the higher pH (refer to Figure 4.30).

A comparison of the four release trends in Figure 4.29 revealed that independent on pH the PCT release from agarose starts very rapidly but then gradually slows down until discharge completion is reached at about 90 minutes. In clear contrast the release curve for chitosan film is for both pH settings much steeper with only a short span of gradually decaying phase and full release thus faster. The PCT release from both polymers, S1-1 and S2-2, on the other hand, is at pH 1.2 and 8 visibly lagging behind the agarose and chitosan cases and interestingly the beginning of discharge is somewhat delayed for these thin-film formulations. As PCT neither swaps charge state nor varies solubility with a pH 1.2 to 8.0 modification, the observation of the highest PCT release rates for a chitosan thin-film, as compared to a thick agarose hydrogel (refer to Figure 4.22 for the release model) and S1-1 or S2-2 thin films, is likely related a more direct access of the dissolving buffer solution to PCT molecules at or in a thin surface deposit and not hydrogel pellet and of a weaker association of the drug with the polymer carrier. Compared to S2-2, the polymer S1-1 has less ionizable sulfonic acid groups ($k_{S1-1} < k_{S2-2}$ in the structure in Figure 4.27), is more crosslinked ($l_{S1-1} > l_{S2-2}$ in the structure in Figure 4.27) and more hydrophobic ($m_{S1-1} > m_{S2-2}$ in the structure in Figure 4.27). The effect of these dissimilarities impact on swelling properties and their entanglement of PCT molecules may explain the lone slight dependence of PCT release on dissolution buffer pH.

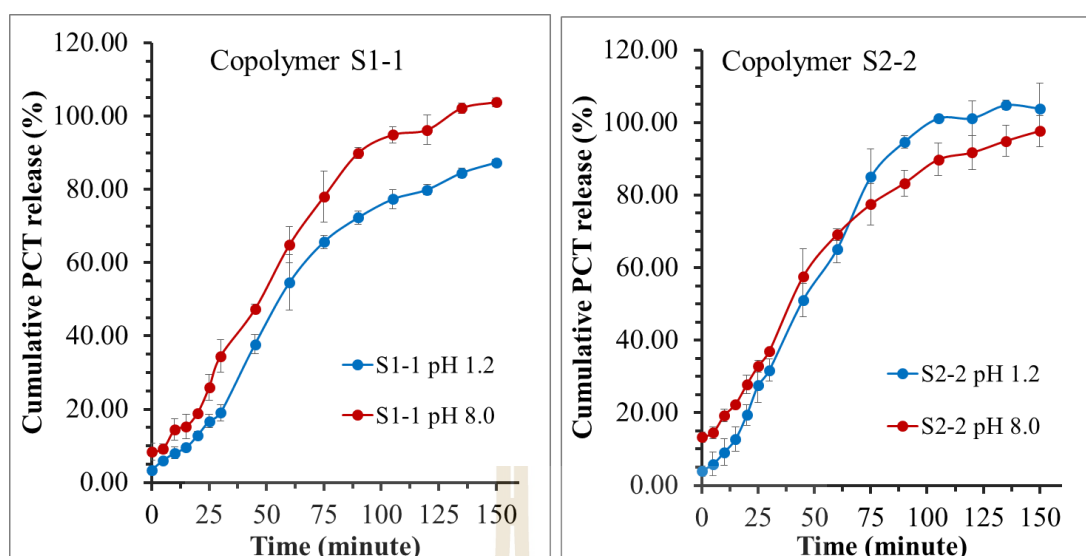


Figure 4.30 Cumulative PCT release (in %) from thin films of the polymers S1-1 (left), and S2-2 (right) at room temperature in 0.1 M K_2SO_4 - H_2SO_4 at pH 1.2 and at slightly alkaline buffer at pH 8.0. Each data point represents the average value of a triplicate repetition and the error bars represent the associated standard deviation.

Based on the pronounced variances in their vertical dimensions (thicknesses) the releases from hydrogel pellets and polymer thin films are meant to be completely different the travel length of stored molecules from the matrix interior to the its solution interface, where complete solution internalization takes place, is significantly varied (refer to Figure 4.31). Accordingly, full content PCT discharge from a ‘three population’ agarose hydrogel in a simple extrapolation of this model would be suggested slower than the one from a ‘one-population’ polymer thin film with only surface-near drug. However, an interesting phenomenon supported by the results of the robotic voltammetry release studies of this chapter was that the PCT release from thin polymer films can be modulated to speedier OR slower release rates as to the agarose reference, just by the playing with choice of the chemical nature of the storing polymeric species. Apparently, the affinity between stored drug and the entrapping

matrix, the matrix crosslinking levels and chemical identity and matrix physical dimensions jointly regulate the time course of drug release in a complex manner.

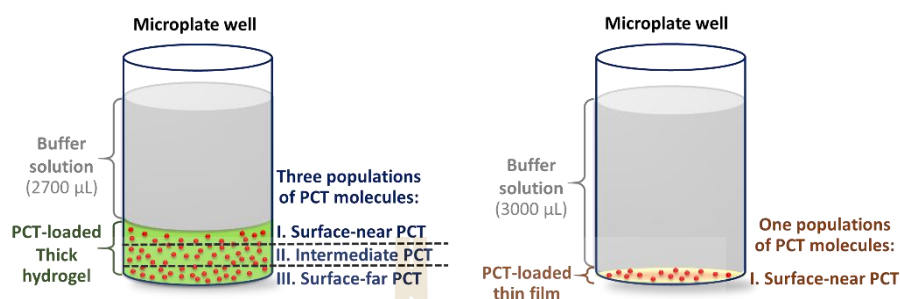


Figure 4.31 Schematic representation of the possible behavior of drug release in the thick and thin hydrogel.

4.2.2.2 Release characteristics of the agarose+chitosan, agarose+S1-1 or S2-2, chitosan+S1-1 or S2-2 and agarose+chitosan+S1-1 or S2-2 PCT formulations.

Since their automated acquisition in the robotic voltammetry workstation was well convenient and reliable, specific PCT release profiles were also determined for four gel- or film-like 2-component and two gel-like 3-component matrix formulations with blends of the materials that have been inspected in pure form regarding their PCT storage or release properties in the previous section. Approached were, to be more exact, the agarose+chitosan, agarose+S1-1, agarose+S2-2, chitosan+S1-1, chitosan+S2-2, agarose+chitosan+S1-1, and agarose+chitosan+S2-2 systems. Figures 4.32 to Figures 4.37 offer the particular cumulative release profiles of the trials and the following conclusions can be drawn from their analysis:

- (1) Agarose+chitosan: For a blend of chitosan with an agarose hydrogel the release characteristics seems to be dominated by agarose component. Chitosan addition does

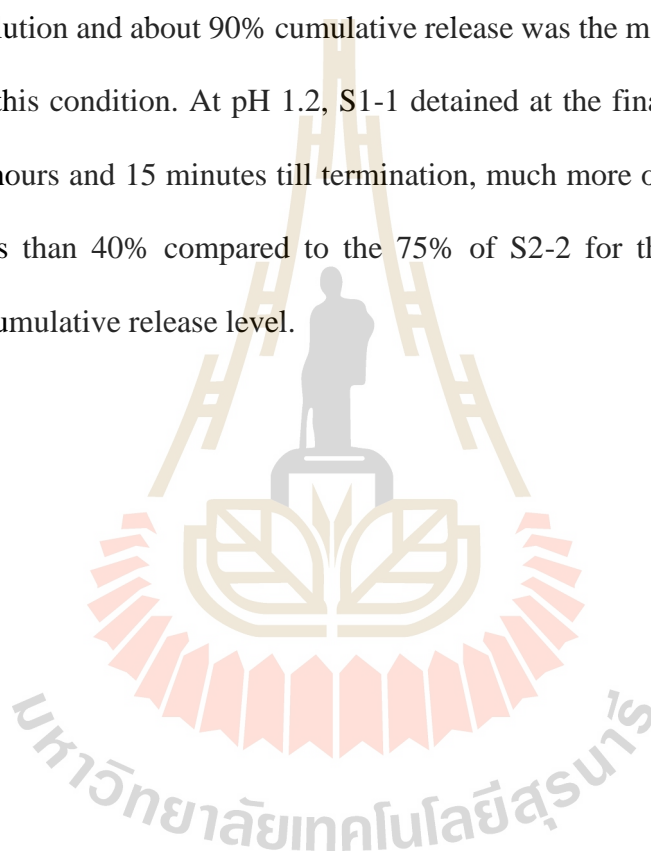
not change the release kinetics at pH 8.0 and 100% release is possible as for the two pure components of the mixture. However, at an acidic pH of 1.2, which is below the pKa of chitosan's NH₂ functionality, complete discharge of the PCT load is for the agarose+chitosan system limited to about 80%; full release is hindered. Apparently, a the charge state of the amino groups along chitosan polymer strings in the agarose hydrogel matrix (cationic at low and neutral at high pH) has an effect on the strength of PCT entrapment and effects cumulative release levels.

(2) Agarose+S1-1, agarose+S2-2: As for agarose+chitosan equivalent the dynamics of PCT release from agarose+S1-1 and agarose+S2-2 drug formulations seems to be dominated by the hydrogel properties. In fact, the addition of polymer S2-2 to an agarose hydrogel leaves its PCT release characteristics at both trialed pH conditions almost unaffected. Polymer S1-1 addition, instead, causes a clear compression of the cumulative release capacity of the hydrogel formulation to about 85% (pH 8.0) and 70% (pH 1.2).

(3) Chitosan+S1-1, chitosan+S2-2: When used in blends with chitosan both, S1-1 and S2-2 presence, abolished the very fast PCT release that was observed for a bare PCT+chitosan formulation. Instead, the release followed more closely the characteristics of the particular bare PCT+polymer formulation. Interestingly, PCT in a chitosan+S1-1 matrix was released to larger cumulative levels at pH 8 and not 1.2 while the departure of the drug from a chitosan+S2-2 matrix was more complete at pH 1.2 instead of 8.0. PCT solubility and molecule charge do not change for the tested pH challenge. Important for the observed effect is the complex interplay of variations in the identities of the functional groups on the polymer strings of the storage matrix. These are actually chitosan's amino (at pH 1.2, protonated and thus cationic and at pH 8.0, neutral) and polymers S1-1 and S2-2 sulfonic acid (at pH 1.2, protonated and thus

neutral and at pH 8.0, deprotonated and thus anionic) groups. Further biasing role is that polymer S1-1 has considerably less sulfonic acid entities, more crosslinking power and larger hydrophobicity as polymer S2-2.

(4) Agarose+chitosan+S1-1 and agarose+chitosan+S2-2: Neither in strongly acidic nor in slightly alkaline release medium these two formulations were able to fully release their adjusted PCT content. At pH 8.0, S1-1 and S2-shared an about similar time course of PCT dissolution and about 90% cumulative release was the maximum possible drug discharge at this condition. At pH 1.2, S1-1 detained at the final stage of dissolution trial, after 3 hours and 15 minutes till termination, much more of its PCT content and just little less than 40% compared to the 75% of S2-2 for this condition was the determined cumulative release level.



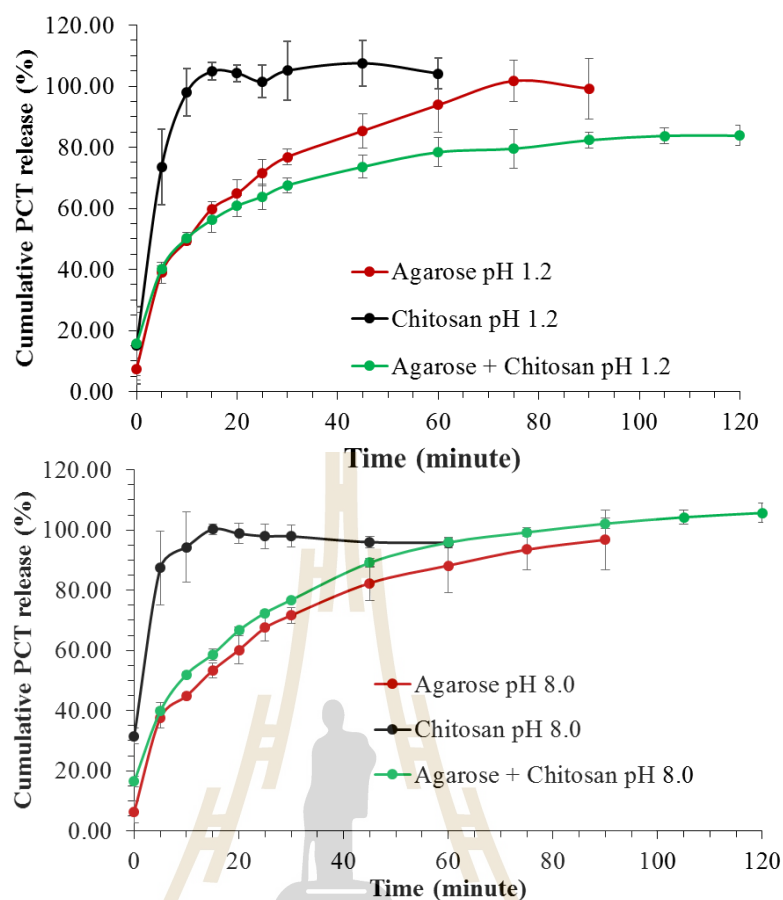


Figure 4.32 Cumulative PCT release (in %) from PCT+agarose+chitosan hydrogel pellets at room temperature in 0.1 M K_2SO_4 - H_2SO_4 at pH 1.2 (top) and at slightly alkaline buffer at pH 8.0 (bottom). Each data point represents the average value of a triplicate repetition and the error bars represent the associated standard deviation.

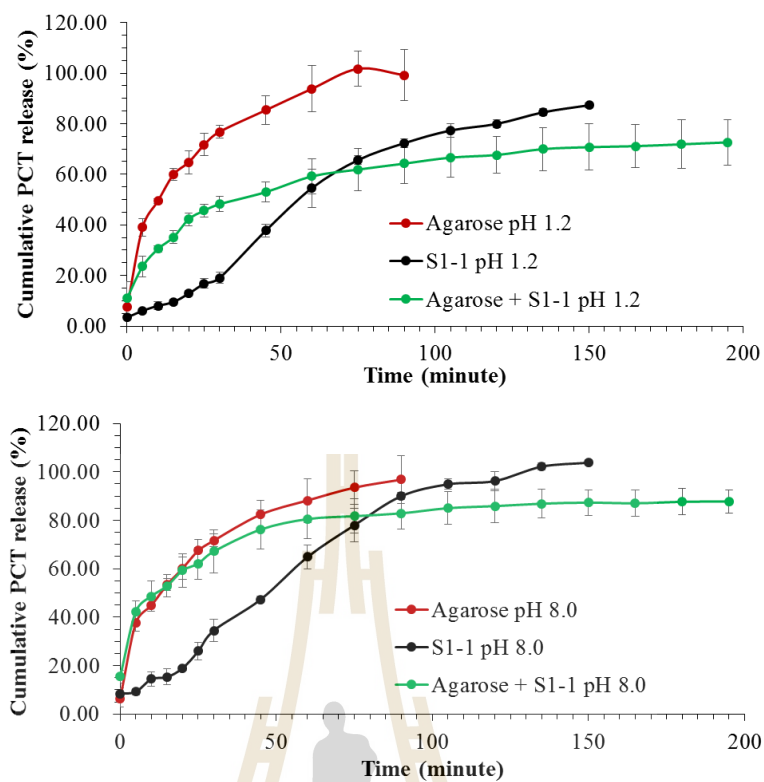


Figure 4.33 Cumulative PCT release (in %) from PCT+agarose+S1-1 hydrogel pellets at room temperature in 0.1 M K_2SO_4 - H_2SO_4 at pH 1.2 (top) and at slightly alkaline buffer at pH 8.0 (bottom). Each data point represents the average value of a triplicate repetition and the error bars represent the associated standard deviation.

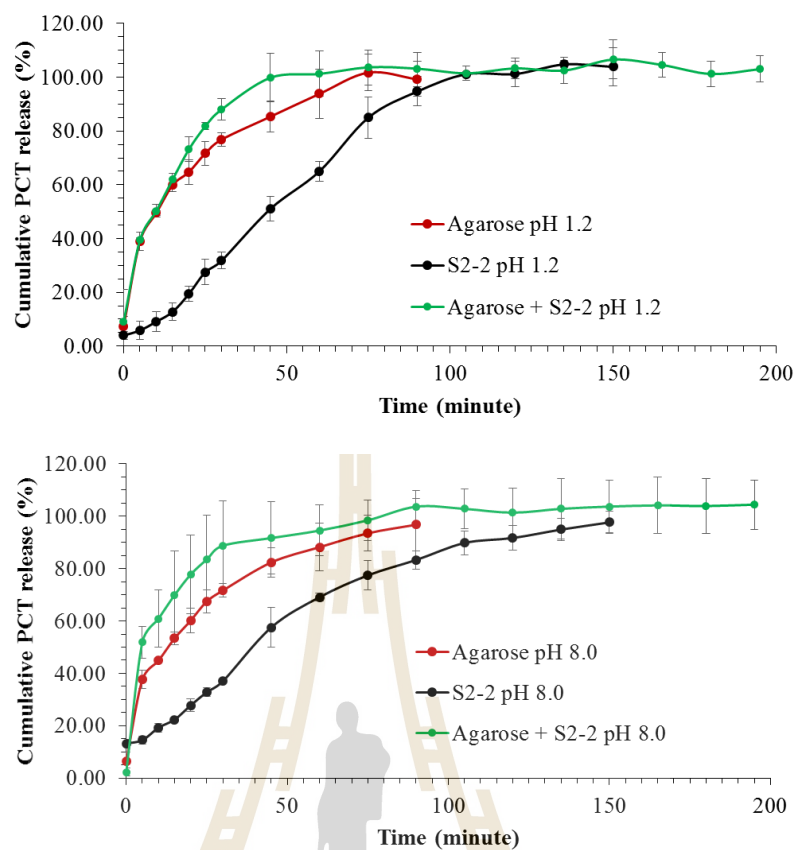


Figure 4.34 Cumulative PCT release (in %) from PCT+agarose+S2-2 hydrogel pellets at room temperature in 0.1 M $K_2SO_4-H_2SO_4$ at pH 1.2 (top) and at slightly alkaline buffer at pH 8.0 (bottom). Each data point represents the average value of a triplicate repetition and the error bars represent the associated standard deviation.

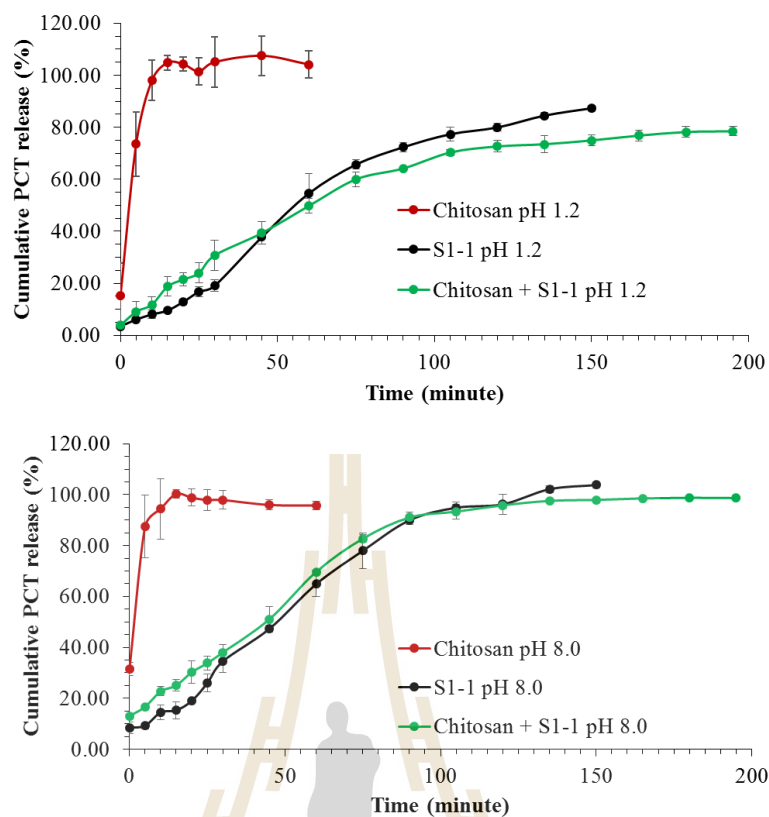


Figure 4.35 Cumulative PCT release (in %) from PCT+chitosan+S1-1 thin films at room temperature in 0.1 M $K_2SO_4-H_2SO_4$ at pH 1.2 (top) and at slightly alkaline buffer at pH 8.0 (bottom). Each data point represents the average value of a triplicate repetition and the error bars represent the associated standard deviation.

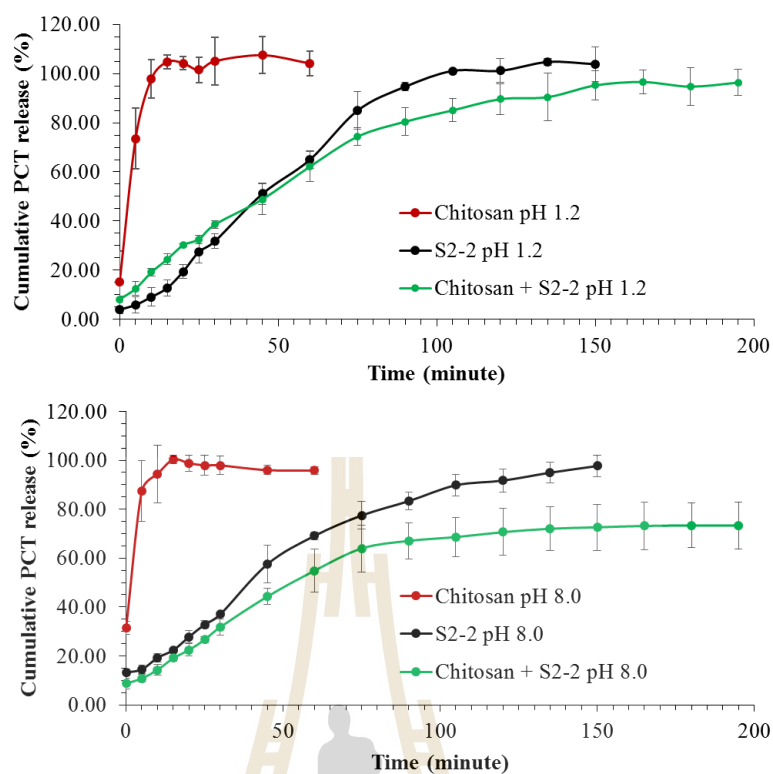


Figure 4.36 Cumulative PCT release (in %) from PCT+chitosan+S2-2 thin films at room temperature in 0.1 M $K_2SO_4-H_2SO_4$ at pH 1.2 (top) and at slightly alkaline buffer at pH 8.0 (bottom). Each data point represents the average value of a triplicate repetition and the error bars represent the associated standard deviation.

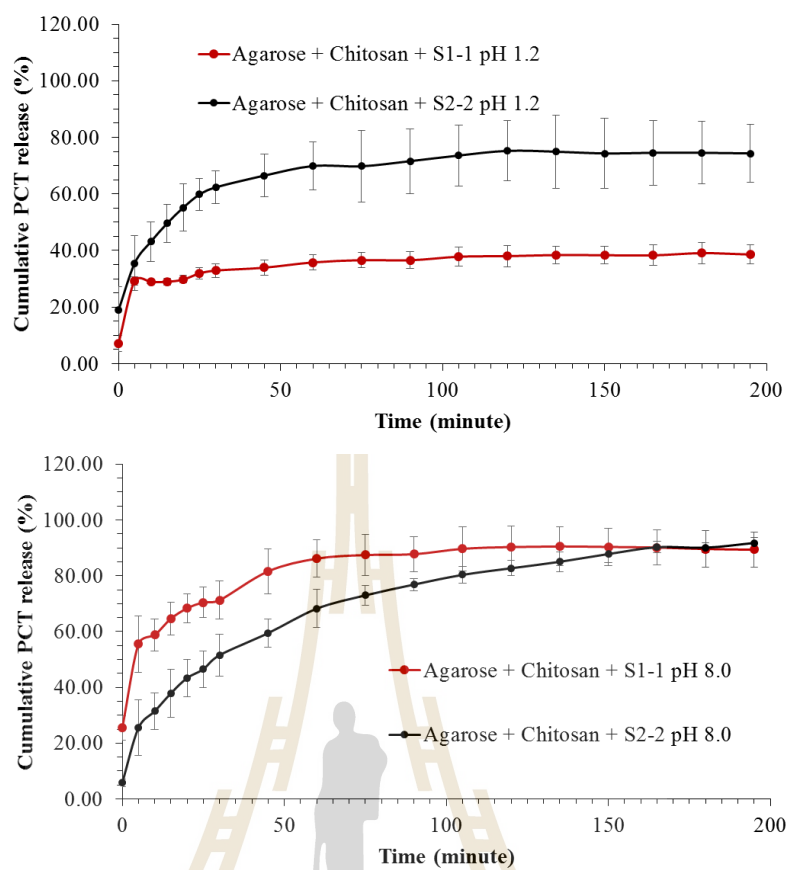


Figure 4.37 Cumulative PCT release (in %) from PCT+agarose+chitosan+S1-1 and PCT+agarose+chitosan+S2-2 hydrogel pellets at room temperature in 0.1 M K_2SO_4 - H_2SO_4 at pH 1.2 (top) and at slightly alkaline buffer at pH 8.0 (bottom). Each data point represents the average value of a triplicate repetition and the error bars represent the associated standard deviation.

4.3 Electrical copper disk electrodes as oxidase biosensor platforms with cathodic of H₂O₂ assessment

Often, glucose oxidase (GOx) biosensors are operated at anodic potentials of e.g. + 600 to + 800 mV vs. RE for the detection of hydrogen peroxide that is released via enzymatic glucose conversion into gluconolactone. Disadvantage is that at the rather strong positive sensor polarization the presence of any other oxidizable compound in the sample solutions would also cause the generation of a biosensor current signal and thus adversely interfere with the glucose determination. The move to cathodic hydrogen peroxide is one of the possible strategies that have been suggested as a solution for interference suppression with oxidase-based biosensors. In the following it will be shown that simple electrical cable copper disk electrodes can actually serve nicely as interference-free cathodic amperometric platforms for H₂O₂ analysis in GOx-based biosensors.

Good GOx biosensor performance depends on the electrochemical reliability and sensitivity of the enzyme-carrying electrode as well as on the ability of the immobilizing matrix to stably hold the biological recognition element in close distance to the signal-transducing electrified sensor surface. Figure 4.38a) shows the end of a completed electrical cable Cu disk electrode as it appears after thorough mechanical polishing on emery paper and finally a cloth soaked with alumina paste. The metal disk is smooth and firmly entrapped in the glass/epoxy insulation.

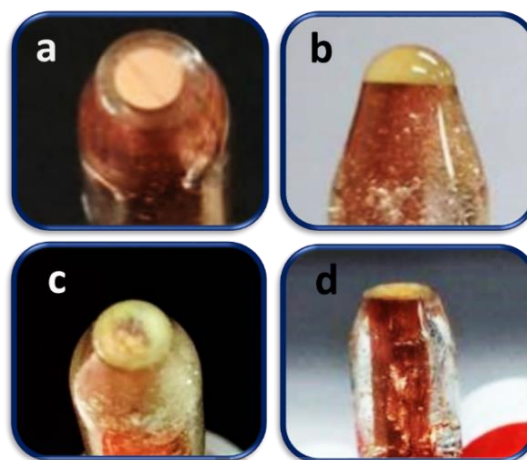


Figure 4.38 Display photographs of the electrical cable used as the precursor for Cu electrode fabrication a) a completed Cu disk electrode b) a Cu disk electrode with a 10 μL drop of a GOx/Nafion solution applied and c) top views and d) the and side views of the modified Cu disk electrode after solvent evaporation, coated with a dry GOx-containing Nafion film.

Easy drop-and-dry coating was used to place a GOx-immobilizing Nafion thin film on polished Cu disks. Figure 4.38(b) to Figure 4.38(d), forming finally electrical cable Cu glucose biosensors of disk geometry. Used for the procedure was a single application of a 10 μL droplet of an aqueous solution of 10 mg/mL GOx in 5% Nafion. As later measurements confirmed the strength of the attachment of the air-dried GOx/Nafion layers to the Cu disks was good enough to survive continuous solution stirring during biosensor calibration and sample measurements in standard addition mode, without noticeable detachment.

Bare versions of the illustrated Cu disk electrodes were tested with respect to their performance for cathodic H_2O_2 amperometry. After GOx/Nafion modification they were then inspected for their quality in serving as glucose biosensor with cathodic H_2O_2 detection. Figure 4.39 shows the outcome of a typical calibration trial in which a

prototype of an electrical cable Cu disk electrode was exposed in a continuously stirred measuring solution to increasing levels of H_2O_2 , while the amperometric current was recorded as a function of time at a potential of -0.15 V vs. reference (Ag/AgCl).

As expected the sequential addition of H_2O_2 aliquots produced well-pronounced stepwise increases in the sensor current, with a response time of 5-10 s. Calibration plots of the averaged background corrected electrode currents versus H_2O_2 concentration were consistently linear up to 1200 mM, with a sensitivity of about $0.65\ \mu\text{A}\ \mu\text{M}^{-1}\ \text{cm}^{-2}$, approaching saturation at higher H_2O_2 concentrations (Figure 4.39(b)). Incremental rises in H_2O_2 concentration as small as $5\ \mu\text{M}$ triggered reliable current steps of matching amplitude and this is considered the practical detection limit of the proposed Cu electrodes (not shown).

The performance cathodic H_2O_2 amperometry at cable Cu disk electrodes for quantitative analyte analysis was evaluated in the standard addition mode by an application for the determination of spiked model samples with known content. A typical original current trace of such a trial with $100\ \mu\text{M}\ \text{H}_2\text{O}_2$ is shown in Figure 4.40(a). The corresponding standard addition plot is shown in Figure 4.40(b).

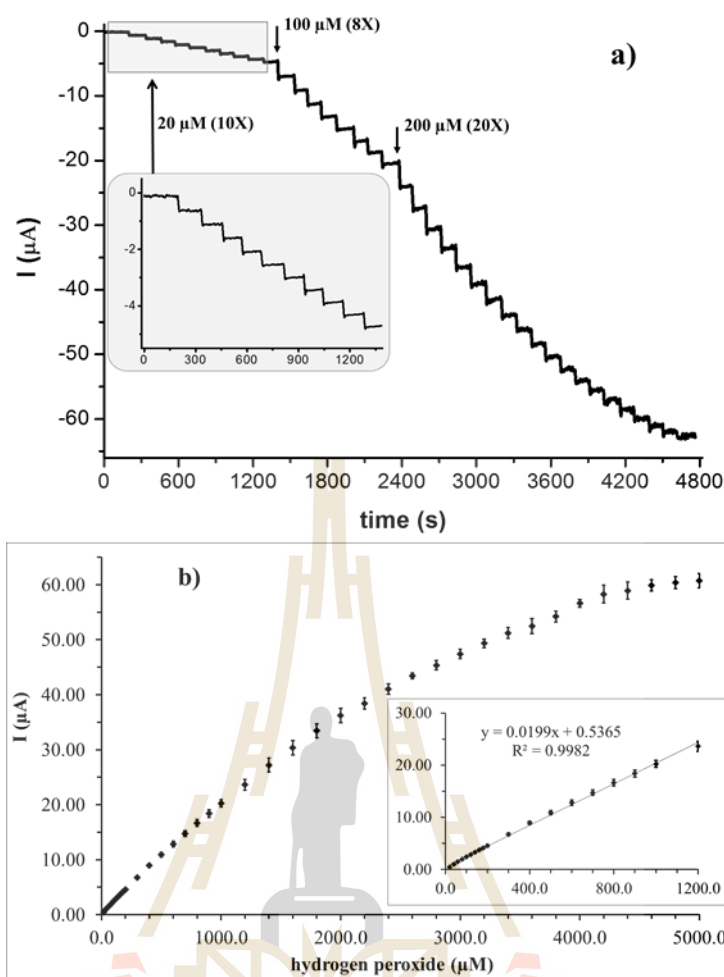


Figure 4.39 Amperometric H_2O_2 calibration measurements via cathodic potential at an cable Cu disk electrode. a) Response of a Cu disk electrode to successive additions of aliquots of a H_2O_2 stock solution to a continuously stirred measuring solution (0.1 M PBS at $\text{pH}=7$). The working electrode potential and stirring rate were -0.15 V vs. reference and 200 rpm, respectively. The inset shows the plot for the first ten additions of H_2O_2 , with zoomed x and y axes. b) Calibration graph constructed with the averaged data from triplicate chronoamperometric trials as shown in the example to the left. Error bars represent the standard deviations for the repeated measurements.

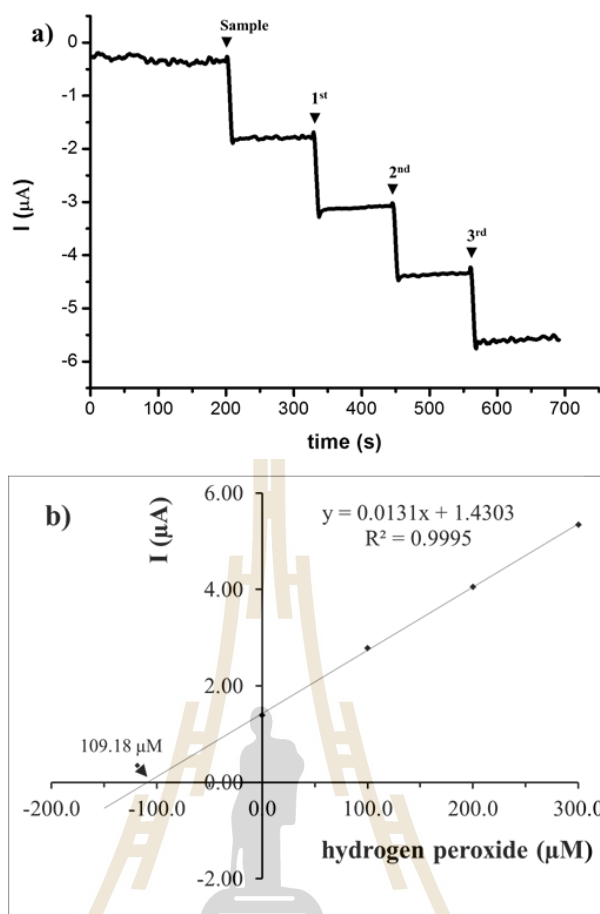


Figure 4.40 Standard addition mode of H_2O_2 quantification via cathodic amperometric at an electrical cable Cu disk electrode in continuously stirred 0.1 M PBS (pH=7) and with -0.15 V vs. RE as detection potential. a) Sensor current response vs. time in course of a $100 \mu\text{M}$ sample supplementation and three $100 \mu\text{M}$ standard additions and b) the corresponding standard addition plot with the regression graph analysis.

The original H_2O_2 concentration in the sample was then obtained from the intersection of the extrapolation of the linear fit ($R^2 = 0.9995$) with the x-axes. In this particular attempt, the analyte concentration measured was $109.2 \mu\text{M}$, compared to its known concentration of $100 \mu\text{M}$. Through triplicate repetitions of the trial the average recovery rate was obtained as 107.6%, with a relative standard deviation of 2.32%.

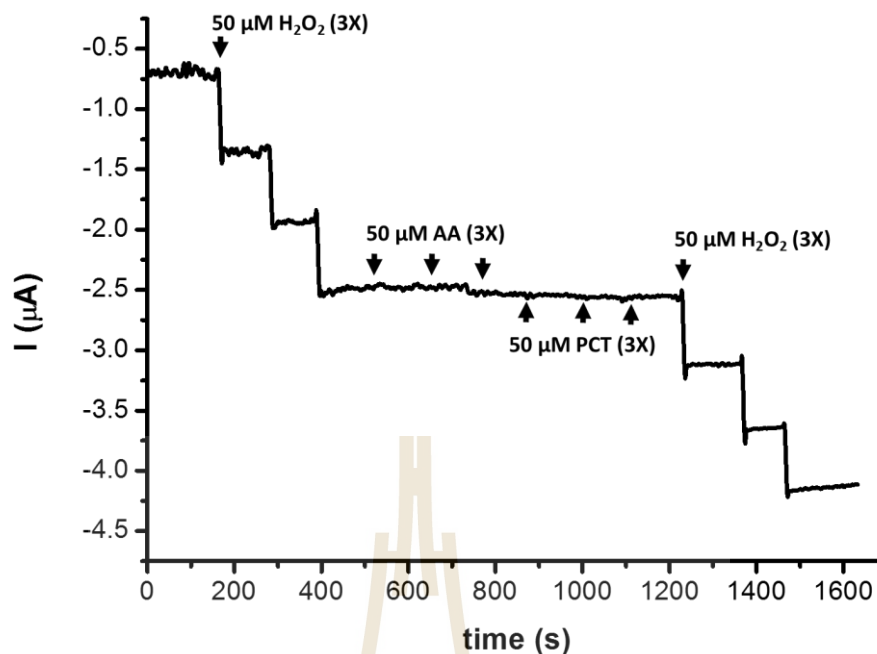


Figure 4.41 Amperometric response of a Cu disk electrode in continuously stirred 0.1 M PBS (pH=7) to successive triplicate additions of 50 mM of analyte (H_2O_2), interferences (ascorbic acid, AA and PCT) and analyte again. The parameters were used -0.15 V vs. reference as working electrode potential and 200 rpm as stirring rate.

Operation of electrical cable Cu electrodes at a negative H_2O_2 detection potential was expected to eliminate interference by compounds that would generate anodic currents at high positive detection potential. Figure 4.41 shows the outcome of an interference study with ascorbic acid and PCT that was supposed to confirm the expectation. Neither ascorbic acid nor the drug, which are common interfering constituents of blood and urine samples, induced the step-like rises in sensor current that were seen for additions of H_2O_2 . This proved that the choice of a cathodic H_2O_2 detection potential indeed was helped to avoid signal disturbance by the interferences such as ascorbic acid and PCT. As electrical cable Cu disk electrodes also showed a reasonable linear range, low detection limit and acceptable average recovery they were

further tested as interference-free cathodic H_2O_2 detection platforms of glucose biosensors.

A coating with a GOx-containing polymeric Nafion layer actually converted the Cu disk electrode to a glucose biosensor that could be operated at negative potential for cathodic detection of H_2O_2 produced by enzymic substrate oxidation. Figure 4.42 displays the outcome of the analytical signals achieved. Figure 4.42(a) shows the amperometric recording from a freshly prepared prototype biosensor operated with a working potential of -0.15 V relative to the reference, in 0.1 M PBS pH=7.0, while sequential additions of aliquots of a stock glucose solution were carried out. Each glucose injection produced an immediate rises in cathodic current, which reached a steady state level in 30-40 s. The resultant plot of background-corrected sensor currents vs. glucose concentrations is shown in Figure 4.42(b). The calibration graph for triplicate trials was linear from 20 μM to 1500 μM , with a slope of 0.22 $\text{nA } \mu\text{M}^{-1}$ (sensitivity of 7 $\text{nA } \mu\text{M}^{-1} \text{ cm}^{-2}$) for a regression through the first 16 data points, and a correlation coefficient of 0.9987 . Increases in glucose concentration as small as 20 μM produced current steps of consistent amplitude and this level is thus the practical detection limit for sample analysis with cable Cu glucose biosensors.

An assessment of the efficiency of sample recovery was approached through quantitative analysis of spiked measuring buffers (model samples) with known glucose content via cathodic amperometry in the standard addition mode. Figure 4.43(a) is a display of a typical amperometric current trace from such a trial, for a 100 μM glucose model sample. Figure 4.43(b) displays the corresponding standard addition graph and the extraction of the sample glucose concentration from the plot identified 109.0 μM as the measured analyte level. Triplicate trial repetition exposed the average recovery rate for the glucose determinations as 106.0 ± 4.1 μM ($n=3$).

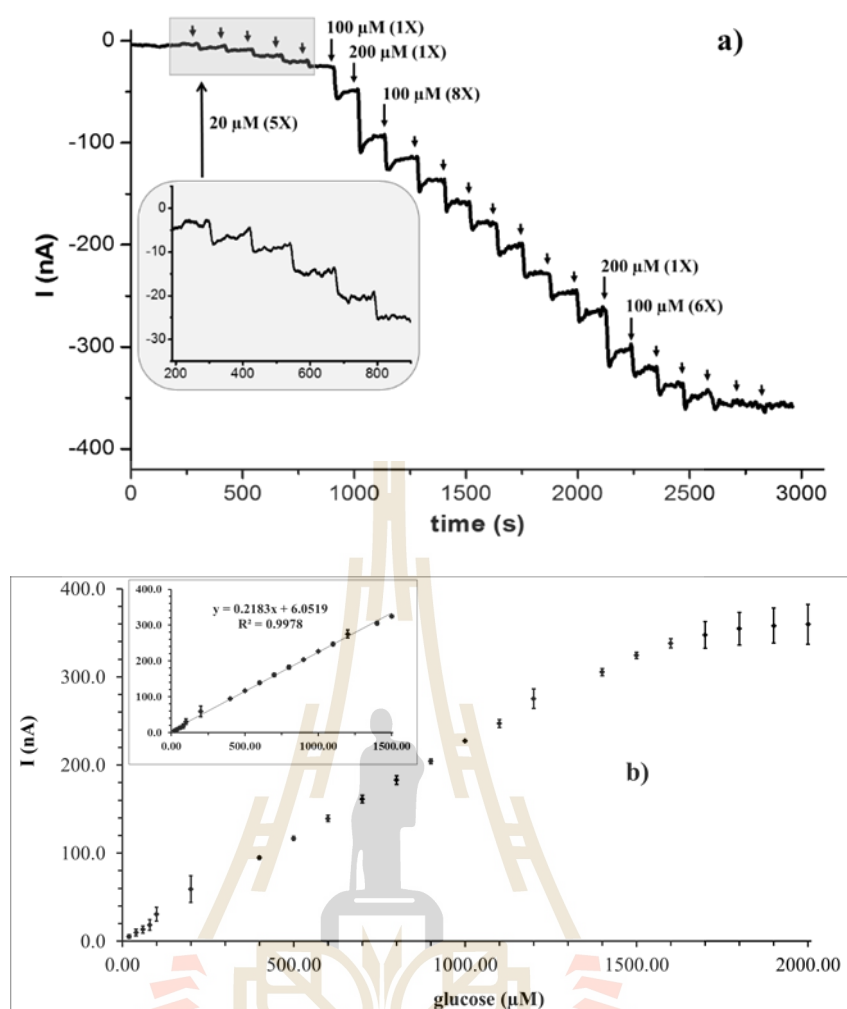


Figure 4.42 Amperometric glucose calibration measurements with cathodic potential. a) Amperometric response of GOx/Nafion-modified cable Cu disk electrode to successive additions of aliquots of a glucose stock solution, in continuously stirred 0.1 M PBS (pH=7). The working electrode potential and stirring rate were set to -0.15 V vs. reference and 200 rpm, respectively. The inset is the I/t curve for the first 5 glucose additions, with zoomed x and y axes. b) Calibration graph constructed with the averaged data from triplicate amperometric trials as shown in the example to the left. The error bars represent the standard deviations for the repeated current measurements.

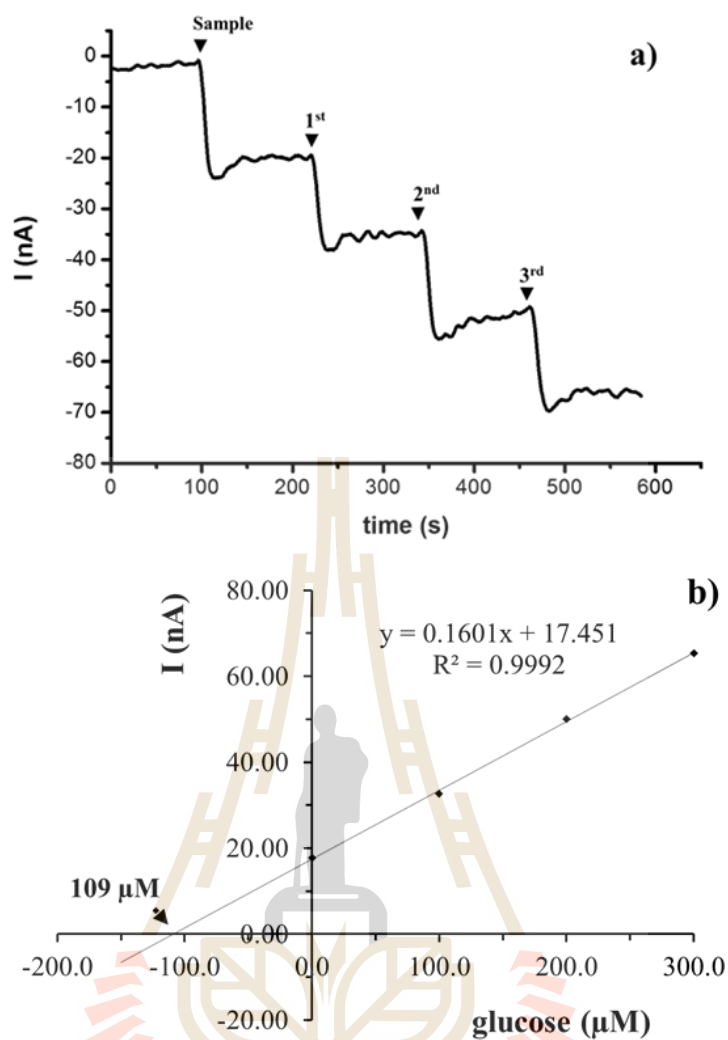


Figure 4.43 Standard addition mode of glucose quantification via cathodic amperometric. a) Amperometric recording of GOx/Nafion-modified cable Cu disk electrode for glucose determination by standard addition. Electrolyte: 0.1 M PBS (pH=7.0); electrode modification: GOx/Nafion; working electrode potential: -0.15 V vs. reference; stirring rate: 200 rpm; adjusted glucose solution concentration: 100 mM; standard additions: 3×100 mM rises. b) Shown the standard addition plot for the analytical run.

Repeated modifications of a single cable Cu disk electrode with a functional GOx/Nafion layer, with surface polishing in between, gave reproducible results. A good reproducibility was also obtained when three separate Cu disk precursor electrodes were identically modified and the consistency of the signals was assessed (refer to Figure 4.44(a)). Figure 4.44(b) shows plots of the background-corrected currents from the individual electrodes as a function of the glucose concentration in the measuring buffer, for seven serial substrate additions. Amplitudes of individual biosensor signals were directly proportional to glucose concentration, with all three regression coefficients settling above 0.999. The slopes of the calibration plots were slightly different; however the standard deviation of only $\pm 12\%$ from the average value is acceptable, given that the electrical Cu cable used to construct the sensors may have differed slightly in cross-sectional area along its length.

The demonstrated analytical performance of cable Cu based glucose biosensors should qualify the tool for application to standard real sample analysis, including use for blood and urine glucose screening from healthy people or clinical patients. The greatest advantage of the novel biosensor described in this study, however, is that its good performance in glucose assays is accomplished with a design that is significantly simpler and cheaper than those of electrodes with other cathodic interference protection.

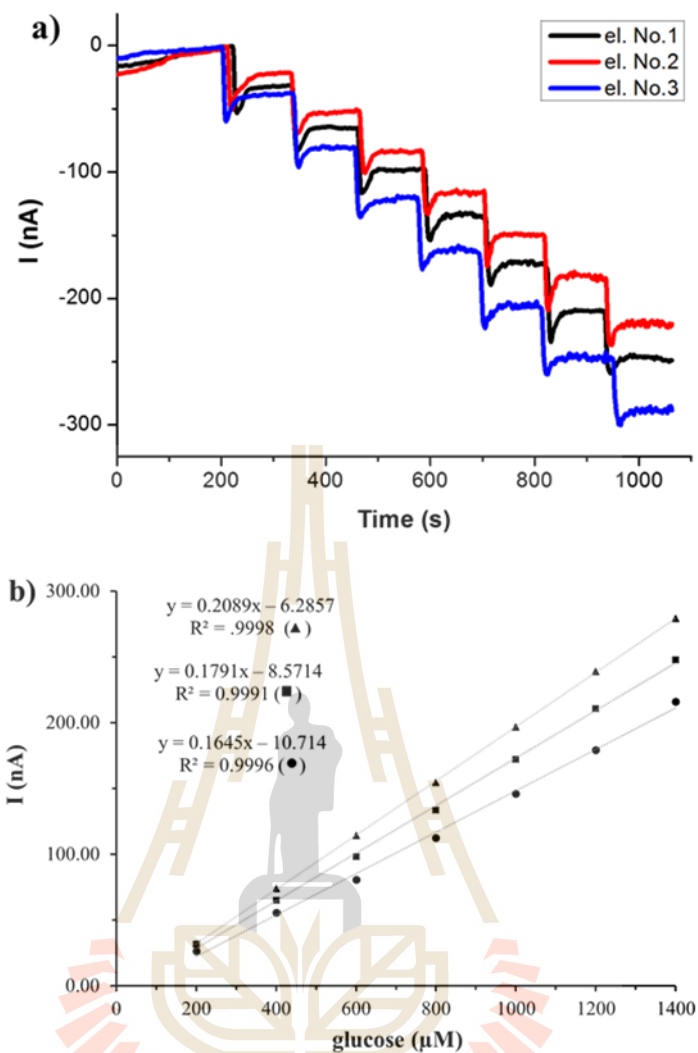


Figure 4.44 Reproducibility of three separate GOx/Nafion-modified Cu electrode at cathodic peroxide detection potential. a) Amperometric glucose calibrations of three separate GOx/Nafion-modified cable Cu disk electrodes. The glucose concentration was raised in 200 μM increments until 1400 μM level in the measuring buffer was reached (Electrolyte: 0.1 M PBS at pH=7.0); electrode modification: GOx/Nafion; working electrode potential: -0.15V vs. reference; stirring rate: 200 rpm). b) The averaged background-subtracted current step amplitudes from three-times measured curves as in a) displayed as a function of the actual glucose concentration.

CHAPTER V

CONCLUSIONS AND OUTLOOK

5.1 Robotic voltammetry for drug product dissolution testing

Accomplished in this dissertation was microtiter plate-based robotic drug quantification that was shown to be capable of screening the many samples from pharmaceutical drug dissolution testing conveniently and accurately, without permanent operator involvement. The methodology was established for Paracetamol[®] (PCT) as model drug of choice and the time courses of the release of this drug were in a series of proof-of-principle trials inspected for commercial tablet formulations, an agarose hydrogel or polymer thin films:

- (1) For sample sets from a standard pharmaceutical dissolution test with the commercial PCT tablets robotic voltammetry generated successfully copies of their known distinct release characteristics. Drug dissolution of the immediate release PCT formulation was, for instance, correctly confirmed as a mono-phasic quick drug discharge process. For the more advanced extended release tablet nicely visualized were, on the other hand, the two phases of the initial quick dissolution of the peripheral drug content followed by slower PCT ejection from the tablet core.
- (2) Incorporation of a computer-controllable syringe pump into the setup for robotic voltammetry and the related gain of triggered microplate

electrolyte filling facilitated an extension from samples of simple tablet dissolution tests to direct release trials on PCT-charged hydrogels and polymer thin films at individual microplate well bottoms. Examined with the approach was PCT release from bare agarose hydrogels, chitosan or synthetic polymer thin films, blends of agarose/chitosan, agarose/synthetic polymers, or chitosan/synthetic polymers and agarose/chitosan/synthetic polymer fusions. For a set of actually 11 different one-, two- or three-component PCT-entrapping systems the specific release profiles were obtained based on the data from automated PCT voltammetry runs and marked differences in the time course of PCT liberation were well evidenced between the individual thick agarose-based hydrogels and thin film polymer systems.

Both the drug content quantification in externally generated PCT samples from traditional tablet dissolution tests and direct screening of PCT in microplates with PCT-loaded hydrogel/polymer implementations worked very well with robotic voltammetry. Compared to the traditional manual electrochemical valuation of dissolution study samples, one at a time, the automation that was reached here for this task work is releasing laboratory staff from monotonous replications of massive numbers of identical measurements. Obvious benefits for users are therefore a pronounced convenience, human error minimization and availability of staff for execution of other tasks. Robotic voltammetry in microplate wells has the potential to make drug release profiling more economic and pleasant, as long as the target compounds are well enough redox active. Accordingly, the established methodology is worth to be considered for more systematic application in pharmaceutical R&D as a complementary analytical assay for authentic drug release trials on targeted storage matrix innovations. Future

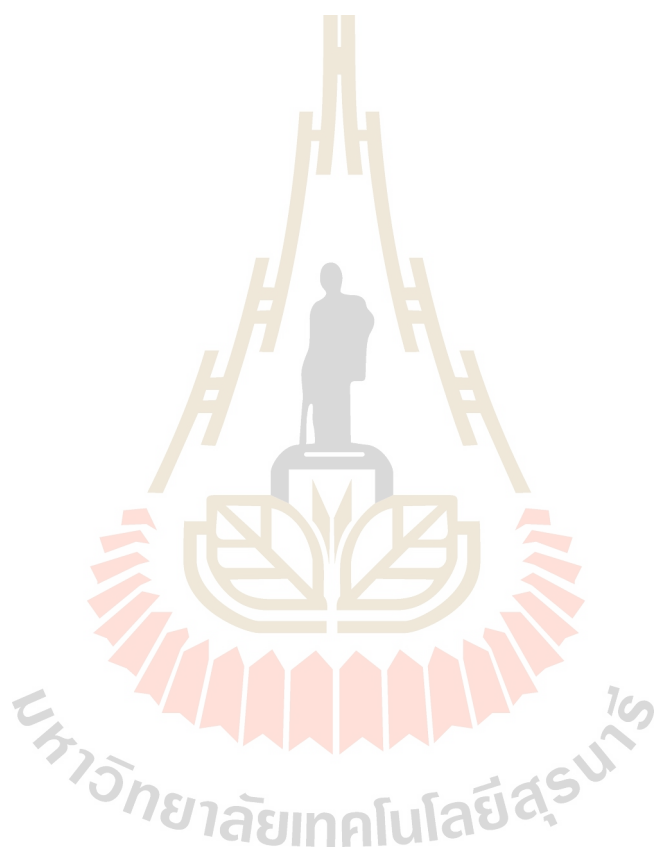
technical advancements could address the incorporation of micro- or nanoscopic sensors for detection limit/sensitivity enhancement, the move from 24- to 96-well microplates for sample throughput increase and the development of software scripts for automated post-trial data readout and release profile construction.

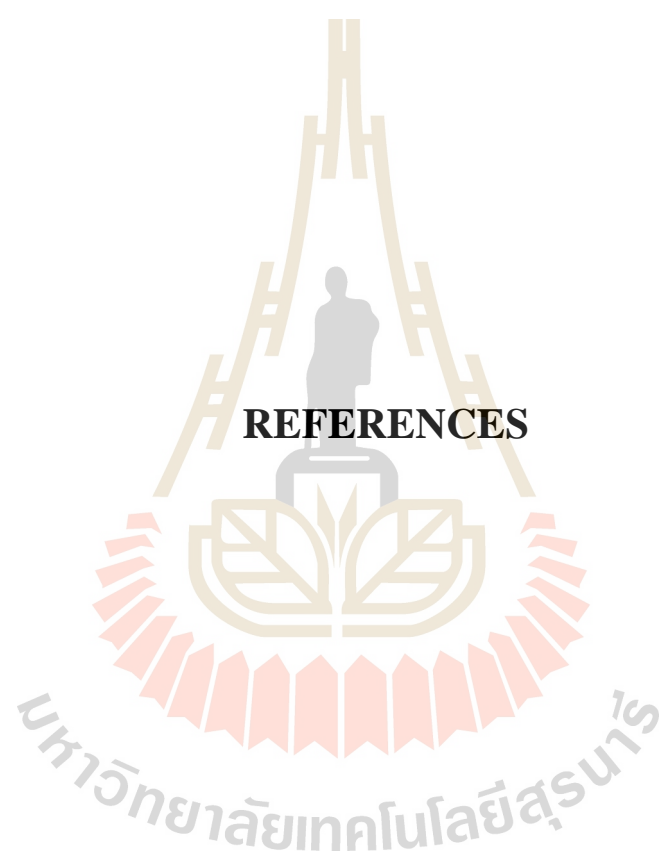
5.2 Cable copper disk electrodes as oxidase biosensor platforms

Electrical cable-based Cu disk electrodes were first assembled and then converted into glucose biosensors by drop-coating with a GOx/Nafion surface layer. The capability of negatively polarized Cu surfaces to electrochemically reduce H_2O_2 made completion of cable Cu glucose biosensors possible at which analyte peroxide was measured at -0.15 V vs. reference. Main advantage of the biosensor operation at cathodic detection potential was the reach of a protection of the acquired current signal against contributions from species that would interfere at the more common anodic polarization. The calibration curve of cable Cu glucose biosensors delivered a linear response up to 1.5 mM, with a practical detection limit of 20 μM at the lower end. With these performance levels the accomplished cable Cu-based tool is suitable for the determination of glucose, whether in targets from food and drink production or in clinical blood or urine samples. On top of the beneficial interference elimination cable Cu glucose biosensors are very easily made from an almost free material. Accordingly, they present a cheap sensor alternative for glucose assessments in academic teaching or industrial research laboratories.

Further work should possibly tackle an extension of the design of Cu-based oxidase biosensors from the macro- to microscopic platform dimension. The valuable assets of miniaturized sensors regarding signal-to-noise ratios and spatial resolution

may well enable local glucose analysis with exquisite sensitivity and detection limit for trace (glucose) trials in small volumes or at tiny objects such as living cells.





REFERENCES

REFERENCES

- Alkire, R. C., Kolb, D. M., Lipkowski, J., and Ross, P. N. (2011). *Bioelectrochemistry: Fundamentals, Applications and Recent Developments* (Vol. 13): John Wiley & Sons.
- Allen, T. M., and Cullis, P. R. (2013). Liposomal Drug Delivery Systems: From Concept to Clinical Applications. **Advanced Drug Delivery Reviews**. 65(1): 36-48.
- Andrade, E. L., Bento, A. F., Cavalli, J., Oliveira, S. K., Freitas, C. S., Marcon, R., Schwanke, R. C., Siqueira, J. M., and Calixto, J. B. (2016). Non-Clinical Studies Required for New Drug Development - Part I: Early in Silico and in Vitro Studies, New Target Discovery and Validation, Proof of Principles and Robustness of Animal Studies. **Brazilian Journal of Medical and Biological Research**. 49(11): e5644.
- Baghayeri, M. (2015). Glucose Sensing by a Glassy Carbon Electrode Modified with Glucose Oxidase and a Magnetic Polymeric Nanocomposite. **Royal Society of Chemistry Advances**. 5(24): 18267-18274.
- Bessems, J. G., and Vermeulen, N. P. (2001). Paracetamol (Acetaminophen)-Induced Toxicity: Molecular and Biochemical Mechanisms, Analogues and Protective Approaches. **Critical Reviews in Toxicology**. 31(1): 55-138.
- Bhattarai, N., Gunn, J., and Zhang, M. Q. (2010). Chitosan-Based Hydrogels for Controlled, Localized Drug Delivery. **Advanced Drug Delivery Reviews**. 62(1): 83-99.

- Bobes, C. F., Abedul, M. T. F., and Costa-Garcia, A. (2001). Pneumolysin Elisa with Adsorptive Voltammetric Detection of Indigo in a Flow System. **Electroanalysis**. 13(7): 559-566.
- Boccaccini, A. R., Cho, J., Roether, J. A., Thomas, B. J. C., Minay, E. J., and Shaffer, M. S. P. (2006). Electrophoretic Deposition of Carbon Nanotubes. **Carbon**. 44(15): 3149-3160.
- Boopathi, M., Won, M. S., and Shim, Y. B. (2004). A Sensor for Acetaminophen in a Blood Medium Using a Cu(II)-Conducting Polymer Complex Modified Electrode. **Analytica Chimica Acta**. 512(2): 191-197.
- Borgmann, S., Radtke, I., Erichsen, T., Blochl, A., Heumann, R., and Schuhmann, W. (2006). Electrochemical High-Content Screening of Nitric Oxide Release from Endothelial Cells. **Chembiochem**. 7(4): 662-668.
- Brahman, P. K., Suresh, L., Lokesh, V., and Nizamuddin, S. (2016). Fabrication of Highly Sensitive and Selective Nanocomposite Film Based on C₆₀/Fullerene-C₆₀/Mwcnts: An Electrochemical Nanosensor for Trace Recognition of Paracetamol. **Analytica Chimica Acta**. 917: 107-116.
- Cheemalapati, S., Palanisamy, S., Mani, V., and Chen, S. M. (2013). Simultaneous Electrochemical Determination of Dopamine and Paracetamol on Multiwalled Carbon Nanotubes/Graphene Oxide Nanocomposite-Modified Glassy Carbon Electrode. **Talanta**. 117: 297-304.
- Chuanuwatanakul, S., Chailapakul, O., and Motomizu, S. (2008). Electrochemical Analysis of Chloramphenicol Using Boron-Doped Diamond Electrode Applied to a Flow-Injection System. **Analytical Sciences**. 24(4): 493-498.

- Clark, L. C., Jr., and Lyons, C. (1962). Electrode Systems for Continuous Monitoring in Cardiovascular Surgery. **Annals of the New York Academy of Sciences**. 102: 29-45.
- Cohen, J. L., Hubert, B. B., Leeson, L. J., Rhodes, C. T., Robinson, J. R., Roseman, T. J., and Shefter, E. (1990). The Development of Usp Dissolution and Drug Release Standards. **Pharmaceutical Research**. 7(10): 983-987.
- Colon, L. A., Dadoo, R., and Zare, R. N. (1993). Determination of Carbohydrates by Capillary Zone Electrophoresis with Amperometric Detection at a Copper Microelectrode. **Analytical Chemistry**. 65(4): 476-481.
- Dai, S., Ravi, P., and Tam, K. C. (2008). Ph-Responsive Polymers: Synthesis, Properties and Applications. **Soft Matter**. 4(3): 435-449.
- Daneshegar, P., Moosavi-Movahedi, A. A., Norouzi, P., Ganjali, M. R., Farhadi, M., and Sheibani, N. (2012). Characterization of Paracetamol Binding with Normal and Glycated Human Serum Albumin Assayed by a New Electrochemical Method. **Journal of the Brazilian Chemical Society**. 23(2): 315-321.
- de Las Heras Alarcon, C., Pennadam, S., and Alexander, C. (2005). Stimuli Responsive Polymers for Biomedical Applications. **Chemical Society Reviews**. 34(3): 276-285.
- de Oliveira, S. M., Siguemura, A., Lima, H. O., de Souza, F. C., Magalhaes, A. A. O., Toledo, R. M., and D'Elia, E. (2014). Flow Injection Analysis with Amperometric Detection for Morpholine Determination in Corrosion Inhibitors. **Journal of the Brazilian Chemical Society**. 25(8): 1399-1406.
- del Valle, E. M. M., Galan, M. A., and Carbonell, R. G. (2009). Drug Delivery Technologies: The Way Forward in the New Decade. **Industrial & Engineering Chemistry Research**. 48(5): 2475-2486.

- Deng, S. Y., Zhang, G. Y., Shan, D., Liu, Y. H., Wang, K., and Zhang, X. J. (2015). Pyrocatechol Violet-Assisted in Situ Growth of Copper Nanoparticles on Carbon Nanotubes: The Synergic Effect for Electrochemical Sensing of Hydrogen Peroxide. **Electrochimica Acta**. 155: 78-84.
- Diebold, S. M. (2005). Physiological Parameters Relevant to Dissolution Testing: Hydrodynamic Considerations. In (pp. 127-191): Taylor & Francis: London, UK.
- Diercks, S., Metfies, K., and Medlin, L. K. (2008). Development and Adaptation of a Multiprobe Biosensor for the Use in a Semi-Automated Device for the Detection of Toxic Algae. **Biosensors and Bioelectronics**. 23(10): 1527-1533.
- Dogan, B., Golcu, A., Dolaz, M., and Ozkan, S. A. (2009). Electrochemical Behaviour of the Bactericidal Cefoperazone and Its Selective Voltammetric Determination in Pharmaceutical Dosage Forms and Human Serum. **Current Pharmaceutical Analysis**. 5(2): 179-189.
- Ensafi, A. A., Ahmadi, N., Rezaei, B., and Abarghoui, M. M. (2015). A New Electrochemical Sensor for the Simultaneous Determination of Acetaminophen and Codeine Based on Porous Silicon/Palladium Nanostructure. **Talanta**. 134: 745-753.
- Erichsen, T., Reiter, S., Ryabova, V., Bensen, E. M., Schuhmann, W., Markle, W., Tittel, C., Jung, G., and Speiser, B. (2005). Combinatorial Microelectrochemistry: Development and Evaluation of an Electrochemical Robotic System. **Review of Scientific Instruments**. 76(6).
- Ezhil Vilian, A. T., Rajkumar, M., and Chen, S. M. (2014). In Situ Electrochemical Synthesis of Highly Loaded Zirconium Nanoparticles Decorated Reduced Graphene Oxide for the Selective Determination of Dopamine and Paracetamol

in Presence of Ascorbic Acid. **Colloids and Surfaces B: Biointerfaces**. 115: 295-301.

Fanjul-Bolado, P., Lamas-Ardisana, P. J., Hernandez-Santos, D., and Costa-Garcia, A. (2009). Electrochemical Study and Flow Injection Analysis of Paracetamol in Pharmaceutical Formulations Based on Screen-Printed Electrodes and Carbon Nanotubes. **Analytica Chimica Acta**. 638(2): 133-138.

Fonseca, W. T., Santos, R. F., Alves, J. N., Ribeiro, S. D., Takeuchi, R. M., Santos, A. L., Assuncao, R. M. N., Filho, G. R., and Munoz, R. A. A. (2015). Square-Wave Voltammetry as Analytical Tool for Real-Time Study of Controlled Naproxen Releasing from Cellulose Derivative Materials. **Electroanalysis**. 27(8): 1847-1854.

Furman, W. B., and Walker, W. H. (1976). *Continuous Flow Analysis: Theory and Practice*: M. Dekker.

Ge, N. J., Wang, D. H., Peng, F., Li, J. H., Qiao, Y. Q., and Liu, X. Y. (2016). Poly(Styrenesulfonate)-Modified Ni-Ti Layered Double Hydroxide Film: A Smart Drug-Eluting Platform. **American Chemical Society Applied Materials & Interfaces**. 8(37): 24491-24501.

Giannos, S. A., Dinh, S. M., and Berner, B. (1995). Temporally Controlled Drug Delivery Systems: Coupling of Ph Oscillators with Membrane Diffusion. **Journal of Pharmaceutical Sciences**. 84(5): 539-543.

Gomez-Mascaraque, L. G., Mendez, J. A., Fernandez-Gutierrez, M., Vazquez, B., and San Roman, J. (2014). Oxidized Dextrins as Alternative Crosslinking Agents for Polysaccharides: Application to Hydrogels of Agarose-Chitosan. **Acta Biomaterialia**. 10(2): 798-811.

- Gray, V., Kelly, G., Xia, M., Butler, C., Thomas, S., and Mayock, S. (2009). The Science of Usp 1 and 2 Dissolution: Present Challenges and Future Relevance. **Pharmaceutical Research**. 26(6): 1289-1302.
- Gupta, V. K., Jain, R., Radhapyari, K., Jadon, N., and Agarwal, S. (2011). Voltammetric Techniques for the Assay of Pharmaceuticals-a Review. **Analytical Biochemistry**. 408(2): 179-196.
- Hanrahan, G., Patil, D. G., and Wang, J. (2004). Electrochemical Sensors for Environmental Monitoring: Design, Development and Applications. **Journal of Environmental Monitoring**. 6(8): 657-664.
- He, N., Xu, L., Wang, T., Du, J., Li, Z., Deng, Y., Li, S., and Ge, S. (2009). Determination of Paracetamol with Porous Electrochemical Sensor. **Journal of Biomedical Nanotechnology**. 5(5): 607-610.
- Hu, H. F., Feng, M., and Zhan, H. B. (2015). A Glucose Biosensor Based on Partially Unzipped Carbon Nanotubes. **Talanta**. 141: 66-72.
- Hughes, J. P., Rees, S., Kalindjian, S. B., and Philpott, K. L. (2011). Principles of Early Drug Discovery. **British Journal of Pharmacology**. 162(6): 1239-1249.
- Hui, J., Li, W., Guo, Y., Yang, Z., Wang, Y., and Yu, C. (2014). Electrochemical Sensor for Sensitive Detection of Paracetamol Based on Novel Multi-Walled Carbon Nanotubes-Derived Organic-Inorganic Material. **Bioprocess and Biosystems Engineering**. 37(3): 461-468.
- Intarakamhang, S., Leson, C., Schuhmann, W., and Schulte, A. (2011). A Novel Automated Electrochemical Ascorbic Acid Assay in the 24-Well Microtiter Plate Format. **Analytica Chimica Acta**. 687(1): 1-6.
- Intarakamhang, S., Schuhmann, W., and Schulte, A. (2013). Robotic Heavy Metal Anodic Stripping Voltammetry: Ease and Efficacy for Trace Lead and

- Cadmium Electroanalysis. **Journal of Solid State Electrochemistry**. 17(6): 1535-1542.
- Intarakamhang, S., and Schulte, A. (2012). Automated Electrochemical Free Radical Scavenger Screening in Dietary Samples. **Analytical Chemistry**. 84(15): 6767-6774.
- Jara-Ulloa, P., Salgado-Figueroa, P., Yanez, C., Nunez-Vergara, L. J., and Squella, J. A. (2012). Voltammetric Determination of Nifedipine on Carbon Nanotubes-Modified Glassy Carbon Electrode: A New Application to Dissolution Test Studies. **Electroanalysis**. 24(8): 1751-1757.
- Jia, W. Z., Wang, K., and Xia, X. H. (2010). Elimination of Electrochemical Interferences in Glucose Biosensors. **Trends in Analytical Chemistry**. 29(4): 306-318.
- Jovanovski, V., Hrastnik, N. I., and Hocevar, S. B. (2015). Copper Film Electrode for Anodic Stripping Voltammetric Determination of Trace Mercury and Lead. **Electrochemistry Communications**. 57: 1-4.
- Kang, X., Wang, J., Wu, H., Liu, J., Aksay, I. A., and Lin, Y. (2010). A Graphene-Based Electrochemical Sensor for Sensitive Detection of Paracetamol. **Talanta**. 81(3): 754-759.
- Kano, K., Takagi, K., Inoue, K., Ikeda, T., and Ueda, T. (1996). Copper Electrodes for Stable Subpicomole Detection of Carbohydrates in High-Performance Liquid Chromatography. **Journal of Chromatography A**. 721(1): 53-57.
- Kataoka, K., Harada, A., and Nagasaki, Y. (2012). Block Copolymer Micelles for Drug Delivery: Design, Characterization and Biological Significance. **Advanced Drug Delivery Reviews**. 64: 37-48.

- Kauffmann, J. M., Pekli-Novak, M., and Nagy, A. (1996). The Potential of Electroanalytical Techniques in Pharmaceutical Analysis. **Acta Pharmaceutica Hungarica**. 66(2): 57-64.
- Kawde, A. N., and Aziz, M. A. (2014). Porous Copper-Modified Graphite Pencil Electrode for the Amperometric Detection of 4-Nitrophenol. **Electroanalysis**. 26(11): 2484-2490.
- Keeley, G. P., McEvoy, N., Nolan, H., Kumar, S., Rezvani, E., Holzinger, M., Cosnier, S., and Duesberg, G. S. (2012). Simultaneous Electrochemical Determination of Dopamine and Paracetamol Based on Thin Pyrolytic Carbon Films. **Analytical Methods**. 4(7): 2048-2053.
- Khor, E., and Lim, L. Y. (2003). Implantable Applications of Chitin and Chitosan. **Biomaterials**. 24(13): 2339-2349.
- Kim, D. W., Cao, X. T., Kim, Y. H., Gal, Y. S., and Lim, K. T. (2017). Block Copolymeric Micelles of Poly(Ethylene Oxide)-B-Poly(Glycidylmethacrylate) for Ph-Triggered Drug Release. **Molecular Crystals and Liquid Crystals**. 644(1): 145-151.
- Kim, S. J., Park, S. J., and Kim, S. I. (2003). Swelling Behavior of Interpenetrating Polymer Network Hydrogels Composed of Poly(Vinyl Alcohol) and Chitosan. **Reactive and Functional Polymers**. 55(1): 53-59.
- Kocak, G., Tuncer, C., and Butun, V. (2017). Ph-Responsive Polymers. **Polymer Chemistry**. 8(1): 144-176.
- Kostewicz, E. S., Abrahamsson, B., Brewster, M., Brouwers, J., Butler, J., Carlert, S., Dickinson, P. A., Dressman, J., Holm, R., Klein, S., Mann, J., McAllister, M., Minekus, M., Muenster, U., Mullertz, A., Verwei, M., Vertzoni, M., Weitschies, W., and Augustijns, P. (2014). In Vitro Models for the Prediction of in Vivo

- Performance of Oral Dosage Forms. **European Journal of Pharmaceutical Sciences**. 57: 342-366.
- Kutluay, A., and Aslanoglu, M. (2014). An Electrochemical Sensor Prepared by Sonochemical One-Pot Synthesis of Multi-Walled Carbon Nanotube-Supported Cobalt Nanoparticles for the Simultaneous Determination of Paracetamol and Dopamine. **Analytica Chimica Acta**. 839: 59-66.
- Levy, G., and Nelson, E. (1961). United States Pharmacopeia and National Formulary Standards, Food and Drug Administration Regulations, and the Quality of Drugs. **New York State Journal of Medicine**. 61: 4003-4008.
- Lin, H., Xu, D.-K., and Chen, H.-Y. (1997). Simultaneous Determination of Purine Bases, Ribonucleosides and Ribonucleotides by Capillary Electrophoresis-Electrochemistry with a Copper Electrode. **Journal of Chromatography A**. 760(2): 227-233.
- Liu, J. H., Li, L., and Cai, Y. Y. (2006). Immobilization of Camptothecin with Surfactant into Hydrogel for Controlled Drug Release. **European Polymer Journal**. 42(8): 1767-1774.
- Lopez, F., Ma, S., Ludwig, R., Schuhmann, W., and Ruff, A. (2017). A Polymer Multilayer Based Amperometric Biosensor for the Detection of Lactose in the Presence of High Concentrations of Glucose. **Electroanalysis**. 29(1): 154-161.
- Mani, V., Devasenathipathy, R., Chen, S. M., Wang, S. F., Devi, P., and Tai, Y. (2015). Electrodeposition of Copper Nanoparticles Using Pectin Scaffold at Graphene Nanosheets for Electrochemical Sensing of Glucose and Hydrogen Peroxide. **Electrochimica Acta**. 176: 804-810.
- Marcus, R. A., and Sutin, N. (1985). Electron Transfers in Chemistry and Biology. **Biochimica et Biophysica Acta - Bioenergetics**. 811(3): 265-322.

- Markle, W., and Speiser, B. (2005). Combinatorial Microelectrochemistry - Part 3. On-Line Monitoring of Electrolyses by Steady-State Cyclic Voltammetry at Microelectrodes. **Electrochimica Acta**. 50(25-26): 4916-4925.
- Markle, W., Speiser, B., Tittel, C., and Vollmer, M. (2005). Combinatorial Micro Electrochemistry - Part 1. Automated Micro Electrosynthesis of Iminoquinol Ether and [1,2,4]Triazolo[4,3-Alpha]Pyridinium Perchlorate Collections in the Wells of Microtiter Plates. **Electrochimica Acta**. 50(14): 2753-2762.
- Millan, A. J., Moreno, R., and Nieto, M. I. (2002). Thermogelling Polysaccharides for Aqueous Gelcasting - Part 1: A Comparative Study of Gelling Additives. **Journal of the European Ceramic Society**. 22(13): 2209-2215.
- Mora, L., Chumbimuni-Torres, K. Y., Clawson, C., Hernandez, L., Zhang, L., and Wang, J. (2009). Real-Time Electrochemical Monitoring of Drug Release from Therapeutic Nanoparticles. **Journal of Controlled Release**. 140(1): 69-73.
- Morgan, M. E., and Freed, C. R. (1981). Acetaminophen as an Internal Standard for Calibrating in Vivo Electrochemical Electrodes. **Journal of Pharmacology and Experimental Therapeutics**. 219(1): 49-53.
- Nair, S. S., John, S. A., and Sagara, T. (2009). Simultaneous Determination of Paracetamol and Ascorbic Acid Using Tetraoctylammonium Bromide Capped Gold Nanoparticles Immobilized on 1,6-Hexanedithiol Modified Au Electrode. **Electrochimica Acta**. 54(27): 6837-6843.
- Niu, X. Y., Zhang, Z. L., and Zhong, Y. H. (2017). Hydrogel Loaded with Self-Assembled Dextran Sulfate-Doxorubicin Complexes as a Delivery System for Chemotherapy. **Materials Science and Engineering: C**. 77: 888-894.
- Obeidat, W. M., Abuznait, A. H., and Sallam, A. S. A. (2010). Sustained Release Tablets Containing Soluble Polymethacrylates: Comparison with Tableted

- Polymethacrylate Ipec Polymers. **An Official Journal of the American Association of Pharmaceutical Scientists**. 11(1): 54-63.
- Otarola, J., Garrido, M., Correa, N. M., and Molina, P. G. (2016). Square Wave Voltammetry: An Alternative Technique to Determinate Piroxicam Release Profiles from Nanostructured Lipid Carriers. **A European Journal of Chemical Physics and Physical Chemistry**. 17(15): 2322-2328.
- Paixao, T. R. L. C., and Bertotti, M. (2004). Development of a Breath Alcohol Sensor Using a Copper Electrode in an Alkaline Medium. **Journal of Electroanalytical Chemistry**. 571(1): 101-109.
- Palanisamy, S., Devasenathipathy, R., Chen, S. M., Ali, M. A., Karuppiah, C., Balakumar, V., Prakash, P., Elshikh, M. S., and Al-Hemaid, F. M. A. (2015). Direct Electrochemistry of Glucose Oxidase at Reduced Graphene Oxide and - Cyclodextrin Composite Modified Electrode and Application for Glucose Biosensing. **Electroanalysis**. 27(10): 2412-2420.
- Pandey, A. P., Singh, S. S., Patil, G. B., Patil, P. O., Bhavsar, C. J., and Deshmukh, P. K. (2015). Sonication-Assisted Drug Encapsulation in Layer-by-Layer Self-Assembled Gelatin-Poly (Styrenesulfonate) Polyelectrolyte Nanocapsules: Process Optimization. **Artificial Cells, Blood Substitutes, and Biotechnology**. 43(6): 413-424.
- Park, J. H., Saravanakumar, G., Kim, K., and Kwon, I. C. (2010). Targeted Delivery of Low Molecular Drugs Using Chitosan and Its Derivatives. **Advanced Drug Delivery Reviews**. 62(1): 28-41.
- Pei, X., Kang, W. J., Yue, W., Bange, A., Heineman, W. R., and Papautsky, I. (2014). Disposable Copper-Based Electrochemical Sensor for Anodic Stripping Voltammetry. **Analytical Chemistry**. 86(10): 4893-4900.

- Prescott, L. F. (1980). Kinetics and Metabolism of Paracetamol and Phenacetin. **British Journal of Clinical Pharmacology**. 10 Suppl 2: 291S-298S.
- Puga, A. M., Lima, A. C., Mano, J. F., Concheiro, A., and Alvarez-Lorenzo, C. (2013). Pectin-Coated Chitosan Microgels Crosslinked on Superhydrophobic Surfaces for 5-Fluorouracil Encapsulation. **Carbohydrate Polymers**. 98(1): 331-340.
- Putzbach, W., and Ronkainen, N. J. (2013). Immobilization Techniques in the Fabrication of Nanomaterial-Based Electrochemical Biosensors: A Review. **Sensors (Basel)**. 13(4): 4811-4840.
- Rainey, F., Kivlehan, F., Chaum, E., and Lindner, E. (2014). Toward Feedback Controlled Anesthesia: Automated Flow Analytical System for Electrochemical Monitoring of Propofol in Serum Solutions. **Electroanalysis**. 26(6): 1295-1303.
- Reanpang, P., Themsirimongkon, S., Saipanya, S., Chailapakul, O., and Jakmune, J. (2015). Cost-Effective Flow Injection Amperometric System with Metal Nanoparticle Loaded Carbon Nanotube Modified Screen Printed Carbon Electrode for Sensitive Determination of Hydrogen Peroxide. **Talanta**. 144: 868-874.
- Reiter, S., Ruhlig, D., Ngounou, B., Neugebauer, S., Janiak, S., Vilkanauskyte, A., Erichsen, T., and Schuhmann, W. (2004). An Electrochemical Robotic System for the Optimization of Amperometric Glucose Biosensors Based on a Library of Cathodic Electrodeposition Paints. **Macromolecular Rapid Communications**. 25(1): 348-354.
- Rodrigues, G., Almeida, F., Ribeiro, S. D., Tormin, T. F., Munoz, R. A. A., Assuncao, R. M. N., and Barud, H. (2016). Controlled Release of Drugs from Cellulose Acetate Matrices Produced from Sugarcane Bagasse: Monitoring by Square-

- Wave Voltammetry. **Drug Development and Industrial Pharmacy**. 42(7): 1066-1072.
- Ronkainen, N. J., Halsall, H. B., and Heineman, W. R. (2010). Electrochemical Biosensors. **Chemical Society Reviews**. 39(5): 1747-1763.
- Rossi, F., Ferrari, R., Castiglione, F., Mele, A., Perale, G., and Moscatelli, D. (2015). Polymer Hydrogel Functionalized with Biodegradable Nanoparticles as Composite System for Controlled Drug Delivery. **Nanotechnology**. 26(1).
- Rowden, A. K., Norvell, J., Eldridge, D. L., and Kirk, M. A. (2006). Acetaminophen Poisoning. **Clinics in Laboratory Medicine**. 26(1): 49-65, viii.
- Ruff, A., Szczesny, J., Zacarias, S., Pereira, I. A. C., Plumere, N., and Schuhmann, W. (2017). Protection and Reactivation of the [Nifese] Hydrogenase from *Desulfovibrio Vulgaris* Hildenborough under Oxidative Conditions. **American Chemical Society Energy Letters**. 2(5): 964-968.
- Ruhlig, D., Schulte, A., and Schuhmann, W. (2006). An Electrochemical Robotic System for Routine Cathodic Adsorptive Stripping Analysis of Ni²⁺ Ion Release from Corroding NiTi Shape Memory Alloys. **Electroanalysis**. 18(1): 53-58.
- Schroeder, A., Kost, J., and Barenholz, Y. (2009). Ultrasound, Liposomes, and Drug Delivery: Principles for Using Ultrasound to Control the Release of Drugs from Liposomes. **Chemistry and Physics of Lipids**. 162(1-2): 1-16.
- Schwarz, M., and Speiser, B. (2009). Combinatorial Micro-Electrochemistry. Part 5. Electrosynthesis Screening of the Electroreductive Coupling of Alpha,Beta-Unsaturated Esters and Allyl Bromides in a Room Temperature Ionic Liquid. **Electrochimica Acta**. 54(14): 3735-3744.

- Selvaraju, T., and Ramaraj, R. (2009). Electrocatalytic Reduction of Hydrogen Peroxide at Nanostructured Copper Modified Electrode. **Journal of Applied Electrochemistry**. 39(3): 321-327.
- ShangGuan, X. D., Zhang, H. F., and Zheng, J. B. (2008). Electrochemical Behavior and Differential Pulse Voltammetric Determination of Paracetamol at a Carbon Ionic Liquid Electrode. **Analytical and Bioanalytical Chemistry**. 391(3): 1049-1055.
- Shiroma, L. Y., Santhiago, M., Gobbi, A. L., and Kubota, L. T. (2012). Separation and Electrochemical Detection of Paracetamol and 4-Aminophenol in a Paper-Based Microfluidic Device. **Analytica Chimica Acta**. 725: 44-50.
- Siepmann, J., Siegel, R. A., and Rathbone, M. J. (2011). *Fundamentals and Applications of Controlled Release Drug Delivery*: Springer Science & Business Media.
- Smyth, W. F., and Woolfson, A. D. (1987). Drug Assays--the Role of Modern Voltammetric Techniques. **Journal of Clinical Pharmacy and Therapeutics**. 12(2): 117-134.
- Somasundrum, M., Kirtikara, K., and Tanticharoen, M. (1996). Amperometric Determination of Hydrogen Peroxide by Direct and Catalytic Reduction at a Copper Electrode. **Analytica Chimica Acta**. 319(1-2): 59-70.
- Sridaeng, D., Weingart, J. J., Chantarasiri, N., Zhe, J., and Hu, J. J. (2010). Postsynthetic Surface Functionalization, Encapsulation, and Releasing Studies of a Novel Polymer Nanocapsule. **Journal of Applied Polymer Science**. 117(2): 706-713.

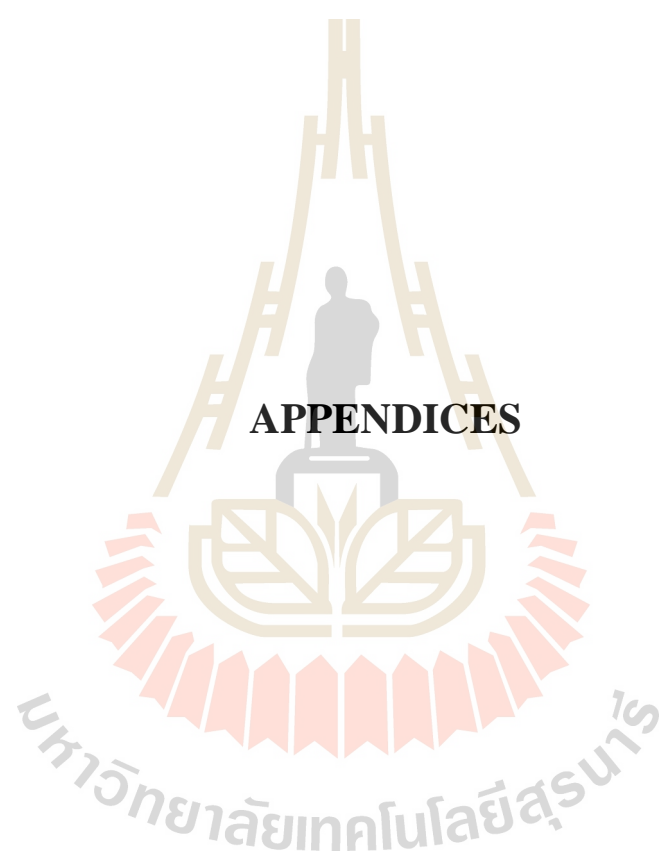
- Suginta, W., Khunkaewla, P., and Schulte, A. (2013). Electrochemical Biosensor Applications of Polysaccharides Chitin and Chitosan. **Chemical Reviews**. 113(7): 5458-5479.
- Sui, C., Preece, J. A., and Zhang, Z. B. (2017). Novel Polystyrene Sulfonate-Silica Microspheres as a Carrier of a Water Soluble Inorganic Salt (KCl) for Its Sustained Release, Via a Dual-Release Mechanism. **Royal Society of Chemistry Advances**. 7(1): 478-481.
- Tanuja, S. B., Swamy, B. E. K., and Pai, K. V. (2017). Electrochemical Determination of Paracetamol in Presence of Folic Acid at Nevirapine Modified Carbon Paste Electrode: A Cyclic Voltammetric Study. **Journal of Electroanalytical Chemistry**. 798: 17-23.
- Tasic, L. M., Jovanovic, M. D., and Djuric, Z. R. (1992). The Influence of Beta-Cyclodextrin on the Solubility and Dissolution Rate of Paracetamol Solid Dispersions. **Journal of Pharmacy and Pharmacology**. 44(1): 52-55.
- Teanphonkrang, S., and Schulte, A. (2017). Automated Quantitative Enzyme Biosensing in 24-Well Microplates. **Analytical Chemistry**. 89(10): 5261-5269.
- Teng, Y., Fan, L., Dai, Y., Zhong, M., Lu, X., and Kan, X. (2015). Electrochemical Sensor for Paracetamol Recognition and Detection Based on Catalytic and Imprinted Composite Film. **Biosensors and Bioelectronics**. 71: 137-142.
- Terse-Thakoor, T., Komori, K., Ramnani, P., Lee, I., and Muchandani, A. (2015). Electrochemically Functionalized Seamless Three-Dimensional Graphene-Carbon Nanotube Hybrid for Direct Electron Transfer of Glucose Oxidase and Bioelectrocatalysis. **Langmuir**. 31(47): 13054-13061.
- Thangaraj, R., Nellaiappan, S., Sudhakaran, R., and Kumar, A. S. (2014). A Flow Injection Analysis Coupled Dual Electrochemical Detector for Selective and

- Simultaneous Detection of Guanine and Adenine. **Electrochimica Acta**. 123: 485-493.
- Theanponkrang, S., Suginta, W., Weingart, H., Winterhalter, M., and Schulte, A. (2015). Robotic Voltammetry with Carbon Nanotube-Based Sensors: A Superb Blend for Convenient High-Quality Antimicrobial Trace Analysis. **International Journal of Nanomedicine**. 10: 859-868.
- Torto, N. (2009). Recent Progress in Electrochemical Oxidation of Saccharides at Gold and Copper Electrodes in Alkaline Solutions. **Bioelectrochemistry**. 76(1-2): 195-200.
- Tunesi, M., Prina, E., Munarin, F., Rodilossi, S., Albani, D., Petrini, P., and Giordano, C. (2015). Cross-Linked Poly(Acrylic Acids) Microgels and Agarose as Semi-Interpenetrating Networks for Resveratrol Release. **Journal of Materials Science: Materials in Medicine**. 26(1).
- Voegel, P. D., and Baldwin, R. P. (1997). Electrochemical Detection in Capillary Electrophoresis. **Electrophoresis**. 18(12-13): 2267-2278.
- Wang, J. (2008). Electrochemical Glucose Biosensors. **Chemical Reviews**. 108(2): 814-825.
- Wang, L. H. (2002). Voltammetric Behavior of Sunscreen Agents at Mercury Film Electrode. **Electroanalysis**. 14(11): 773-781.
- Wilson, C. G., and Crowley, P. J. (2011). *Controlled Release in Oral Drug Delivery*: Springer.
- Wischke, C., Neffe, A. T., Steuer, S., Engelhardt, E., and Lendlein, A. (2010). Ab-Polymer Networks with Cooligoester and Poly(N-Butyl Acrylate) Segments as a Multifunctional Matrix for Controlled Drug Release. **Macromolecular Bioscience**. 10(9): 1063-1072.

- Yang, G. C., Wang, L., Yang, Y. S., Chen, X. S., Zhou, D. F., Jia, J. B., and Li, D. F. (2012). 4-Phosphatephenyl Covalently Modified Glassy Carbon Electrode for Real-Time Electrochemical Monitoring of Paracetamol Release from Electrospun Nanofibers. **Electroanalysis**. 24(10): 1937-1944.
- Ye, J., and Baldwin, R. P. (1994). Determination of Amino Acids and Peptides by Capillary Electrophoresis and Electrochemical Detection at a Copper Electrode. **Analytical Chemistry**. 66(17): 2669-2674.
- Yi, S., Chung, Y. J., Kim, T. E., Shin, H. S., Yoon, S. H., Cho, J. Y., Jang, I. J., Shin, S. G., and Yu, K. S. (2011). Pharmacokinetics of Extended-Release Versus Conventional Tramadol/Acetaminophen Fixed-Dose Combination Tablets: An Open-Label, 2-Treatment, Multiple-Dose, Randomized-Sequence Crossover Study in Healthy Korean Male Volunteers. **Clinical Therapeutics**. 33(6): 728-737.
- Yi, S. J., Kim, T. E., Jeon, H. W., Shin, H. S., Yoon, S. H., Cho, J. Y., Yu, K. S., Jang, I. J., and Shin, S. G. (2010). Comparative Pharmacokinetics of Extended-Release Versus Conventional Tramadol/Acetaminophen Fixed-Dose Combination Tablets in Healthy Volunteers. **Clinical Pharmacology & Therapeutics**. 87: S87-S88.
- You, X. R., Kang, Y., Hollett, G., Chen, X., Zhao, W., Gu, Z. P., and Wu, J. (2016). Polymeric Nanoparticles for Colon Cancer Therapy: Overview and Perspectives. **Journal of Materials Chemistry B**. 4(48): 7779-7792.
- Zamora-Mora, V., Velasco, D., Hernandez, R., Mijangos, C., and Kumacheva, E. (2014). Chitosan/Agarose Hydrogels: Cooperative Properties and Microfluidic Preparation. **Carbohydrate Polymers**. 111: 348-355.

Zhu, Z., Garcia-Gancedo, L., Flewitt, A. J., Xie, H., Moussy, F., and Milne, W. I. (2012). A Critical Review of Glucose Biosensors Based on Carbon Nanomaterials: Carbon Nanotubes and Graphene. **Sensors (Basel)**. 12(5): 5996-6022.





APPENDICES

APPENDIX A

SOLUTION PREPARATION

A.1 Preparation of chemical solutions

1. A dispersion of CNT of 20 mg/ml carbon nanotube (P3-SWNT) in water; it is used for the electrophoretic deposition of the GCE (preparation of WE): 20 mg of CNT was dissolved in DI water in 1 mL eppendorf tube. The solution was suspended in ultrasonic bath.

2. Potassium chloride solution of 0.1 M of KCl as supporting electrolyte of drug determination. 3.7278 g of KCl was dissolved in DI water and transfer in to a 500 mL volumetric flask. The solution was made up to volume with water.

3. 0.1 M of K_2SO_4 - H_2SO_4 as medium solution of drug dissolution testing and voltammetry drug measurement.

A) The Medium solution of drug dissolution testing; 8.713 g of K_2SO_4 was dissolved in 0.1 M H_2SO_4 and transfer in to 500 mL volumetric flask. The solution was made up to volume with water. The pH was adjusted to 1.02 by 0.1 M H_2SO_4 solution addition.

B) The solution A) was mixed with 0.1 M KCl and the pH was adjusted to 1.02 by 0.1 M H_2SO_4 solution addition.

4. 0.1 M PBS buffer solution pH 7.0 as measuring buffer and supporting electrolyte for H_2O_2 determination. 0.1 M PBS buffer solution pH 7.0 was prepared by mixing 0.1 M Sodium phosphate dibasic anhydrous (Na_2HPO_4) and 0.1 M Sodium dihydrogen phosphate ($NaH_2PO_4 \cdot H_2O$).

5. The glucose and hydrogen peroxide (H_2O_2) were purchased from CARLO ERBA Reagents S.A.S., the stock solution of hydrogen peroxide (H_2O_2) was freshly prepared daily by diluting 30% H_2O_2 solution in DI water.

6. Nafion perfluorinated ion-exchange resin, 10% wt. dispersion in water were purchased from Sigma-Aldrich.

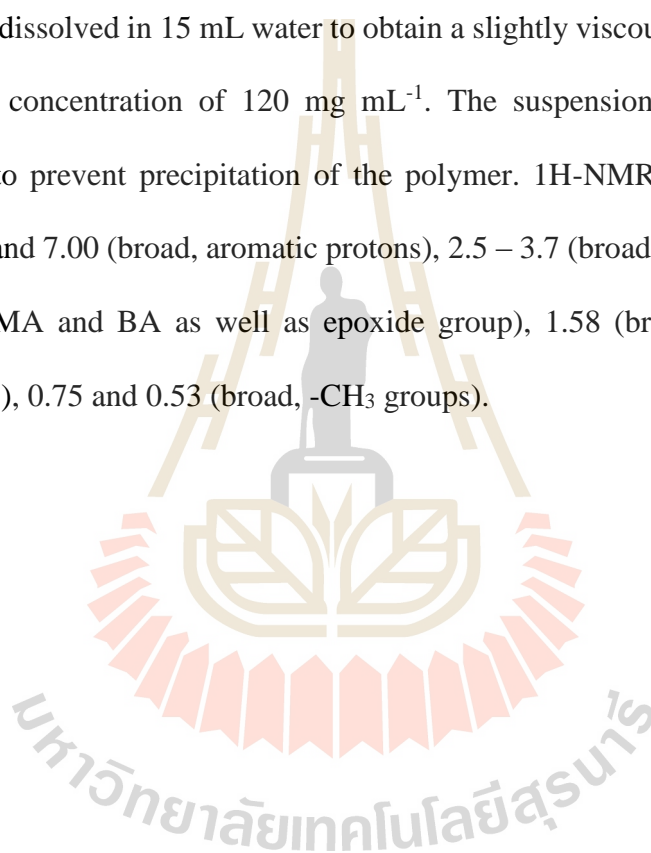
7. A stock standard solution of 1 M ascorbic acid in water: 1.76 g of L (+) Ascorbic acid (AA) was dissolved in DI water and transferred in to a 10 mL volumetric flask. The solution was made up to the volume with DI water.

8. A stock standard solution of 1 mM a 4-cetamidophenol (paracetamol) in water: 15 mg of $\text{C}_8\text{H}_9\text{NO}_2$ (PCT) was dissolved in DI water and transferred in to 10 mL volumetric flask. The solution was made up to the volume with DI water.

9. Glucose oxidase (G7141-250KU, type X-S, from *Aspergillus niger*) (Lyophilized ~ 75% protein, 1.83 G solid; 136300 units/G solid) (Molecular Weight: 160 kDa) were purchased from Sigma-Aldrich.

10. The copolymers P(SS-GMA-BA)-S1 and P(SS-GMA-BA)-S2 reveal nominal compositions of 50 mol% SS, 30 mol% GMA, 20 mol% BA (S1) and 80 mol% SS, 10 mol% GMA, 10 mol% BA, respectively. The synthesis and characterization of polymer P(SS-GMA-BA)-S2 was described earlier in ref. Lopez et al (Lopez *et al.*, 2017). Polymer P(SS-GMA-BA) was prepared analogously with the respective composition of comonomers. Synthesis of poly(styrene sulfonate-co-glycidyl methacrylate-co-butyl acrylate), P(SS-GMA-BA)-S1. Under an argon atmosphere, the comonomers sodium 4-vinylbenzenesulfonate (1 g, 4.85 mmol, 50 mol%, SS), glycidyl methacrylate (414 mg; 2.91 mmol, 30 mol%, GMA) and butyl acrylate (249 mg; 1.94 mmol, 20 mol%, BA) were dissolved in a mixture of isopropyl alcohol (10 mL) and water (7 mL). The reaction mixture was deaerated by argon bubbling and 2.5 mg of

AIBN (= 2,2'-azobis(2-methylpropionitrile); recrystallized from hot toluene, stored at 4 °C) were added. The colorless mixture was heated to 70 °C and stirred overnight. The clear and colorless solution was cooled down to room temperature and the product was precipitated by adding 30 mL of tetrahydrofuran. The colorless precipitate was separated by centrifugation (4,000 rpm, 15 minutes), washed with 3 mL of isopropyl alcohol and dried under reduced pressure to yield 1.8 g of a gel. Finally, the crude polymer was dissolved in 15 mL water to obtain a slightly viscous polymer suspension with a mass concentration of 120 mg mL⁻¹. The suspension was stored at room temperature to prevent precipitation of the polymer. ¹H-NMR (200.13 MHz, D₂O) δ/ppm: 7.56 and 7.00 (broad, aromatic protons), 2.5 – 3.7 (broad, overlapping signals -CH₂O- of GMA and BA as well as epoxide group), 1.58 (broad, -CH₂- and -CH-backbone, SS), 0.75 and 0.53 (broad, -CH₃ groups).



APPENDIX B

DESIGN OF SOFTWARE FOR THE EXECUTION OF ROBOTIC ELECTROCHEMICAL ANALYSIS IN 24- WELL MICROTITER PLATES

A description of the software and abbreviations used for script design for voltammetry and the command of x, y, and z micro-positioning and the command of buffer suction pump system control robotic software are provided in Table B.1.

Table B.1 Listed parameters and abbreviations of voltammetric techniques used in software script of the robotic electrochemical device.

Abbreviation	Implication
E begin	Potential where a scan starts. The applicable range of the potential is $-2V$ to $+2V$.
E start	Potential where a CV scan started. This value must be between E vtx1 and E vtx2.
E vtx1	Potential where a scan direction is reversed (CV only) The applicable range of the potential is $-2 V$ to $+2 V$.
E end	Potential where a measurement stops.
E vtx2	Potential where a scan direction is reversed (CV only). The applicable range of the potential is $-2 V$ to $+2 V$.

Table B.1 Listed parameters and abbreviations of voltammetric techniques used in software script of the robotic electrochemical device (Continued).

Abbreviation	Implication
E amp	Amplitude (of square wave pulse (SWV) and sine wave (acV). Values are half peak-to-peak (SWV) or rms (acV).
E cond	Potential applied before the deposition stage is started. Is only relevant when $t_{\text{cond}} > 0$ s.
E dep	Potential applied during the deposition stage. Is only relevant when $t_{\text{dep}} > 0$ s.
E stby	Potential applied after the measurement is finished.
scan rate	The applied scan rate. The applicable range depends on the value of E step.
t pulse	The pulse time
Freq	The frequency of the square wave or ac signal
n scans	Number of a scans for CV
t cond	Conditioning time
t dep	Deposition time
t eq	Equilibration time. During this stage E or E start is applied
PUM -1	For suction buffer solution
PUM 1	For releasing buffer solution
PUM valve 0	Aspire from valve 0 (suction solution)
PUM valve 1	Dispense from valve 1 (releasing solution)

APPENDIX C

ROBOTIC ELECTROCHEMICAL ANALYSIS OF DRUG DISSOLUTION SAMPLES

C.1 The loading drug solution in microtiter plate-based assessment of PCT calibration curve

Figure C.1 is listing the solutions volumes of PCT to be loaded in to the 24 well microtiter plates for robotic quantification. Wells A1, B1, C1, and D1 were water-filled for electrode cleaning, well A2 had bare 0.1 M $K_2SO_4-H_2SO_4-KCl$ solution pH 1.02, the other rest wells were standard addition of PCT measurement for calibration curves.

D	C	B	A	
H ₂ O	H ₂ O	H ₂ O	H ₂ O	1
800	100	10	blank	2
1000	150	20	2	3
1200	200	40	4	4
1400	400	60	6	5
1600	600	80	8	6

Figure C.1 Assignment of standard PCT solution loaded in the 24-well microtiter plate used for drug calibration trial.

C.3 The loading drug stability testing and the software script in microtiter plate-based assessment of PCT solution

Figure C.2 is listing the solutions volumes of PCT to be loaded in to the 24 well microtiter plates for robotic quantification. The microtiter plate were controlled direction by computer, its movable as positions x- and y- axis. The measurement sequence was running calibration curve, and then measuring 10 μM or 80 μM PCT solution, and finally running calibration curve. The plate of stability measuring as wells #1, #3, and #5 were water-filled for electrode cleaning, well #2, #4, and #6 were standard addition of PCT measurements.

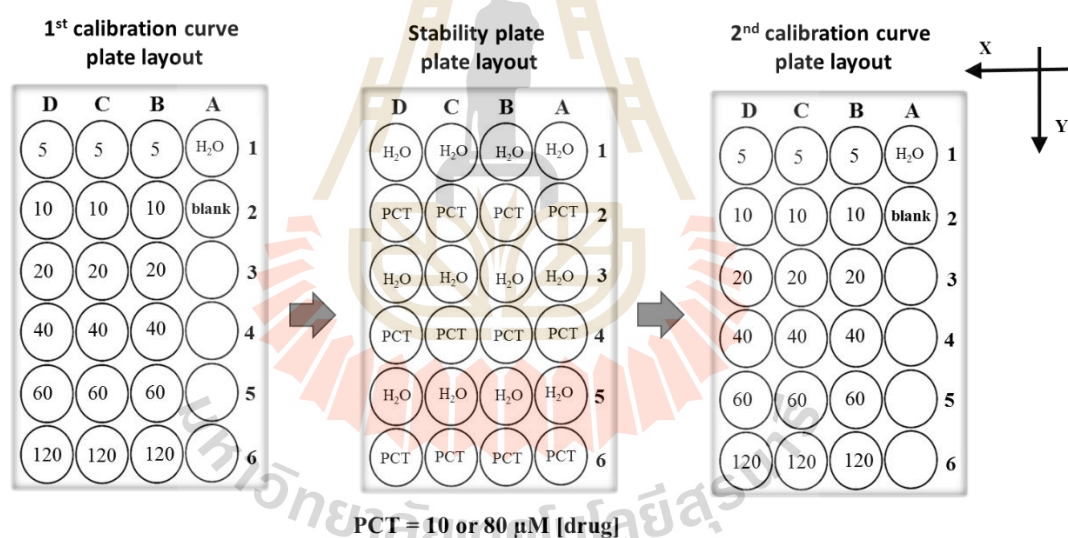


Figure C.2 Assignment of standard PCT solution loaded in the 24-well microtiter plate used for drug stability testing via calibration method.

C.4 The software script in automation assessment dissolution profile of drug

Table C.4 The Notepad software script for robotic voltammetric quantification of PCT in dissolution profile via normal calibration method for the plate layout refer to refers Figure 4.8.

1		2	3	4	5	7	8	9	10	11	15	16	17		
Well No.	Command		E_{begin} (V)	E_{end} (V)	E_{step} (mV)	E_{pk} (mV)	E_{end} (V)	E_{step} (V)	E_{start} (V)	scan rate (V/s)	t_{pk} (s)	t_{end} (s)	t_{step} (s)	t_{end} (s)	
A	1	WAIT	10												
A	2	POT	DPV	0.1	0.9	5	25	0	0	0	0.02	0.07	10	0	5
A	3	POT	DPV	0.1	0.9	5	25	0	0	0	0.02	0.07	10	0	5
A	4	POT	DPV	0.1	0.9	5	25	0	0	0	0.02	0.07	10	0	5
A	5	POT	DPV	0.1	0.9	5	25	0	0	0	0.02	0.07	10	0	5
A	6	POT	DPV	0.1	0.9	5	25	0	0	0	0.02	0.07	10	0	5
A	1	WAIT	10												
B	1	WAIT	10												
B	2	POT	DPV	0.1	0.9	5	25	0	0	0	0.02	0.07	10	0	5
B	3	POT	DPV	0.1	0.9	5	25	0	0	0	0.02	0.07	10	0	5
B	4	POT	DPV	0.1	0.9	5	25	0	0	0	0.02	0.07	10	0	5
B	5	POT	DPV	0.1	0.9	5	25	0	0	0	0.02	0.07	10	0	5
B	6	POT	DPV	0.1	0.9	5	25	0	0	0	0.02	0.07	10	0	5
B	1	WAIT	10												
C	1	WAIT	10												
C	2	POT	DPV	0.1	0.9	5	25	0	0	0	0.02	0.07	10	0	5
C	3	POT	DPV	0.1	0.9	5	25	0	0	0	0.02	0.07	10	0	5
C	4	POT	DPV	0.1	0.9	5	25	0	0	0	0.02	0.07	10	0	5
C	5	POT	DPV	0.1	0.9	5	25	0	0	0	0.02	0.07	10	0	5
C	6	POT	DPV	0.1	0.9	5	25	0	0	0	0.02	0.07	10	0	5
C	1	WAIT	10												
D	1	WAIT	10												
D	2	POT	DPV	0.1	0.9	5	25	0	0	0	0.02	0.07	10	0	5
D	3	POT	DPV	0.1	0.9	5	25	0	0	0	0.02	0.07	10	0	5
D	4	POT	DPV	0.1	0.9	5	25	0	0	0	0.02	0.07	10	0	5
D	5	POT	DPV	0.1	0.9	5	25	0	0	0	0.02	0.07	10	0	5
D	6	POT	DPV	0.1	0.9	5	25	0	0	0	0.02	0.07	10	0	5
D	1	WAIT	10												
A	1	WAIT	10												
Stop the script execution with a stop-command															
A	1	STOP													

C.5 The calculation of percentage drug dissolution profile

The calculation PCT in tablet sample (for example in 650 mg/tablet)

The concentration of PCT 650 mg/300 mL in dissolution medium, (molecular weight PCT are 151.16 g/mole)

$$\begin{aligned} \text{Conc. of PCT} &= 650 \text{ mg} / 300 \text{ mL} = 2.167 \text{ g/L} \\ &= (2.167 \text{ g/L}) / (151.16 \text{ g/mole}) \\ &= 0.01433 \text{ mole/L} \quad \dots\dots\dots C_i \end{aligned}$$

(The concentration of PCT 325 mg/tablet is 7.165 mmole/L)

Therefore, the concentration of PCT dilution in robotic system is:

$$C_i V_i = C_o V_o$$

C_i = PCT concentration, mole/L

V_i = PCT volume, μL

C_o = final releasing concentration of PCT, mole/L

V_o = final volume of PCT in well (3 mL)

$$(0.01433 \text{ mole/L}) \times (15 \mu\text{L}) = C_o \times (3000 \mu\text{L})$$

$$C_o = 71.65 \times 10^{-6} \text{ mole/L} \quad \dots\dots\dots C_o$$

Then, the percentage drug release was calculated by the following equation:

$$\text{Cumulative of PCT released (\%)} = C_t / C_o \times 100$$

C_t = PCT concentration released ($t > 0$), mole/L

C_o = final releasing concentration of PCT, mole/L

APPENDIX D

**ROBOTIC ELECTROCHEMICAL ANALYSIS OF
CONTROLLED DRUG RELEASE FROM THE
NATURAL AND ARTIFICIAL POLYMERS**

D.1 The evaluation of PCT release using robotic SWV

Table D.1 The parameters for drug SWV.

Parameters (SWV)	Conditions
E_{begin} (V)	0.15
E_{end} (V)	0.85
E_{step} (V)	0.007
E_{ampl} (V)	0.025
E_{cond} (V)	-0.2
E_{dep} (V)	-0.2
Freq (Hz)	100
t_{cond} (s)	30
t_{dep} (s)	0
t_{eq} (s)	3

D.2 Robotic software script for 'in well' drug release profiling

Table D.2 The software script for automation the profiling drug release using SWV.

		1		2	3	4	5	7	8	9	10	11	15	16	17
Well No.	Command		E_{begin} (V)	E_{end} (V)	E_{step} (mV)	E_{pts} (mV)	E_{cond} (V)	E_{dep} (V)	E_{stand} (V)	freq (Hz)	t_{pts} (s)	t_{cond} (s)	t_{dp} (s)	t_{eq} (s)	
	Pumpdirection		Valve No. (0 or 1)	Volume (μ L)	Speed (μ L/s)										
A	1	WAIT	10												
A	2	POT	SWV	0.15	0.85	7	25	-0.2	-0.2	0	0.02	0.07	30	0	3
B	1	POT	SWV	0.15	0.85	7	25	-0.2	-0.2	0	0.02	0.07	30	0	3
B	2	POT	SWV	0.15	0.85	7	25	-0.2	-0.2	0	0.02	0.07	30	0	3
B	3	POT	SWV	0.15	0.85	7	25	-0.2	-0.2	0	0.02	0.07	30	0	3
B	4	POT	SWV	0.15	0.85	7	25	-0.2	-0.2	0	0.02	0.07	30	0	3
B	5	POT	SWV	0.15	0.85	7	25	-0.2	-0.2	0	0.02	0.07	30	0	3
B	6	POT	SWV	0.15	0.85	7	25	-0.2	-0.2	0	0.02	0.07	30	0	3
A	1	WAIT	10												
A	2	POT	SWV	0.15	0.85	7	25	-0.2	-0.2	0	0.02	0.07	30	0	3
C	1	POT	SWV	0.15	0.85	7	25	-0.2	-0.2	0	0.02	0.07	30	0	3
C	2	POT	SWV	0.15	0.85	7	25	-0.2	-0.2	0	0.02	0.07	30	0	3
C	3	POT	SWV	0.15	0.85	7	25	-0.2	-0.2	0	0.02	0.07	30	0	3
C	4	POT	SWV	0.15	0.85	7	25	-0.2	-0.2	0	0.02	0.07	30	0	3
C	5	POT	SWV	0.15	0.85	7	25	-0.2	-0.2	0	0.02	0.07	30	0	3
C	6	POT	SWV	0.15	0.85	7	25	-0.2	-0.2	0	0.02	0.07	30	0	3
A	1	WAIT	10												
A	2	POT	SWV	0.15	0.85	7	25	-0.2	-0.2	0	0.02	0.07	30	0	3
D	1	POT	SWV	0.15	0.85	7	25	-0.2	-0.2	0	0.02	0.07	30	0	3
D	2	POT	SWV	0.15	0.85	7	25	-0.2	-0.2	0	0.02	0.07	30	0	3
D	3	POT	SWV	0.15	0.85	7	25	-0.2	-0.2	0	0.02	0.07	30	0	3
D	4	POT	SWV	0.15	0.85	7	25	-0.2	-0.2	0	0.02	0.07	30	0	3
D	5	POT	SWV	0.15	0.85	7	25	-0.2	-0.2	0	0.02	0.07	30	0	3
D	6	POT	SWV	0.15	0.85	7	25	-0.2	-0.2	0	0.02	0.07	30	0	3
A	1	WAIT	10												
A	2	POT	SWV	0.15	0.85	7	25	-0.2	-0.2	0	0.02	0.07	30	0	3
A	3	WAIT	10												
A	3	PUMP	-1	0	2700	500									
A	3	PUMP	+1	1	2700	500									
A	3	POT	SWV	0.15	0.85	7	25	-0.2	-0.2	0	0.02	0.07	30	0	3
A	4	WAIT	10												
A	4	PUMP	-1	0	2700	500									
A	4	PUMP	+1	1	2700	500									
A	4	POT	SWV	0.15	0.85	7	25	-0.2	-0.2	0	0.02	0.07	30	0	3
A	5	WAIT	10												
A	5	PUMP	-1	0	2700	500									
A	5	PUMP	+1	1	2700	500									
A	5	POT	SWV	0.15	0.85	7	25	-0.2	-0.2	0	0.02	0.07	30	0	3
A	3	POT	SWV	0.15	0.85	7	25	-0.2	-0.2	0	0.02	0.07	30	0	3

Table D.2 The software script for automation the profiling drug release using SWV (Continued).

Well No.	1		2	3	4	5	7	8	9	10	11	15	16	17
	Command		E_{begin} (V)	E_{end} (V)	E_{step} (mV)	E_{pk} (mV)	E_{end} (V)	E_{step} (V)	E_{start} (V)	freq (Hz)	t_{pk} (s)	t_{end} (s)	t_{dp} (s)	t_{eq} (s)
	Pumpdirection		Valve No. (0 or 1)	Volume (μ L)	Speed (μ L/s)									
A	4	POT SWV	0.15	0.85	7	25	-0.2	-0.2	0	0.02	0.07	30	0	3
A	5	POT SWV	0.15	0.85	7	25	-0.2	-0.2	0	0.02	0.07	30	0	3
A	3	POT SWV	0.15	0.85	7	25	-0.2	-0.2	0	0.02	0.07	30	0	3
A	4	POT SWV	0.15	0.85	7	25	-0.2	-0.2	0	0.02	0.07	30	0	3
A	5	POT SWV	0.15	0.85	7	25	-0.2	-0.2	0	0.02	0.07	30	0	3
A	3	POT SWV	0.15	0.85	7	25	-0.2	-0.2	0	0.02	0.07	30	0	3
A	4	POT SWV	0.15	0.85	7	25	-0.2	-0.2	0	0.02	0.07	30	0	3
A	5	POT SWV	0.15	0.85	7	25	-0.2	-0.2	0	0.02	0.07	30	0	3
A	3	POT SWV	0.15	0.85	7	25	-0.2	-0.2	0	0.02	0.07	30	0	3
A	4	POT SWV	0.15	0.85	7	25	-0.2	-0.2	0	0.02	0.07	30	0	3
A	5	POT SWV	0.15	0.85	7	25	-0.2	-0.2	0	0.02	0.07	30	0	3
A	3	POT SWV	0.15	0.85	7	25	-0.2	-0.2	0	0.02	0.07	30	0	3
A	4	POT SWV	0.15	0.85	7	25	-0.2	-0.2	0	0.02	0.07	30	0	3
A	5	POT SWV	0.15	0.85	7	25	-0.2	-0.2	0	0.02	0.07	30	0	3
A	3	POT SWV	0.15	0.85	7	25	-0.2	-0.2	0	0.02	0.07	30	0	3
A	4	POT SWV	0.15	0.85	7	25	-0.2	-0.2	0	0.02	0.07	30	0	3
A	5	POT SWV	0.15	0.85	7	25	-0.2	-0.2	0	0.02	0.07	30	0	3
A	2	WAIT	500											
A	3	POT SWV	0.15	0.85	7	25	-0.2	-0.2	0	0.02	0.07	30	0	3
A	4	POT SWV	0.15	0.85	7	25	-0.2	-0.2	0	0.02	0.07	30	0	3
A	5	POT SWV	0.15	0.85	7	25	-0.2	-0.2	0	0.02	0.07	30	0	3
A	2	WAIT	500											
A	3	POT SWV	0.15	0.85	7	25	-0.2	-0.2	0	0.02	0.07	30	0	3
A	4	POT SWV	0.15	0.85	7	25	-0.2	-0.2	0	0.02	0.07	30	0	3
A	5	POT SWV	0.15	0.85	7	25	-0.2	-0.2	0	0.02	0.07	30	0	3
A	2	WAIT	500											
A	3	POT SWV	0.15	0.85	7	25	-0.2	-0.2	0	0.02	0.07	30	0	3
A	4	POT SWV	0.15	0.85	7	25	-0.2	-0.2	0	0.02	0.07	30	0	3
A	5	POT SWV	0.15	0.85	7	25	-0.2	-0.2	0	0.02	0.07	30	0	3
A	2	WAIT	500											
A	3	POT SWV	0.15	0.85	7	25	-0.2	-0.2	0	0.02	0.07	30	0	3
A	4	POT SWV	0.15	0.85	7	25	-0.2	-0.2	0	0.02	0.07	30	0	3
A	5	POT SWV	0.15	0.85	7	25	-0.2	-0.2	0	0.02	0.07	30	0	3
A	2	WAIT	500											
A	3	POT SWV	0.15	0.85	7	25	-0.2	-0.2	0	0.02	0.07	30	0	3
A	4	POT SWV	0.15	0.85	7	25	-0.2	-0.2	0	0.02	0.07	30	0	3
A	5	POT SWV	0.15	0.85	7	25	-0.2	-0.2	0	0.02	0.07	30	0	3
A	1	WAIT	10											
A	2	POT SWV	0.15	0.85	7	25	-0.2	-0.2	0	0.02	0.07	30	0	3
B	1	POT SWV	0.15	0.85	7	25	-0.2	-0.2	0	0.02	0.07	30	0	3
B	2	POT SWV	0.15	0.85	7	25	-0.2	-0.2	0	0.02	0.07	30	0	3
B	3	POT SWV	0.15	0.85	7	25	-0.2	-0.2	0	0.02	0.07	30	0	3

Table D.2 The software script for automation the profiling drug release using SWV (Continued).

1		2	3	4	5	7	8	9	10	11	15	16	17	
Well No.	Command		E_{begin} (V)	E_{end} (V)	E_{step} (mV)	E_{pk} (mV)	E_{end} (V)	E_{step} (V)	E_{start} (V)	freq (Hz)	t_{pk} (s)	t_{end} (s)	t_{dp} (s)	t_{eq} (s)
	Pumpdirection		Valve No. (0 or 1)	Volume (μ L)	Speed (μ L/s)									
B	4	POT SWV	0.15	0.85	7	25	-0.2	-0.2	0	0.02	0.07	30	0	3
B	5	POT SWV	0.15	0.85	7	25	-0.2	-0.2	0	0.02	0.07	30	0	3
B	6	POT SWV	0.15	0.85	7	25	-0.2	-0.2	0	0.02	0.07	30	0	3
A	1	WAIT	10											
A	2	POT SWV	0.15	0.85	7	25	-0.2	-0.2	0	0.02	0.07	30	0	3
C	1	POT SWV	0.15	0.85	7	25	-0.2	-0.2	0	0.02	0.07	30	0	3
C	2	POT SWV	0.15	0.85	7	25	-0.2	-0.2	0	0.02	0.07	30	0	3
C	3	POT SWV	0.15	0.85	7	25	-0.2	-0.2	0	0.02	0.07	30	0	3
C	4	POT SWV	0.15	0.85	7	25	-0.2	-0.2	0	0.02	0.07	30	0	3
C	5	POT SWV	0.15	0.85	7	25	-0.2	-0.2	0	0.02	0.07	30	0	3
C	6	POT SWV	0.15	0.85	7	25	-0.2	-0.2	0	0.02	0.07	30	0	3
A	1	WAIT	10											
A	2	POT SWV	0.15	0.85	7	25	-0.2	-0.2	0	0.02	0.07	30	0	3
D	1	POT SWV	0.15	0.85	7	25	-0.2	-0.2	0	0.02	0.07	30	0	3
D	2	POT SWV	0.15	0.85	7	25	-0.2	-0.2	0	0.02	0.07	30	0	3
D	3	POT SWV	0.15	0.85	7	25	-0.2	-0.2	0	0.02	0.07	30	0	3
D	4	POT SWV	0.15	0.85	7	25	-0.2	-0.2	0	0.02	0.07	30	0	3
D	5	POT SWV	0.15	0.85	7	25	-0.2	-0.2	0	0.02	0.07	30	0	3
D	6	POT SWV	0.15	0.85	7	25	-0.2	-0.2	0	0.02	0.07	30	0	3
A	1	WAIT	10											
Stop the script execution with a stop-command														
A	1	STOP												

D.3 PCT release profiling from covering matrix trials via robotic SWV in the calibration mode

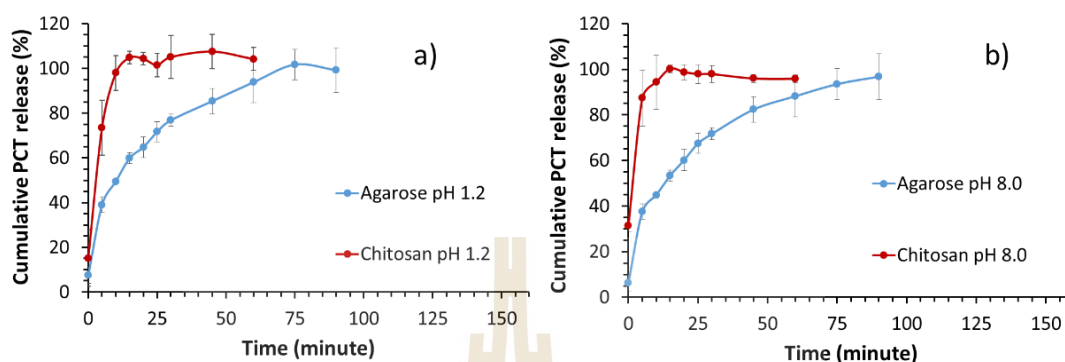


Figure D.1 Cumulative PCT release (in %) from the chitosan and agarose in 0.1 M $K_2SO_4-H_2SO_4$ at a) pH=1.2, and b) slightly alkaline buffer at pH 8.0. Each data point represents the average value of a triplicate repetition and the error bars represent the associated standard deviation.

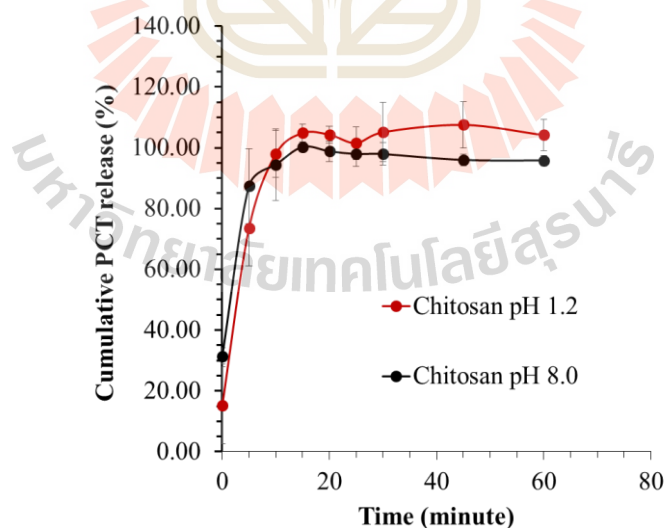


Figure D.2 Cumulative PCT release (in %) from the chitosan in 0.1 M $K_2SO_4-H_2SO_4$ at pH=1.2 (red), and slightly alkaline buffer at pH 8.0 (black).

D.4 The calculation of percentage cumulative drug releasing

The percentage drug release was calculated by the following equation:

$$\text{Cumulative of PCT release} = \text{Ci/Co} \times 100$$

Where

Ci = the concentration of PCT released with hydrogel

Co = the concentration of PCT loaded with hydrogel



APPENDIX E

PUBLICATIONS

Publication outputs:

Jaikaew, W., Patanakul, R., and Schulte, A.* (2016). Electrical Cable-Based Copper Disk Electrodes as Oxidase Biosensor Platforms with Cathodic H₂O₂ Readout. *Electroanalysis*, 28(10): 2408-2414.

Manuscript in preparations:

- 1) In Vitro Tablet Dissolution Testing with Final Sample Analysis via Robotic Drug Voltammetry in Microplate Format.

Wajee Jaikaew¹, Panida Khunkaewla¹, Albert Schulte^{2*}

¹School of Chemistry, Institute of Science, Biochemistry-Electrochemistry Research Unit, Institute of Science, and Center of Excellence (CoE) in Advanced Functional Materials, Institute of Science, Suranaree University of Technology, Nakhon Ratchasima 30000, Thailand

²Biomolecular Science and Engineering, Vidyasirimedhi Institute of Science and Technology, Rayong 21210, Thailand

- 2) Programmed Microplate Drug Voltammetry as Convenient and Reliable Non-Manual Tool for Quantitative Hydrogel Release Profiling.

Wajee Jaikaew¹, Panida Khunkaewla¹, Thomas Erichsen², Adrian Ruff², Wolfgang Schuhmann², Albert Schulte^{3*}

¹School of Chemistry, Institute of Science, Biochemistry-Electrochemistry Research Unit, Institute of Science, and Center of Excellence (CoE) in Advanced Functional Materials, Institute of Science, Suranaree University of Technology, Nakhon Ratchasima 30000, Thailand

²Lehrstuhl für Analytische Chemie und Zentrum für Elektrochemie, Ruhr-Universität Bochum, D-44780 Bochum, Germany

³Biomolecular Science and Engineering, Vidyasirimedhi Institute of Science and Technology, Rayong 21210, Thailand

3) Discharge Behavior of Drug-loaded Agarose Hydrogel Amalgams with Natural and Synthetic Polymers: Contrasts from Robotic Microplate Electroanalysis.

Wajee Jaikaew¹, Panida Khunkaewla¹, Thomas Erichsen², Adrian Ruff², Wolfgang Schuhmann², Albert Schulte^{3*}

¹School of Chemistry, Institute of Science, Biochemistry-Electrochemistry Research Unit, Institute of Science, and Center of Excellence (CoE) in Advanced Functional Materials, Institute of Science, Suranaree University of Technology, Nakhon Ratchasima 30000, Thailand

²Lehrstuhl für Analytische Chemie und Zentrum für Elektrochemie, Ruhr-Universität Bochum, D-44780 Bochum, Germany

³Biomolecular Science and Engineering, Vidyasirimedhi Institute of Science and Technology, Rayong 21210, Thailand

Electrical Cable-based Copper Disk Electrodes as Oxidase Biosensor Platforms with Cathodic H₂O₂ Readout

Wajee Jaikaew,^[a, c] Rungrueng Patanakul,^[b] and Albert Schulte^{*,[a, c, d]}

Dedicated to Professor W. Schuhmann on the Occasion of his 60th Birthday

Abstract: We report the first utilization of copper disk electrodes as suitable cathodic transducer platforms for glucose biosensors. Simple and cheap Cu disk electrodes were fabricated from ordinary electrical cable by cementing into a glass tube with epoxy resin and subsequent polishing to expose the active area. Glucose oxidase was immobilized on the electrode tips by entrapment in dropped and dried polymeric Nafion deposits. At a H₂O₂ detection potential of -0.15 V vs. a reference electrode, the linear response range of fabricated cable Cu glucose biosensors was 20–1500 μ M, with a sensitivity of about 700 nA μ M⁻¹ cm⁻². Quantitative analysis of glucose-supplemented buffer solutions showed a recovery of 106 \pm

4% ($n=3$). The principal advantage of the glucose biosensors described in this study, compared to other options, is the simplicity of the cathodic H₂O₂ readout, which exploits cheap and readily available electrical cable, without any extra surface modification with catalytically active micro- or nanomaterials. The analytical performance of the biosensor is competitive and suggests potential applications in routine glucose testing, in particular in academic teaching and research laboratories. The work is also a starting point for transfer of the methodology from simple cable Cu electrodes to arrays of miniaturized Cu sensors, using a combination of microlithography, electroforming and molding (LIGA).

Keywords: Enzyme biosensor · amperometry · copper · hydrogen peroxide · cathodic detection

1 Introduction

Amperometric enzyme biosensors based on oxidases have over the past few decades become widely used analytical tools, with applications in biotechnology, medicine and the life sciences [1]. The reason for the popularity of oxidase biosensors is their marked selectivity, achievable with simple electrode transducers and technically undemanding constant-potential detection of hydrogen peroxide, the by-product of the enzyme-catalysed reaction. Commercial sensors based on glucose oxidase (GOx) were the prototypes and are still the most widely used examples, because of their application to blood glucose monitoring. The current state of (blood) glucose biosensing and the various existing sensor designs are well described in a number of recent review articles [2]. However, despite the predominant use of GOx oxidases for other substrates than glucose have also been used successfully: alcohols, mono- and diamines, galactose, lactate, cholesterol, glutamate, xanthine, sarcosine, sulphite, pyruvate, urate, choline, glutathione sulphhydryl, oxalate, lysine and nicotinamide adenine dinucleotide are some examples of important analytes that can be assayed with biosensors containing the appropriate oxidases.

The assembly of functional amperometric oxidase-based biosensors relies to a great extent on the application-oriented choice of electrode shape, size and material, the immobilization strategy and, because H₂O₂ is prone to electrooxidation and -reduction, the polarity of the signal-generating detection potential. Commonly used

electrode platforms are bare or chemically modified disks of platinum, gold, glassy carbon or carbon pastes, with active disk diameters on the nano- to millimetre scale. For active redox protein immobilization, entrapment in thin films of natural or synthetic polymers and covalent oxidase bonding to functional groups on the electrode surface or to thin-film electrode surface modifications are feasible approaches. Anodic H₂O₂ amperometry, at detector potentials of $+0.5$ – $+0.8$ V, relative to a reference electrode, is then used to convert oxidase activity into a proportional electrical signal, for substrate quantification.

The use of an unselectively strong positive polarization for efficient H₂O₂ detection is a significant weakness of

[a] W. Jaikaew, A. Schulte
School of Chemistry, Institute of Science, Suranaree University of Technology
Nakhon Ratchasima, Thailand
*e-mail: schulte@sut.ac.th

[b] R. Patanakul
Synchrotron Light Research Institute, Nakhon Ratchasima, Thailand

[c] W. Jaikaew, A. Schulte
Biochemistry and Electrochemistry Research Unit
Suranaree University of Technology, Nakhon Ratchasima, Thailand

[d] A. Schulte
Centre of Excellence in Advanced Functional Materials
Suranaree University of Technology, Nakhon Ratchasima, Thailand.

Full Paper

ELECTROANALYSIS

many oxidase-based biosensors, as it makes them susceptible to interference by electron transfer reactions involving redox active species other than the enzymically produced target. Unwanted contributions to the signalling current confound sample quantification, particularly in complex samples containing only trace amounts of enzyme substrate. Body fluids, for instance, may contain detectable levels of anodically electroactive substances such as ascorbate and uric acid and, during medication, electro-oxidizable drugs such as 4-acetamidophenol (Paracetamol®). Blood and urine electroanalysis with GOx-based detectors in the routine anodic H₂O₂ detection mode is thus a good example of the need for protection against chemical interference with sensor signalling by other components of the sample. Detailed information on glucose biosensor signal interference and an introduction to the available strategies for elimination of such interference are available in a recent review [3]. To summarize briefly, one option is to cover the immobilized enzyme with a coating that either is selectively permeable to the oxidase substrate but excludes interfering compounds (e.g. Nafion, with the advantage of charge repulsion) or incorporates oxidizing biocatalysts such as horseradish peroxidase (HRP) or ascorbic acid oxidase or other compounds (e.g. the metal oxides PbO₂, MnO₂, CeO₂) that remove interferents by oxidation before they reach the detector surface. Another approach is to reduce the detection potential of the electrode transducer to a value below that at which interference occurs. Tailored Prussian blue, metallized carbon and HRP sensor adaptations can, for instance, facilitate measurement of H₂O₂ by reduction, rather than oxidation, at a negative potential. It is also possible to use a synthetic redox mediator with a lower reduction potential, replacing the O₂/H₂O₂ couple as indicator of the enzymic reaction. The redox mediator, in its oxidized state, may be utilized as a dissolved species, like O₂ in aerated sample solutions, or integrated into the immobilization matrix as a functional part of a redox polymer. Finally, the electrode potential of oxidase biosensors can also be reduced by exploiting direct electron transfer (DET) between the electrode platform and immobilized enzyme and measuring the (amperometric) current signal reacted to enzyme recycling, with a negative voltage stimulus close to the protein's formal potential, which is about -400–500 mV, depending on the experimental conditions [4].

The reported solutions for low-potential oxidase biosensor readouts often involve costly catalytically active micro- or nanomaterials and/or complex immobilization layer designs, so the methodology is still a subject of intense research activities in these field(s). However, copper and Cu-modified electrodes have not yet been explored as low-potential signal transducers in oxidase-based biosensors. Their use as detectors in sugar chromatography is well established [5] and they have also been used in the electroanalysis of amino acids and peptides [6], purines [7], phenols [8], alcohols [9] and heavy metal ions [10]. The motivation for the present work was

a report of the successful use of Cu electrodes for cathodic amperometry of H₂O₂, which has not yet been exploited in oxidase biosensors [11]. H₂O₂ has also been detected with noble metal or carbon sensors that had been chemically modified with copper micro- and nanomaterials [12]. We first demonstrated that disk electrodes made of ordinary Cu wire, with no special micro- or nanoscopic surface modification, were capable of measuring H₂O₂ at low cathodic potentials with a linear response up to 1200 μM. In a further exploration of this property we found that a simple 'drop and dry' coating with a thin film of Nafion containing GOx can convert cathodic H₂O₂ Cu sensors into sensitive biosensors for glucose with resistance to interference by other oxidizable substances. Calibration curves for unmodified (H₂O₂-detecting) and GOx-modified (glucose-detecting) versions of the Cu electrodes with negative detection potential are presented, together with tests for interference and assessments of recovery rates in the analysis of 'spiked' model samples.

2 Experimental

2.1 Reagents and Solutions

All chemicals used in this study were of analytical grade and purchased through SM Chemical Supplies Co. Ltd. (Bangkok, Thailand) or Italmar Co. Ltd (Bangkok, Thailand) and, unless otherwise mentioned, were products of Carlo Erba Reagents (Cornaredo, Italy). Ultrapure water for aqueous solution preparation came from a reverse osmosis-deionization system. 0.1 M phosphate buffers (PBS) were made with monobasic sodium phosphate monohydrate (NaH₂PO₄·H₂O) and anhydrous dibasic sodium phosphate (Na₂HPO₄). Aqueous stock solutions of glucose, ascorbic acid and 4-acetamidophenol (Acros Organics) were prepared on the day of use while fresh aqueous H₂O₂ stock solutions were made by diluting commercial 30% (w/w) aqueous H₂O₂ solution containing stabilizer. The enzyme component of the biosensors of this study, GOx from *Aspergillus niger* (type X-S, 136300 units/g, Sigma Aldrich), was stored in aliquots (20 mg/mL) at -20 °C. The polymer for immobilization matrix formation was commercial Nafion® perfluorinated resin, obtained as 10% (w/v) dispersion in water (Sigma Aldrich).

2.2 Cu Electrode Fabrication and GOx Immobilization

The starting material for Cu disk electrode manufacture was poly(vinyl chloride)-insulated electrical cable with a metal core of circular cross-section (Phelps Dodge Int. Corp., PD-THW 750 V PVC 70° TIS 11-2531). The plastic insulation was stripped from an approximately 5 cm length of cable and the bare Cu wire, of about 2 mm diameter, was then sealed with a two-component insulating epoxy resin, (2-Ton Epox-Fix from Altec Chemical Pte. Ltd., Singapore), into a glass tube of slightly larger inner

Full Paper

diameter. Care was taken that the Cu wire protruded at the top of the assembly, to be used for electrical connection to the electrochemical amplifier, while at the bottom the glass rim and wire disk face were roughly aligned. After curing the epoxy resin overnight at room temperature, abrasion with rough emery paper was used to expose the embedded Cu disk. The disk and its surrounding glass/epoxy rim were then finely polished to a mirror-like appearance by continuous circular movements on increasingly fine emery paper and, finally, the same treatment on a soft polishing pad soaked with alumina suspensions of 1–2 μM and then 0.4 μm particle diameter. The outcome at this stage was a glass/polymer-embedded Cu disk electrode of approximately 2 mm diameter that could be used either for H_2O_2 amperometry or as the precursor in glucose biosensor construction.

To demonstrate the suitability of bare Cu electrodes as cathodic platforms in oxidase-based biosensors they were modified with a surface deposit of polymeric Nafion blended with the enzyme GOx. As in previously published attempts with other precursor electrodes [13] the active layer was constructed by simple drop-and-dry application of a mixture of equal volumes of 20 mg/mL GOx stock solution and commercial 10% aqueous Nafion dispersion. With the Cu electrode shaft inverted, 10 μL of this mixture were dropped onto the disk face and complete solvent evaporation was allowed to take place. Dried electrodes with the enzyme/Nafion top coat were thoroughly rinsed with distilled water and then their glucose response was checked by amperometric calibration measurements.

2.3 Apparatus and Electrochemical Measurements

Freshly prepared Cu electrodes or Cu-based glucose biosensors were dipped into 0.1 M PBS as measuring buffer and supporting electrolyte, and were used as working electrodes in a beaker-type electrochemical cell, connected to a Gamry Reference 600™ potentiostat. A coiled platinum wire and an Ag/AgCl/saturated KCl reference electrode (ALS Co., Ltd., Tokyo, Japan) completed the three-electrode cell arrangement as counter and reference electrodes, respectively. In routine test trials the cathodic monitoring of added (bare Cu electrodes) or enzymatically produced (Cu-based glucose biosensors) H_2O_2 was performed with the Cu platform polarized to -0.15 V vs. reference electrode and the electrolyte stirred at 200 rpm.

3 Results and Discussion

Good biosensor performance depends on the electrochemical reliability and sensitivity of the enzyme-carrying electrode and the ability of the immobilizing matrix to hold the biological recognition element close to the signal-transducing surface. Figs 1A and B show the electrical Cu cable used for biosensor preparation and one completed cable Cu electrode, respectively.

ELECTROANALYSIS

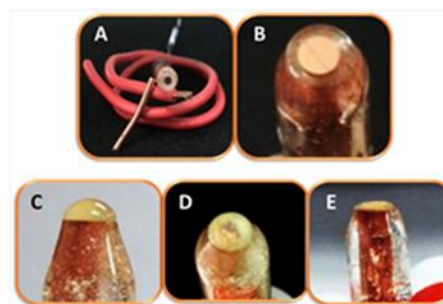


Fig. 1. Digital photographs of (A) the electrical cable used as the precursor for Cu electrode fabrication (B) a completed Cu disk electrode (C) a Cu disk electrode with a 10 μL drop of a GOx/Nafion solution applied and (D) and (E) the top- and side-views of the modified Cu disk electrode after solvent evaporation, coated with a dry GOx-containing Nafion film.

Polishing of the end of the glass tube with fine emery paper and alumina paste exposed a uniformly smooth Cu disk of about 2 mm-diameter, insulated by the adjacent glass/epoxy sheath. A simple drop-and-dry coating procedure was used to modify simple cable Cu disk electrodes by coating them with a GOx-immobilizing Nafion thin film, forming the prototype cable Cu glucose biosensors. Figs 1C–1E show the cable Cu disk electrode after application of a 10 μL droplet of an aqueous solution of 10 mg/mL GOx and 5% Nafion. The liquid was placed on top of the electrode (1C) and evaporation of water formed a dry Nafion polymer with entrapped enzyme (1D, 1E). Note that air-dried GOx/Nafion layers were adhesive enough to survive continuous solution stirring during biosensor calibration and sample measurements in standard addition mode, without noticeable detachment.

The ability of a bare cable Cu disk electrode to detect H_2O_2 at cathodic potentials with appropriate analytical performance was investigated by calibration trials in which the sensor was exposed to increasing levels of the analyte in a continuously stirred measuring solution, while the amperometric current was recorded as a function of time. Figure 2A is a typical current trace, obtained with a Cu working electrode at -0.15 V vs. reference. The sequential addition of H_2O_2 aliquots produced stepwise increases in the sensor current, with a response time of 5–10 s. Calibration plots of the averaged background-corrected electrode currents versus H_2O_2 concentration were consistently linear up to 1200 μM , with a sensitivity of about $0.65 \mu\text{A} \mu\text{M}^{-1} \text{cm}^{-2}$, approaching saturation at higher H_2O_2 concentrations (Figure 2B). Incremental rises in H_2O_2 concentration as small as 5 μM triggered reliable current steps of matching amplitude and this is considered the practical detection limit of the proposed Cu electrodes.

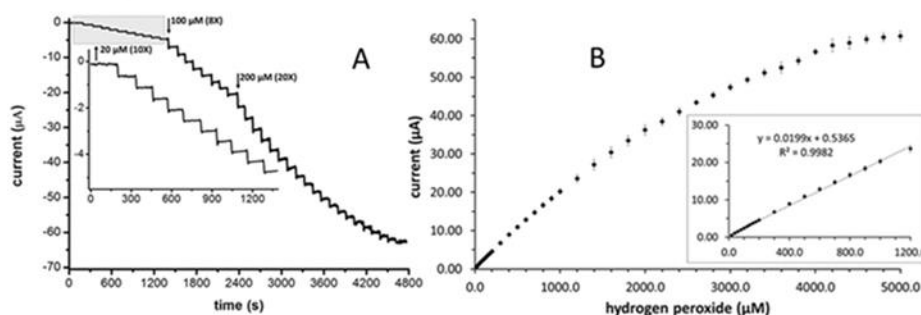


Fig. 2. (A) Response of a Cu disk electrode to successive additions of aliquots of a H_2O_2 stock solution to a continuously stirred measuring solution (0.1 M PBS (pH 7)). The working electrode potential and stirring rate were -0.15 V vs. reference and 200 rpm, respectively. The inset shows the I/t curve for the first ten additions of H_2O_2 , with zoomed x and y axes. (B) Calibration graph constructed with the averaged data from triplicate chronoamperometric trials as shown in the example to the left. Error bars represent the standard deviations for the repeated measurements.

Operation of the Cu electrode at negative H_2O_2 detection potential was expected to eliminate interference by compounds that would generate anodic currents at high positive detection potential. Fig. 3 shows the outcome of the interference study: neither ascorbic acid nor the drug Paracetamol[®], which may be interfering constituents of blood and urine, induced the step-like rises in sensor current that were seen with equal additions of H_2O_2 .

The performance of cable Cu disk electrodes, in the standard addition mode, was evaluated by determining their ability to determine accurately the known analyte concentration of spiked electrolytes. An example of the original current trace in such an analytical trial with $100 \mu\text{M}$ H_2O_2 and the corresponding calibration plot are shown in Fig. 4. In this particular attempt, the analyte

concentration measured was $109.2 \mu\text{M}$, compared to its known concentration of $100 \mu\text{M}$. An average apparent recovery of 107.6% ($107.6 \pm 2.5 \mu\text{M}$, $n=3$) was obtained from the triplicate measurements. The reasonable linear range, low detection limit and acceptable average recovery suggested the feasibility of using Cu disk electrodes as interference-free cathodic H_2O_2 detection platforms.

Coating with a GOx-containing polymeric Nafion layer converted the Cu disk electrode to a glucose biosensor that could be operated at negative potential for cathodic detection of H_2O_2 produced by enzymic substrate oxidation. Fig. 5A shows an amperometric recording from a freshly prepared prototype electrode operated with a working potential of -0.15 V relative to the reference,

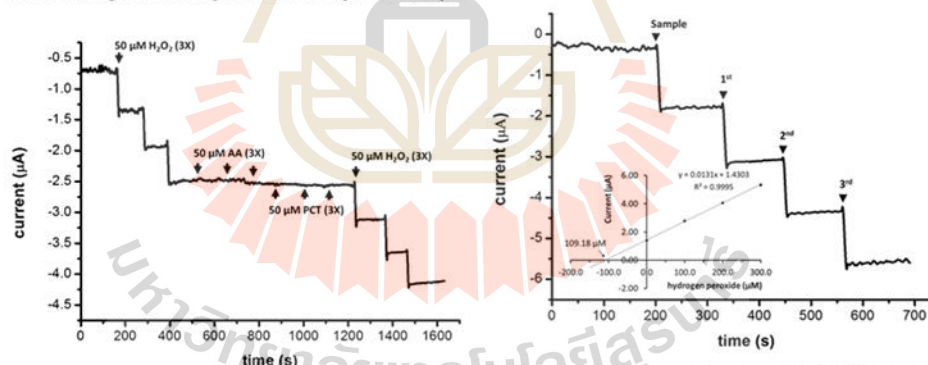


Fig. 3. Amperometric response of a Cu disk electrode in continuously stirred 0.1 M PBS (pH 7) to successive triplicate additions of $50 \mu\text{M}$ of analyte (H_2O_2), interferents (ascorbic acid, AA and paracetamol, PCT) and analyte again. The parameters for detection were as in Figure 2.

Fig. 4. Amperometric recording of a cable Cu disk electrode for H_2O_2 determination in continuously stirred 0.1 M PBS (pH 7) by standard addition. Adjusted H_2O_2 concentration: $100 \mu\text{M}$; standard additions: $3 \times 100 \mu\text{M}$ increments. The parameters for detection were as in Figure 2. The inset is the standard addition plot for the analytical run.

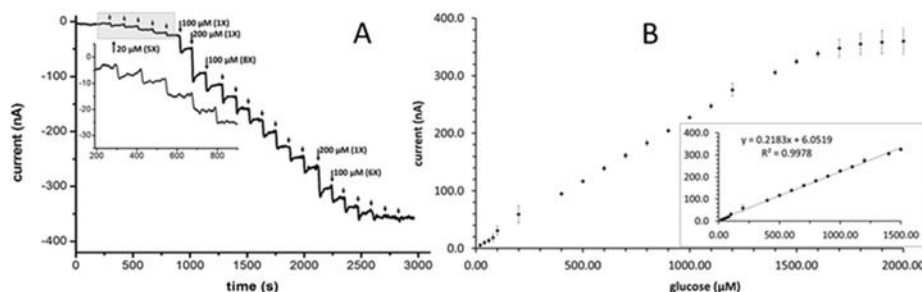


Fig. 5. (A) Amperometric response of GOx/Nafion-modified cable Cu disk electrode to successive additions of aliquots of a glucose stock solution, in continuously stirred 0.1 M PBS (pH 7). The working electrode potential and stirring rate were set to -0.15 V vs. reference and 200 rpm, respectively. The inset is the I/t curve for the first 5 glucose additions, with zoomed x and y axes. (B) Calibration graph constructed with the averaged data from triplicate amperometric trials as shown in the example to the left. The error bars represent the standard deviations for the repeated current measurements.

in 0.1 M PBS pH 7.0, and with 1 aliquots of stock glucose solution added sequentially. Each glucose injection produced an immediate (within <5 s) rise in cathodic current, while the final steady state current was reached in 30–40 s, which is a little longer than is needed to establish a constant H_2O_2 signal in unmodified Cu electrodes. The resultant plot of background-corrected sensor current vs. glucose concentration is shown in Fig. 5B. The calibration graph for triplicate trials was linear from 20 to 1500 μ M, with a slope of $0.22 \text{ nA } \mu\text{M}^{-1}$ (sensitivity of $7 \text{ nA } \mu\text{M}^{-1} \text{ cm}^{-2}$) for regression through the first 16 data points, and a correlation coefficient of 0.9987. Increases in glucose concentration as small as 20 μ M produced current steps of matching amplitude and this is the practical detection limit for sample analysis with cable Cu glucose biosensors. Assessment of the efficiency of sample recovery was made by addition of glucose standards in spiked measuring buffers. Fig. 6 shows a typical amperometric current trace from such an analysis, for addition of 100 μ M glucose. The inset of Fig. 6 shows the standard addition plot, which gave 109.0 μ M as the measured analyte level. From triplicate repetitions of this trial the average recovery of glucose was calculated to be $106.0 \pm 4.1 \%$ ($n=3$).

Repeated modifications of a single cable Cu disk electrode with a functional GOx/Nafion layer, with surface polishing in between, gave reproducible results, as evidenced by the small error bars of triplicate measurements (see Fig. 5B, for example). Good reproducibility was also obtained when three separate Cu disk precursor electrodes were identically modified and the consistency of the signals assessed. Fig. 7 shows plots of the background-corrected currents from the individual electrodes as a function of the glucose concentration in the measuring buffer, for 7 serial substrate additions. Amplitudes of individual biosensor signals were directly proportional to glucose concentration, with all three regression coefficients >0.999 . The slopes of the calibration plots were slightly

different, however the standard deviation of only $\pm 12 \%$ from the average value is considered acceptable, given that the Cu wires used to construct the sensors may have differed slightly in cross-sectional area.

The demonstrated analytical performance of cable Cu-based glucose biosensors should in principle qualify the tool for future application to standard samples, including blood and urine from healthy people or clinical patients. The greatest advantage of the novel biosensor described in this study, however, is that its good performance in glucose assays is accomplished with a design that is significantly simpler and cheaper than those of similar electrodes with cathodic interference protection.

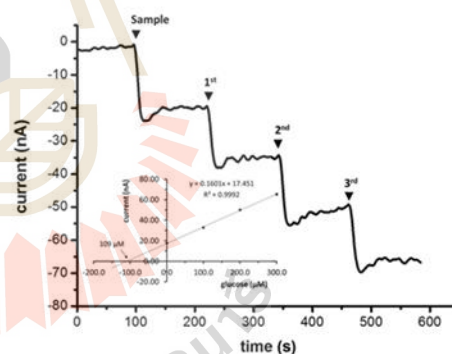


Fig. 6. Amperometric recording of GOx/Nafion-modified cable Cu disk electrode for glucose determination by standard addition. Electrolyte: 0.1 M PBS (pH 7.0); electrode modification: GOx/Nafion; working electrode potential: -0.15 V vs. reference; stirring rate: 200 rpm; adjusted glucose solution concentration: 100 μ M; standard additions: $3 \times 100 \mu\text{M}$ rises. The inset is the standard addition plot for the analytical run.

Full Paper

ELECTROANALYSIS

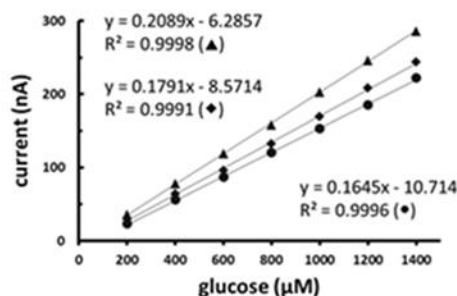


Fig. 7. Amperometric glucose calibrations of three separate GOx/Nafion-modified cable Cu disk electrodes. Electrolyte: 0.1 M PBS (pH 7.0); electrode modification: GOx/Nafion; working electrode potential: -0.15 V vs. reference; stirring rate: 200 rpm; the glucose concentration was raised in 200 μ M increments from 0 to 1400 μ M and the background-subtracted current step amplitudes displayed as a function of the actual glucose concentration.

4 Conclusions

Electrical cable-based Cu disk electrodes have been fabricated and converted into glucose biosensors by drop-coating with a GOx/Nafion surface layer. The ability of Cu electrodes to measure H_2O_2 by reduction made it possible to operate completed cable Cu glucose biosensors at -0.15 V vs. reference for analyte quantifications, the negative detection potential eliminating interference by other substances. The calibration curve showed a linear response up to 1.5 mM, with a practical detection limit of 20 μ M at the lower end. With these performance characteristics the novel cable Cu glucose biosensors are suitable for quantification of glucose, whether in extracts from food and drink production or in clinical blood or urine samples. These sensors are simple, cheap and easily made for quantitative glucose measurement and are recommended, for instance, as an economical option for school and university teaching as well as for professional clinical and biotechnology laboratories.

Copper is one of the few metals that works well in the fabrication of microelectrode arrays through the synchrotron radiation-supported LIGA process (LIGA, Lithography, Galvanoformung (Electroplating), Abformung (Molding)). Our further work will focus on an extension of the confirmed analytical performance of Cu-based oxidase biosensors from macro- to microscopic platforms dimension. The known benefits of microelectrodes in terms of signal amplification (through the enhanced mass transport properties of miniaturized sensors) and noise reduction (through smaller capacitive currents) should help to achieve advanced Cu-based (glucose) oxidase microbiosensors with an exquisite sensitivity and detection limit for trace (glucose) biosensing.

Acknowledgements

We acknowledge the kind financial support of this study by the Thailand Research Fund (TRF), through Basic Research Grant BRG 56800013, the TRF and Suranaree University of Technology (SUT), through their joint Royal Golden Jubilee Ph.D. Program Grant No. PHD/0168/2554 and the Centre of Excellence in Advanced Functional Materials from SUT and The Office of the Higher Education Commission under the National Research University (NRU) project of Thailand. Special appreciation goes to Dr. David Apps, Biochemistry Reader (retired), Centre for Integrative Physiology, Edinburgh University, Scotland, who helped by reading the manuscript and with language improvement.

References

- [1] S. Borgmann, A. Schulte, S. Neugebauer, W. Schuhmann in *Bioelectrochemistry: Fundamentals, Applications and Recent Developments, Volume 13 (Advances in Electrochemical Sciences and Engineering)* (Eds.: R. C. Alkire, D. M. Kolb, J. Lipkowsky), Wiley-VCH Verlag GmbH & Co. KGaA, Weinheim, 2012, pp. 1–84.
- [2] a) A. G. A. Aggidis, J. D. Newman, G. A. Aggidis, *Biosens. Bioelectron.* 2015, 74, 243–262. b) M. Taguchi, A. Pitsyn, E. S. McLamore, J. C. Claussen, *J. Diabetes Sci. Technol.* 2014, 8, 403–411; c) B. Lim, Y. P. Kim, *Adv. Biochem. Eng. Biotechnol.* 2014, 140, 203–219; d) M. M. Rahman, A. J. Ahammad, J. H. Jin, S. H. Ahn, J. J. Lee, *Sensors* 2010, 10, 4855–4886; e) E. H. Yoo, S. Y. Lee, *Sensors* 2010, 10, 4558–4576; f) J. Wang, *Chem. Rev.* 2008, 108, 814–825; g) J. D. Newman, A. P. Turner, *Biosens. Bioelectron.* 2005, 20, 2435–2453; h) E. Wilkins, P. Atanasov, *Med. Eng. Phys.* 1996, 18, 237–288.
- [3] W.-Z. Jia, K. Wang, X.-H. Xia, *Trends Anal. Chem.* 2010, 29, 306–318.
- [4] T. Terse-Thakoor, K. Komori, P. Ramnani, I. Lee, A. Mulchandani, *Langmuir* 2015, 31, 13054–13061; b) H. Hu, M. Feng, H. Zhang, *Talanta* 2015, 141, 66–72; c) S. Palanisami, R. Devasenathipathy, S.-M. Chen, A. M. Ajmal, C. Karpuriah, V. Balakumar, P. Prakash, M. S. Elshikh, F. M. A. Al-Hemaid, *Electroanalysis* 2015, 27, 2412–2420; M. Baghayeri, *RSC Advances* 2015, 5, 18267–18274.
- [5] N. Tordo, *Bioelectrochem.* 2009, 76, 195–200; b) P. D. Voegel, R. P. Baldwin, *Electrophoresis* 1997, 18, 2267–2278; c) K. Kano, K. Takagi, K. Inoue, T. Ikeda, T. Ueda, *J. Chromatogr.* 1996, 721, 53–57; d) L. A. Colon, R. Dadoo, R. N. Zare, *Anal. Chem.* 1993, 65, 476–481.
- [6] J. Ye, R. P. Baldwin, *Anal. Chem.* 1994, 66, 2669–2674.
- [7] H. Lin, D. K. Xu, H. Y. Chen, *J. Chromatogr.* 1997, 760, 227–233.
- [8] A.-N. Kawde, A. Aziz, *Electroanalysis*, 2014, 26, 2484–2490.
- [9] T. R. L. C. Paixao, M. Bertotti, *J. Electroanal. Chem.* 2004, 571, 101–109.
- [10] Y. Jovanovski, N. I. Hrastnik, S. B. Hočevar, *Electrochem. Commun.* 2015, 57, 1–4; b) X. Pei, W. Kang, W. Yue, A. Bange, W. R. Heineman, I. Papautsky, *Anal. Chem.* 2014, 86, 4893–4900.
- [11] M. Somasundrum, K. Kirtikara, M. Tanticharoen, *Anal. Chim. Acta.* 1996, 319, 59–70.
- [12] V. Mani, R. Devasenathipathy, S. M. Chen, S. F. Wang, P. Devi, Y. Tai, *Electrochim. Acta* 2015, 176, 804–810; b) S. Y.

Full Paper

ELECTROANALYSIS

- Deng, G. Y. Zhang, D. Shan, Y. H. Liu, K. Wang, X. J. Zhang, *Electrochim. Acta* **2015**, *155*, 78–84; c) T. Selvaraju, R. Ramaraj, *J. Appl. Electrochem.* **2009**, *39*, 321–327.
- [13] J. Rishpon, S. Gottesfeld, C. Campbell, J. Davey, T. A. Zawodzinski Jr., *Electroanalysis* **1994** *6*, 17–21; b) A. A. Karyakin, E. E. Karyakina, L. Gorton, O. A. Bobrova, L. V. Lu-

kachova, A. K. Gladilin, A. V. Levashov, *Anal. Chem.* **1996**, 4335–4341.

Received: March 14, 2016
Accepted: May 25, 2016
Published online: July 8, 2016

SPECIAL ISSUE



CURRICULUM VITAE

Name: Wajee Jaikaew
Status: Ph.D.candidate (Chemistry)
Birthday: 28th March 1988
Place of Birth: Nakhon Ratchasima, Thailand
Nationality: Thai

Educations:

- Primary Education 1994-1999: Ban Nong Khanak School, Nakhon Ratchasima, Thailand.
Secondary Education
Lower and higher school form: 2000-2005: Sukphaibunwiriyawittaya School, Nakhon Ratchasima, Thailand.
- Tertiary Education
B. Sc. (Chemistry), Rajamangala University of Technology Isan, Nakhon Ratchasima, Thailand, 2006-2010.
- Enrolled as a Ph.D. student in 2012

Scholarship

The Royal Golden Jubilee (RGJ) Ph.D. Programme, Thailand, 2012.